T.C. ISTANBUL KÜLTÜR UNIVERSITY
INSTITUTE OF GRADUATE STUDIES

SEISMIC BEHAVIOR OF THE CONTENTS OF SEISMICALLY ISOLATED BUILDINGS

Masters of Applied Science Thesis

Zakirullah HAJI ABDUL QADUS

1301014014

Department: Civil Engineering

Programme: Structural Engineering

Supervisor: Prof. Dr. Cenk ALHAN

JUNE 2021

T.C. ISTANBUL KÜLTÜR UNIVERSITY
INSTITUTE OF GRADUATE STUDIES

SEISMIC BEHAVIOR OF THE CONTENTS OF SEISMICALLY ISOLATED BUILDINGS

Masters of Applied Science Thesis

Zakirullah HAJI ABDUL QADUS

1301014014

Date of Submission: 12 April 2021

Date of defence examination: 3 June 2021

Supervisor and Chairperson: Prof. Dr. Cenk ALHAN

Members of Examining Committee:

Assist. Prof Dr. Gökhan YAZICI

Assist. Prof Dr. Erdal COŞKUN

JUNE 2021

ACKNOWLEDGEMENT

I would like to keep my special courtesy to Prof. Dr. Cenk ALHAN. Despite his busy schedule, he managed to guide, lead, supervise, motivate, assist and support me throughout the thesis. Additionally, his efforts, expertise and work discipline is exemplary, which led me to complete my thesis. His teachings and insightful comments are based on a practical approach, by showing computer-based modeling of structures and providing necessary materials to understand the topic deeply, which an engineer needs to achieve during his education to become a future structural engineer. I would also like to thank Research Assistant Zafer KANBİR for his assistance and advice in my thesis. I would love to thank Istanbul Kultur University, especially Civil Engineering Department members for sharing their valuable knowledge, professionalism and mentoring in my bachelor and as well as in master studies. Last but not least, I am deeply thankful to my precious parents, for their love, care, kindness and for their unlimited support they provided me throughout my education career and dedicate this research to my family and humanity.

Zakirullah, HAJI ABDUL QADUS

University	**:**	**İstanbul Kültür University**
Institute	**:**	**Institute of Graduate Studies**
Programme	**:**	**Structural Engineering**
Department	**:**	**Civil Engineering**
Supervisor	**:**	**Prof. Dr. Cenk ALHAN**
Degree Awarded and Date	**:**	**MSc Thesis – June 2021**

ABSTRACT

SEISMIC BEHAVIOR OF THE CONTENTS OF SEISMICALLY ISOLATED BUILDINGS

Zakirullah Haji Abdul Qadus

Seismic isolation is an emerging earthquake resistant design technology. It particularly reduces floor accelerations as compared to fixed base buildings. Thus, it is very successful in protecting the contents of buildings. In previous studies, the extents of the content protection was assessed by investigating the floor accelerations only. However, particularly vibration sensitive contents such as electronic devices, computers, testing machines, etc are located on racks which are mounted on various floors of buildings. Therefore, it is essential to assess the acceleration levels sustained at the rack floors rather than just taking floor accelerations into account. In order to shed light to this issue, in this thesis, acceleration response behaviour of benchmark racks with rack natural periods that are located at different levels of a benchmark seismically isolated building are assessed when the building is subjected to historical and synthetic near-fault ground motion records. The building and the rack systems are modelled as a combined structural system which takes the building-rack interaction into account. Results are reported in the form of comparative plots and failure probabilities when certain acceleration trash hold limits are considered.

Üniversite	**:**	**İstanbul Kültür Üniversitesi**
Enstitüsü	**:**	**Lisansüstü Eğitim Enstitüsü**
Programı	**:**	**Yapı Mühendisliği (İngilizce)**
Anabilim Dalı	**:**	**İnşaat Mühendisliği**
Tez Danışmanı	**:**	**Prof. Dr. Cenk ALHAN**
Tez Türü ve Tarihi	**:**	**Yüksek Lisans – Haziran 2021**

KISA ÖZET

SİSMİK İZOLASYONLU BİNALARDAKİ İÇERİĞİN SİSMİK DAVRANIŞI

Zakirullah Haji Abdul Qadus

Sismik izolasyon, gelişmekte olan depreme dayanıklı bir tasarım teknolojisidir. Özellikle ankastre binalara kıyasla kat ivmelerini azaltır. Böylece, binaların içeriğini korumada çok başarılıdır. Önceki çalışmalarda, içerik korumanın kapsamı yalnızca kat ivmelerinin incelenmesi ile yapılmıştır. Bununla birlikte, özellikle elektronik cihazlar, bilgisayarlar, test makineleri vb. titreşime duyarlı içerikler binaların çeşitli katlarına monte edilmiş raflarda yer almaktadır. Bu nedenle, sadece kat ivmelerini hesaba katmak yerine raf katlarındaki ivme düzeylerini değerlendirmek gerekir. Bu konuya ışık tutmak amacıyla, bu tezde sismik izolasyonlu binaların farklı seviyelerinde yer alan farklı doğal periyotlara sahip rafların ivme tepki davranışı değerlendirilmektedir. Bina, tarihi ve sentetik yakın fay yer hareket kayıtlarına tabi tutulduğunda bina ve raf sistemleri, bina-raf etkileşimini hesaba katan birleşik bir yapısal sistem olarak modellenmiştir. Sonuçlar, belirli ivme eşiği sınırları göz önüne alındığında karşılaştırmalı grafikler ve başarısızlık olasılıkları şeklinde rapor edilmiştir.

TABLE OF CONTENTS

LIST OF FIGURES

LIST OF TABLES

LIST OF ABBREVIATIONS

AFAD	: Afet Ve Acil Durum Müdürlüğü (Disaster and Emergency Management Authority)
USGS	: United States Geological Survey
VSD	: Vibration Sensitive Devices
CBI	: Connecting Business Initiative
DLH	: Demiryollar, Limanlar Ve Hava Meydanları İnşaatı Genel Müdürlüğü (General Directorate of Railways Harbors And Airports Construction)
DBE	: Design Base Earthquake
MCE	: Maximum Credible Earthquake
LDRBs	: Low Damping Rubber Bear
HDRBs	: High Damping Rubber Bearings
LRBS	: Lead Rubber Bearings Isolation System
TFP	: Triple Friction Pendulum
PEER	: Pacific Earthquake Engineering Research Center
ATC	: Applied Technology Council
EPS	: Earthquake Protective Systems
FEMA	: Federal Emergency Management Agency
CSA	: Canadian Standards Association
BWOR	: Building Without Rack
BWR	: Building With Rack
TFA	: Top Floor Acceleration
J161	: Joint Number 161
R_D	: Rack Dependent
R_I	: Rack Independent

LIST OF SYMBOLS

C	: the amplitude scale factor
φ	: the phase angle of the sinusoidal component
η	: damping factor
n	: parameter controlling the sharpness of the pulse envelope curve,
t0	: the start time of the pulse (s)
$\omega p=2\pi/Tp$	: the pulse frequency (rad/s)
F_Q	: characteristic force (kN)
F_y	: yield force (kN)
D_y	: yield displacement (mm)
K_1	: pre-yield stiffness Kn/m or N/mm
K_2	:post-yield stiffness Kn/m or N/mm
α	: post to pre yield stiffness ratio
ke	: Effective Stiffness Kn/m or N/mm
a	: Ground motion acceleration. (m/s^2)
v(t)	: Velocity time dependent function (m/s)
a(t)	: Acceleration time dependent (m/s^2)
T_0	: isolation period based on post yielding stiffness
W	: total weight of the building
g	: the gravitational acceleration (m/s^2)
Q/W	: the nominal characteristic force ratio
ζ_p	: decaying or damping factor
ω_p	: the sinusoid frequency (rad/s)
t	: the time in unit of seconds (s)
s	: the initial amplitude of the velocity pulse.
v_p	: peak ground velocity (m/s)
T_p	: pulse period (s)

$\sqrt{(1-\zeta_p^2)}$: defined to meet the T_p in velocity pulse period simulation of near-fault ground motion

t_p : time of peak ground velocity (s)

Mw : moment magnitude

r : distance from the fault relationships (km)

ω : Natural frequency (rad/s)

$\ddot{u}_t$: Total acceleration (g)

$\ddot{u}_r$: Relative acceleration or structural acceleration (g)

$\ddot{u}_g$: Ground motion acceleration (g)

$\dot{u}$: Relative velocity (m/s)

u : Relative displacement (m)

μ : Friction coefficient

e : Eccentricity (m)

E_c : Bearing compressive modulus (MPa)

E_c : Concrete elastic modulus (MPa)

E_s : Steel elastic modulus (MPa)

Ee :Elastic strain energy (kN.m)

Eh : Hysteretic damping energy (kN.m)

1 INTRODUCTION

1.1 Background

The research for specific purpose raised from the real need. Earthquake is one of the very important natural fact, which really affects daily life. Structure's performance depends upon the structure design type. Intensity of the earthquake is the first parameter, which determines the consequences. Closer the structure to the fault, it gets more prone to earthquake damage. Its effect can last for short and long period of time depending upon the type and damage level.

Earthquake is a natural phenomenon, which is explained by different theories and proved by different hypothesis. According to Wald (2019) written about the science of earthquake for "The Green Frog News" tectonic plates, fault lines and some other factors are the main causes, due to which earth crust movement happens. U.S. Geological Survey (2017) reported that in past two decades thousands of life's and millions of dollars is lost around the world due to earthquake.

Since history, scholars have tried to tackle the earthquake problem. Beside conventional construction methods, seismic isolation was also on the agenda. Bayraktar et al (2012) and Makris (2018) mention in their studies, the historical development and importance given to the seismic isolation. Historical and monumental structures were designed with the care of protecting it in any upcoming earthquake. Since some decades, the traditional approach were effective but as soon as the population grew, the earthquake problem took different dimension due to high- rise buildings, growing population and urbanization .This urged the professionals to take serious steps to save human and economic losses.

As per technological advances, more and more mechanical instruments and equipment's are used for precision and comfort. Earthquake movement creates vibrations and some of the devices are sensitive to vibration. The sensitivity level of devices varies regarding their function and properties. Different devices can withstand up to different vibration levels. VSD (vibration sensitive devices) are used for different purposes such as in laboratory, research field, hospitals, defense headquarters, and industries. Regarding the protection and importance of VSD, Alhan and Sahin (2011) have explained in the research study project. During earthquake, non-isolated structures may collapse partially or wholly depending upon the intensity and magnitude of the earthquake.

1.2 Seismic Isolation Applications in Turkey

To comprehend the overall scenario of seismic isolator applications in Turkey, investigation will be followed by two steps. First, general overview of the region will be detailed. Secondly, what steps were taken to reach to application will be summarized.

1.2.1 General Overview

Turkey is among the earthquake prone countries. 42% of Turkey is covered by first-degree seismic zone. Earthquakes are constantly on the agenda and every five years earthquake poses with losses of life and property (AFAD, 2014: 14). The North Anatolian Fault extends from East to West covering 1,400-kilometer-long (870-mile-long), which exhibited a systematic progression of major earthquake events USGS (Seismicity study in Turkey). Ambraseys and Jackson (2000) in their study explain the active tectonics of Turkey. Turkey is located in the Mediterranean, Alps, Himalayan earthquake zone. These are active earthquake zones. Alps mountain ranges are the result of the movements of Asia and Europe continents towards each other. Likewise, the unification of India and the Asian Continents resulted the Himalayas (Erdik et al, 1999), (JICA, 2004: 28). Tan et al (2007) in their study compiled the specification of historic earthquakes and the focal mechanism parameters dated from 1938 till 2004 covering 108 destructive earthquake data, among them are nearly 30 earthquakes which were over M_w = 6.0 across the country. The data base also includes the deadly earthquakes of North Anatolian Fault ($M \geq 6.5$) between 1939–1957.

To sum up, the historic events clearly tell us the seismicity of Turkey. Consequently, earthquakes have economic facts also. Şahin and Kılınç (2016) mention the economic effects of earthquakes in Turkey between 1980-2014. And in this study the total human and economic losses and primay, secondary and tertiary effects of earthquakes on the daily life are also detailed. According to CBI (2019) report, as Turkey's economy grew over in 20 years, the earthquake risk also raised. Earthquakes affected 30 thousand work places and businesses resulting in total loss of 200 billion Turkish Lira. But due to the extensive research in this field, the professionals are now able to put serious measures to prevent the relative losses. Invention of seismic isolation became very effective which helped the structures to dissipate energy.

1.2.2 Renaissance, Revival

Makris (2018) mentions the traditional and historical applications of seismic isolation. Its traces can be found in the existing structures and historical monuments. Since 1990s, seismic isolation is developed into a feasible and effective seismic safety technique, with either lead-rubber bearings, natural rubber bearings, or single-concave sliding bearings supporting large buildings and bridges. Seismic isolation enjoyed growing worldwide recognition for the seismic safety of civil structures following the 1994 Northridge, California and the 1995 Kobe, Japan earthquakes (Makris, 2018).

In the general overview section, the devastating effects of earthquakes are reviewed from the researches. Very high floor accelerations in rigid structures and inter-story drifts in elastic structures are the main responses of conventional buildings, which is not promising and securing to the structural and non-structural elements. Post-earthquake functioning of both elements are reliably ensured by seismic isolation.

Seismic isolation application came into the agenda in Turkey after Kocaeli 1999 Mw7.4 Earthquake, which struck at 03.01 am in the morning. As a result, thousands of lives were lost, half a million people were homeless (C.Scawthorn, G.S. Jhonson, 2000) . Post-earthquake articles A. Barka, H.S. Akyüz et al (1999) and R.Gore (2020), reports were published by different organizations such as RMS Reconnaissance Team about the earthquake which comprise the building failure reasons, the economic effects, and so on.

Just after the tragic event, with new day and new hope the importance of functionality of buildings post-earthquake start gaining momentum. New official codes and various instructions were developed to motivate and modulate the proceeding applications. After 2000, at first, passive control technologies were used as earthquake resistant. Due to the lack of official seismic isolation code, professionals used US and European codes. The different approaches in design parameters and testing led to incompatible results. In 2018, first Turkish "seismic isolation design code for building was released". Different projects started adopting the code. After 2011 Van earthquake, hospitals were nonfunctional due to structural and non-structural damages. As there was no legislation to conserve the post-earthquake functioning of hospitals. The Ministry of health in 2013 released a regulation and specification for the hospitals comprising of over 100 beds in seismic zone 1 and 2 to be mandatorily seismically isolated. Research as "seismic isolation code development and application in turkey" is published by Erdik et al (2018).

Kocaeli (1999) Earthquake damaged lots of existing and under construction buildings. The Atatürk International Airport was one of them. Airport was nearly 70 km away from the rupture point. It was to be finished but all of a sudden, the earthquake damaged the roof to column structure of the terminal (Figure 1.1). The project study carried out by Constantinou et al (1999) for the seismic evaluation and retrofit of airport. As a result of static and dynamic analysis, structural strengthening and roof base isolation were installed (Figure 1.2) and were completed within 12 weeks period of time.

Figure 1.1: Observed Damage to the Terminal Building; base of third story column (left) and base of roof truss connection to column (right). (Constantinou et al, 1999)

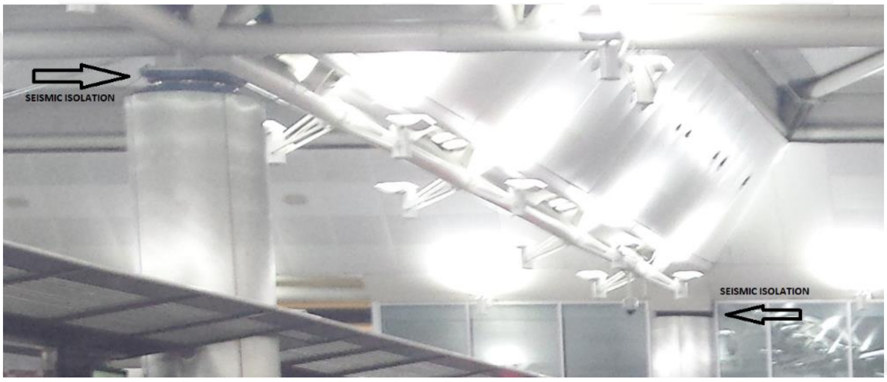

Figure 1.2: Seismic Isolation of terminal building

Base isolation is widely preferred for retrofitting of existing buildings. Because its economical, time saving and a promising solution. Conventional method of retrofitting is time consuming due to its application on each floor and introduction of new structure members in some cases. In Japan, base isolation is widely used for retrofitting and new building.

Gurup Apartment located in Moda District Istanbul near the Marmara Sea, is the very first residential building retrofitted with base isolation. After examination, building is found to be incapable to withstand earthquake forces. Karayiğit, Özkul (2019) studied the performance criteria, analysis, and application details of the building. The building consists of eleven stories. Figure 1.3 is the plan of building. Figure 1.4 is the design spectrum of existing Gurup apartment, which is generated by using variables of response spectrum of the earthquakes depending on site location per DLH (2008). The two level of safety is used to evaluate the performance of the building in push over analysis; firstly, using Design Basis Earthquake (DBE), secondly Maximum Credible Earthquake (MCE) with return period of 475 years and 2,475 years, respectively. As a result, foundation was reinforced. 27 Lead Rubber Bearings (LRBs) and six sliders were installed as base isolation in the base floor which is capable of 280 mm maximum displacement.

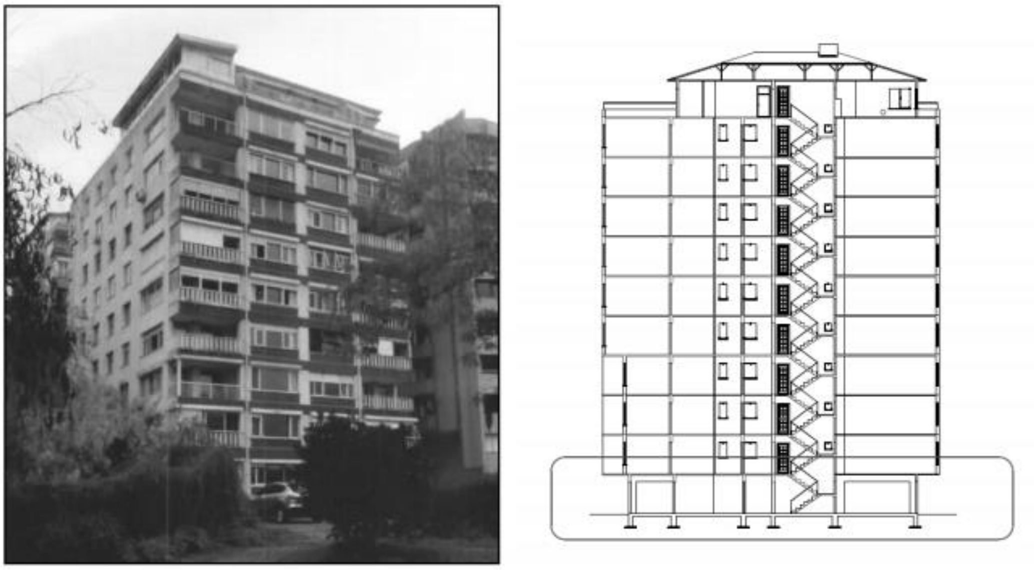

Figure 1.3: view of the building and the isolation level (Karayiğit, Özkul, 2019)

Basaksehir Cam and Sakura City Hospital located in Istanbul, is the world's largest base-isolated building with an area of 1 million m^2. Figure 1.4 is the perspective veiw of the City Hospital, which was initiated in May 2020. The hospital is made of six building facilities which includes general, cardiovascular, physical therapy, and rehabilitation treatment services.

The hospital is designed to be fully functional after the earthquake. For "immediate occupancy", triple friction pendulum (TFP) is selected as base isolation to fulfil design criteria. Figure 1.5 is one of the TFP in base floor. In total, 2068 triple friction pendulum (TFP) are installed which have 700mm capacity of displacement resulting in reduction of seismic forces.

Figure 1.4: Başakşehir Çam & Sakura City Hospital (Arup, 2018)

Figure 1.5: TFP installed in base floor (Reference)

Kutahya City Hospital Project is located in seismic region 2. The project includes total 500 beds for General Hospital and 100 beds for Physical Therapy and Rehabilitation Hospital. Yamanturk, Dogruoz (2019) in their study, mention the application of double pendulum in the project. The City Hospital is designed to be fully functional after earthquake. A total of 498 seismic isolators are installed with moment resisting frame and have 560 mm maximum deformation capacity.

Figure 1.6 shows the ground work for the isolator and Figure 1.7 is the completion of installation. Top floor acceleration as per study is expected to be 0.18g. The study also shows the importance of base isolation in seismic regions.

Figure 1.6: Foundation work for isolator installion (Yamanturk, Dogruoz, 2019)

Figure 1.7: Installed double friction pendulum isolator view (Yamanturk, Dogruoz, 2019)

1.3 Motivation and Aim

Near-fault earthquakes are more destructive for structures and their contents. In near-fault regions, the amplitudes of vibrations are higher than far-fault. This study is inspired by sorrowful events in post-earthquakes, where devices are halted instead of functioning. In emergency situations, especially the devices in hospitals, should function prior to and post-earthquake and this can only be possible if proper precautions are taken. For protection of such devices and for earthquake risk mitigation on buildings and its contents such as sensitive devices, seismic base isolation is an emerging alternative. In this study, Sap2000 computer analysis program is used to assess the seismic response of the contents placed on racks located in different floors of a benchmark base-isolated building model subjected to earthquake excitation.

Earthquake generates vibration, which is really harmful for vibration sensitive devices. Alhan and Sahin (2011) discussed the importance of the protection of VSD devices. We use seismic isolation in the structure, which absorbs the seismic energy without transferring to the superstructure and reduces equivalent seismic forces. In near-fault earthquakes, seismic isolated structures suffer from high-amplitude and long-period vibrations originating from the earthquake. Although the isolated structure may survive the earthquake, its content, specially VSD, may not protected as required, i.e. VSD devices may suffer damage. VSD may become non-functional and useless, which in turn would stop the health care, telecommunications and other important industrial facilities. The purpose of this thesis is to understand the extent of protection of the VSD devices placed on racks which are housed in base-isolated buildings especially in near-fault regions.

1.4 Thesis Structure

This thesis includes six chapters. In the first chapter, an introduction, inspiration for the topic, thesis structure and limitations are explained. In the second chapter, seismic isolation, vibration sensitive equipment, literature review and near-fault earthquakes are elaborated. In chapter three, selection of structural model, rack model, materials and method are detailed. In chapter four, historic and synthetic earthquake selection, generation, and evaluation method and approach are described. Following chapter four, discussion of the results is explained in chapter five. In chapter six, general conclusion of the study are given.

1.5 Limitations

Some limitations apply and some assumptions are accepted in this research. The geometry of the building is symmetrical. Vertical earthquake effects are not taken into account. Structure-soil interaction is not taken considered.

2 GENERAL PARTS AND LITERATURE REVIEW

Seismic isolation decreases the effective earthquake forces by extending the dominant period of the structural system. Isolation provides damping, it absorbs the energy at the level of the isolation system which reduces the energy transmission to the structure. Thus, both floor accelerations and relative floor drift ratios are reduced below the desired limits. For such systems, the main challenge arises in case of near-fault earthquakes. Near-fault earthquakes lead the system into larger displacments (Heaton et al, 1995: Alhan and Öncü-Davas,2016).

S. Grimaz,P. maliSan(2014) and Mohammadia, Nouri(2017) in their studies explain the complexity involved in understanding the near-fault earthquakes. Various fault types, rupture, forward directivity and inter-related resulting motion, all is the content of near-faults. One by one observation and detailed studies of inter-related parts of near-fault earthquakes and in turn their effects on base isolation additionally to their contents is still so limited.

Base isolation is used to minimize the floor accelerations and protect the contents. In near-fault earthquakes, base isolation systems may face challenges. Makris(2000) study suggests additional protective system for base isolated building in near-fault earthquakes due to the large and unreturnable displacement of isolated buildings.

Lu Shun, Fu Lin (2008), investigated the isolated and non-isolated building differences in terms of floor acceleration and vibration depletion or weakening. Super-structure of isolated structure is observed to have 10% acceleration reaction of sub-structure. While the non-isolated building is seen to have vibration increment. Additionally, resulting natural frequency of non-isolated structure is found as 24.7Hz, while isolated structure as nearly half of the non-isolated structure as 11.5Hz. Moreover, isolated structure resulted significantly, in reduction of vibration as compared to conventional structures. Seismic isolated structure is observed under one-third octave vibration spectra (G. Gordon, 1999) to be safer for VSD, having 25db vibration decreasing performance.

The base isolation mechanism as a passive control system engages during ground motion. Sub-structure moves back and forth, maintaining the rhythm with ground motion while greatly protecting the super-structure with its contents. Base isolation does not allow the vibration to enter to the building such that the relevant frequencies which will cause structure vibration will be filtered out by base isolation and only other frequencies which does not contribute to the structure vibration enters. In other words, Figure 1.1 shows how seismic isolation technology shifts dominant period of the structure and in turn it decreases the earthquake forces. (Erdik et al, 2018)

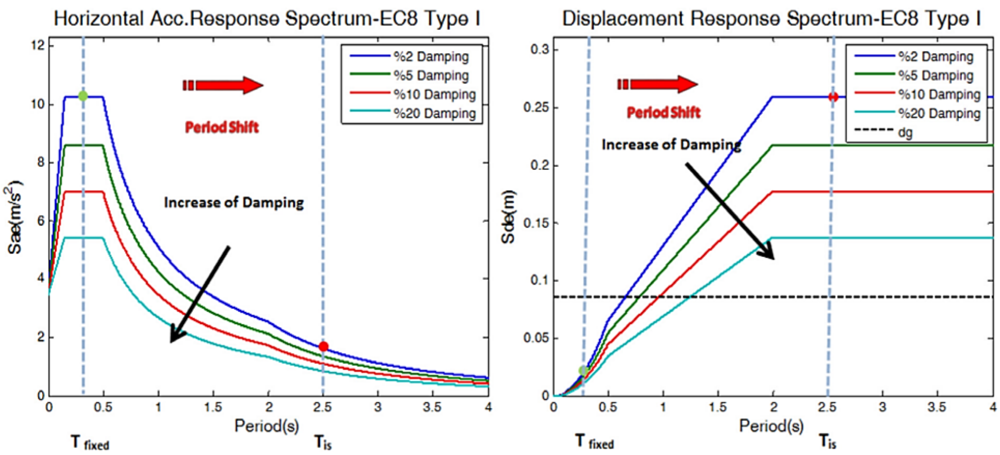

Figure 2.1: Advantage of seismic isolation through the lengthening of dominant vibration period and increment in damping to limiting extreme deformation (Erdik et al, 2018).

2.1 Seismic Isolation Background

Carpani (2017) and Makris (2018) in their study discuss base isolation from a historical perspective. David Stevenson (1868), a Scottish engineer, invented the first aseismic joint (a rolling-bearing device), which aimed to protect the toppling of lamp table carrying lighting apparatus. Figure 2.2 is taken from Stevenson (1868).

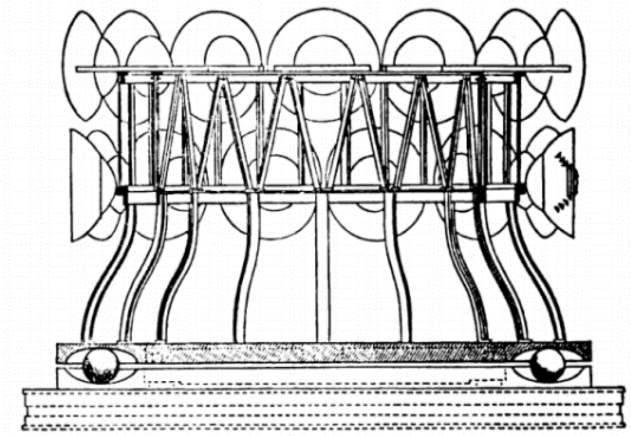

Figure 2.2 : Section of the lamp table provided with aseismic joint. Stevenson (1868).

Jhon milne (1884), for an experiment purpose in Japan built a wooden structure, laid on four cast-iron balls. During this session, Milne changed the dimension of iron balls by adding round grains to create rolling friction. As a result, Milne found out building being stable in wind loads such that the floor acceleration decreased six times than on the ground outside. John Milne's work is studied by Carpani (2017).

2.1.1 Earthquake Protective Systems

Structure protecting systems are classified into active, passive, and hybrid systems. Buckle (2000) in his study, elaborates about the earthquake shielding systems and explains the importance of seismic isolation. In this study, epecially base isolation or passive protection systems are invistigated and it also includes many other notable researches, which are conducted for passive protection in different countries.

Figure 2.3 is the categorized chart type of earthquake securing systems. It is devided into three main categories. Active protective systems include input devices and actuators in a structure integrated in the field of real-time recording devices. Passive protective systems are the most used (base isolation). Hybrid is the combination of active and passive protective system.

Warn, Ryan(2012) in their study, breifly introduce the two basic types of seismic isolation technology simply as bearings which is composed of elastomeric and sliding bearings. Elastomeric bearings are lead-rubber bearings, low and high damping natural or synthetic rubbers. Sliding bearings are single, double and triple friction pendulum. Technical specification of both types of bearings are detailed in the research and several other conducted studies are also mentioned.

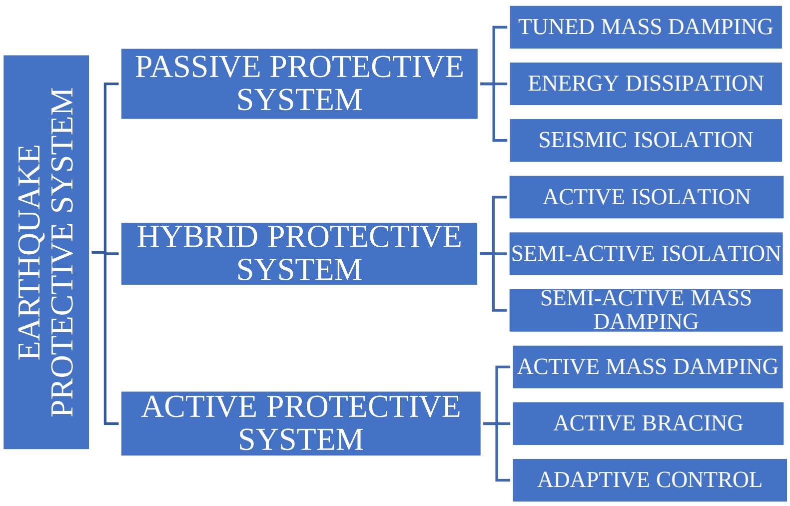

Figure 2.3 : Family of earthquake protective system. Buckle (2000)

2.2 Technical and Economical Comparison of Fixed-base and Seismic Isolated Buildings

Earthquake is a natural fact, it cannot be undermined and neglected. The neglegence results in both types of losses i.e human life's as well as economy. As per studies the technical comparison of conventioal and seismic isolated buildings are studied in various researches. Figure 2.4 illustrates the fundamental behaviour demonstration of isolated and non-isolated buildings.

Kishor (2010) , Kishor et al (2011), Kabeer and kumar (2014) studied the response of conventional and base isolated buildings with analytical and experimental analysis. A better performance of base isolation is observed when compared to fixed base building. Base isolation can offer servicable conditions post-earthquake and 20% decrement of reinforcement is achieved. Figure 2.4 clearly illustrates the fundamental response differences of fixed base and seismic isolated buildings.

Martin Lashgari (2014), in his Phd thesis studied the comparative cost-benefit analysis of fixed base and isolated buildings. It included six model buildings, five conventional and one base isolated building. Performance assement methodology introduced by PEER and ATC (Applied Technology Council) is used in his study which helps to evaluate probable risk included like casualities, duration, repair and maintenace cost. Beside the intial cost of base isolation, it performs better than fixed base building and isolated building can be functional post-earthquake.

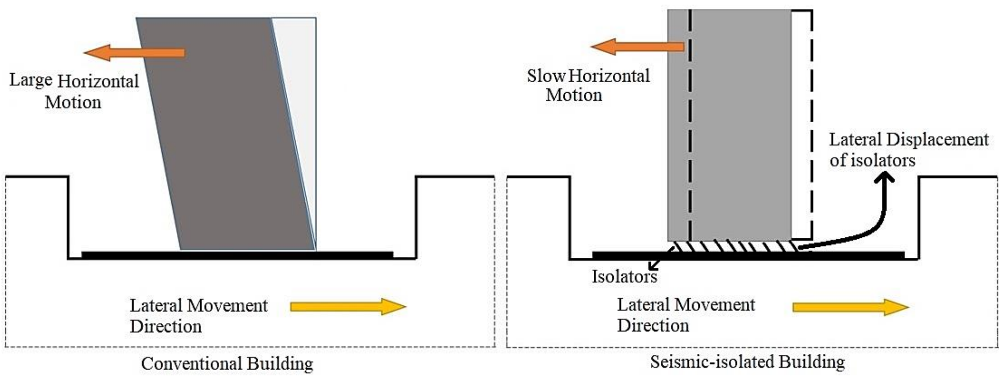

Figure 2.4:Comparison of Convetional (fixed base) and seismic base isolation.(S.N. Fathima (2016))

2.3 Vibration Sensitve Equipment and Isolation

Konstantinidis, Nikfar (2014) in their study, shed light on importance of contents and the list mentioned per FEMA and CSA of non-strucutral components and contents. In the study, related economic effect is also compiled. Non-structural elements which are the important assets of a company, hospital, labortory, defense and etc are detailed. In small, moderate, or large scale earthquakes, buildings as well as contents are important to be protected to save time and money. Since last two decades, severel research studies have been carried out to protect the structure. “Immidiate occupancy” and “operational performace level” are recommended for design level earthquakes. However, very few attention is paid to the protection of the non-structural components which relates to the overall performance of the building design. In some cases, the content of building may be 60%-80% more expensive than the structure itsself.

Alhan and Sahin (2011) in their study, suggest that base isolation system can be a good option for the protection of vibration sensitive contents and buildings but emphasizing on the importance of undertanding the behaviour of the isolation sytem due to very limited allowance value for floor accelerations to maintain the functioning of devices. In the study base-isolated three different height benchmarks structures -three, six and ten story- possessing different properties are analyzed under bi-directional time history analysis. In the study, flexible super-structure of seismic isolated building is found out to have larger floor accelerations than stiff super-structure. And increase in the flexibility of upperstructure is directly proportional to the increase of max floor acceleration. The seismically isolated rigid super-structure possesed same peak floor acceleration or small amount increment towards top floor but in flexible super-structure drastically decreased toward middle floors while greatly increased towards top floor. In the study, middle floors are suggested for protecting VSD due to minimum acceleration, then down floors and at last top floors.

Non-structural elements also include plumbing, electric, mechanic, HVAC, VSD equipment and etc. Vibration sensitive equipment are among non-structural elements. Different codes have guidelines for the vibration exceedance limit and criteria for the sensitivity of the equipement. Such as in Table 2.1 from different research different particle velocity for building is given. According to DIN 4150, visible damage and historic and ancient buildings are 4mm/s and 2 mm/s particle velocity.

Table 2.1 Criteria of vibration to label damage in buildings

Category	Source	Particle Velocity mm/s (in/s)
Industrial Buildings	Wiss (1981)	100 (4)
Buildings of Substantial Construction	Chae	100 (4)
Residential	Nichols, *et al.*, Wiss (1981)	50 (2)
Residental, New construction	Chae	50 (2)
Residential, Poor Condition	Chae	25 (1)
Residential, Very Poor Condition	Chae	12.5 (0.5)
Buildings Visibly Damaged	DIN 4150	4 (0.16)
Historic Buildings	Swiss Standard	3 (0.12)
Historic and Ancient Buildings	DIN 4150	2 (0.08)

Maximum admissible acceleration levels of certain model hard drives in working and non-working situation are listed in following several researches (Gordon 1991; Inaudi and Kelly 1993; Alhan and Gavin 2005; Gavin and Zaicenco 2007; Ungar 2007; Ismail et al. 2009a). Worksafe Technologies Corporation (2010). Depending on hard drive type, proper functioning can be achieved within the bearable peak acceleration limits of 0.2g and 1.0g. According to Iemura et al (2007) In practice, as a safety of factor, acceptable acceleration can be lowered up to some merit.

2.4 Earthquake Records

Earthquake generates ground excitation which can be recorded by seismograph instrument. The recorded data are the real event motions having several components. Real earthquake records are stored in different databases by different sources for example PEER, USGS etc.

Different analysis methods are used for seismic performance check of structures under earthquake loads. However, among all analysis methods time history analysis gives the real response of structure in real event ground motion. Time history analysis method can be applied on structures using historic or synthetically generated earthquake records, which are explained briefly in the following subsections.

2.4.1 Historic Earthquake records

Historic Earthquake records are the real earthquake motion records which are collected by seismograph instrument. They can be either far-fault or near-fault earthquake records. Atmaca et al (2018) in a study briefly explain the fundamental method, basis of selection, and scaling of earthquake records and also compare the structural responses to real and scaled earthquakes. Near-fault earthquakes are available in a limited number and the related problem is explained in subsection.

2.4.2 Near-fault Earthquake Problem

Near-fault or near-field means closer to the fault. Definition for near-fault is disputed among scholars. Mohraz (1994), in context of fault distance, classifies earthquakes into three as near, mid and far field earthquakes. According to his study, below 20 km is near-field, 20 km-50 km is mid-field and above 50 km is far-field. But per UBC-97 Code, near-fault is ranging from 0 km-15 km from the earthquake epicenter and above15 km are known as far-fault earthquakes.

In near-field earthquakes, several factors define the problem of its nature. S. Grimaz,P. maliSan(2014) and Mohammadia, Nouri(2017) in their study disclose the main problem in near-field earthquake arising from the fault types such as strike-slip, dip-slip, magnitude and rupture principle. Structures located in near-fault regions are exposed to several types of challenges by earthquake mainly focusing on the breakage mechanism (fault types, focal depth) and its features. In the study different terminology is explained such as vertical seismic component, hanging-wall, fling-step, directivity, velocity pulse and rotational seismic components. The earthquake of different magnitude as intensity can pose different threats to structures. Structure is subjected to horizontal motion containing large period with high amplitude or pulses and opens a door to vertical ground motion. In some cases, studies concluded that the rotational effects of ground motions are also effective in near-field earthquakes.

Near-field earthquake effects in a study conducted by Hall and Ryan (2000) on six story base-isolated building using computer model in compliance with UBC97 shows that near-field earthquakes can lead structure into nonlinear response if the building is put under assumed Mw = 7.0 earthquake or severe shaking of Northridge 1994 earthquake. In another study, Makris(2000) in his observation found out, isolated structural system with high friction forces in near-fault can go permanent displacement. After his thorough examination of numbers of dissipation systems in near-fault ground motion, he suggested usage of equivalent linear damping along with low friction dissipiation with viscous dampers in near-fault regions. Likewise, Chengjiang Lu (2012) compiled near-fault ground motion effects from various research review. In this study, the influence of near-fault ground motion on fixed base buildings, base-isolated and controlled buildings, bridges, and special buildings are mentioned.

Near-fault earthquakes have higher acceleration and less frequncy unlike far-fault earthquakes which have higher frequency. Figure 2.5 illustrates the difference for near-field and far-field earthquakes having longer periods, large velocity pulses. Near-field possess fling effect and ground directiviy effect. Daei, poursha(2016) and Davas (2018) in different research review, explain the near-fault earthquakes related different terms such as forward directivity, backward directivity and normal directivity and the near-fault characteristics.

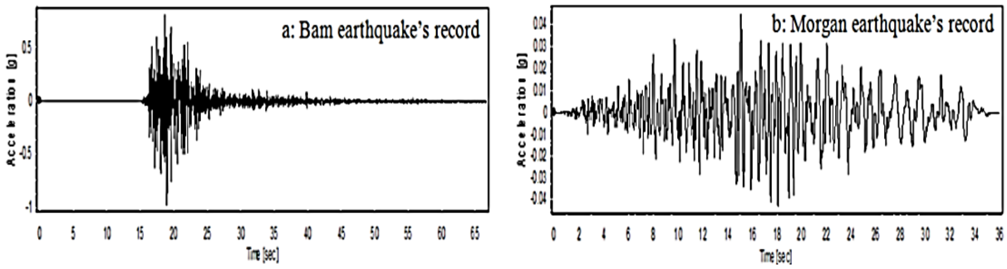

Figure 2.5: comparison of (a) Near-fault and (b) far-fault earthquakes (Najafi, Tehranizadeh, 2013)

2.4.3 Synthetic Earthquake

Synthetic or generated earthquakes are the alternative for simulating near-field earthquakes, adopted for systematically analyzing the structures under time history analysis. Öncü-Davas (2018), in her dissertation study mentions the near-fault earthquake problems like insufficiency of parametric historical earthquake data in the past and studies of last two decades to systematically understand near-fault earthquake of different ranges and the methodology adopted to simulate the near fualt earthquakes. Likewise, (Makris and Chang, 2000; Menun and Fu, 2002; Agrawal and He, 2002; He, 2003; He and Agrawal, 2008) used analytic pulse models to simulate the near-fault earthquakes. Different methodologies or different recommended pulse models for near-fault earthquakes are detailed in Öncü-Davas (2011).

Of the mentioned above, Agrawal and He model equations are given below. He and Agarwal (2008) time dependent function of velocity and acceleration is given in Eq. (2.1) and Eq. (2.2).

$$v(t) = Ct^{n}e^{-\beta t}\sin(\omega_p t + \varphi) \qquad t \geq t_0 \qquad (2.1)$$

$$a(t) = Ct^{n}e^{-\beta t}\left[\left(\frac{n}{t} - \eta\right)\sin(\omega_p t + \varphi) + \omega_p \cos(\omega_p t + \varphi)\right] \qquad t \geq t_0 \qquad (2.2)$$

The derivative of velocity time dependent function (Eq 2.1) gives the acceleration function (Eq 2.2). In Eq. (2.1) and Eq. (2.2), C is the amplitude scale factor, φ being the phase angle of the sinusoidal component, η is the damping factor, n is the parameter controlling the sharpness of the pulse envelope curve, t_0 is the start time of the pulse, ωp=2π/Tp is the pulse frequency, and Tp is the pulse period. By using He and Agarwal(2008) pulse model, the real earthquake can be characterized, if the aforementioned parameters are properly determined. Öncü-Davas (2018) briefly explains the variable characterization and nonlinear least squares method. Moreover, the model is seen to simulate the dominant kinematic properties of the near-fault motion better than other pulse models.

Agarwal and He (2002) pulse model is suitable for parametric studies of near-fault earthquakes, when n, parameter controlling the sharpness of the pulse envelope curve in He and Agarwal(2008) is neglected by equating (n=0). (Dicleli and Buddaram, 2007; V. Amiri et al, (2008); Alhan and Sürmeli, 2015; and Davas, 2018) in their study, point out the effective simulation of near-fault earthquake by using Agrawal and He (2002) pulse model in parametric analysis of their structures under time history analysis. Eq. (2.3) to Eq.(2.7) are the pulse model veloctiy ($\dot{u}(t)$) and acceleration ($\ddot{u}(t)$) equations, respectively, presented by Agarwal and He (2002).

$$\dot{u}(t) = se^{-\zeta_p\omega_p t}\sin\,\omega_p\sqrt{(1-\zeta_p^2)}t \qquad (2.3)$$

$$\ddot{u}(t) = se^{-\zeta_p\omega_p t}\left[-\zeta_p\omega_p \sin\omega_p\sqrt{(1-\zeta_p^2)}t + \omega_p\sqrt{(1-\zeta_p^2)}\cos\,\omega_p\sqrt{(1-\zeta_p^2)}t\right] \qquad (2.4)$$

(Dicleli and Buddaram, 2007; Alhan and Sürmeli, 2015; and Davas, 2018) used this pulse model in their studies where the variables are described as: ζ_p is the decaying or damping factor, ω_p is the sinusoid frequency, t is the time in unit of seconds, s is the initial amplitude of the velocity pulse. Simulation of near-fault ground motion with peak velocity, v_p, T_p as a pulse period and ζ_p damping factor, s and ω_p are the model parameters to be chosen to meet the v_p and $T_p$values. At first, ω_p is computed using the Eq.(2.5). Then Eq.(2.5) is substituted in Eq.(2.3).

$$\omega_p = \frac{2\pi}{\left(T_p\sqrt{(1-\zeta_p^2)}\right)} \tag{2.5}$$

Eq.(2.4) is settled to zero for finding t. then t_p is calculated using Eq.(2.6). here t_p is the time of peak ground velocity.

$$t_\mathrm{p} = \frac{\tan^{-1}\left(\frac{1}{\zeta_\mathrm{p}^2}-1\right)}{\left(\omega_\mathrm{p}\sqrt{(1-\zeta_\mathrm{p}^2)}\right)} \tag{2.6}$$

Now s, the initial amplitude of the velocity pulse, is calculated by substituting t_p in Eq.(2.3) and equating it to peak ground velocity V_p.

$$s = \frac{v_p}{\left(e^{-\zeta_p\omega_p t_p}\sin\,\omega_p\sqrt{(1-\zeta_p^2)t_p}\right)} \tag{2.7}$$

According to Dicleli and Buddaram (2007), maximum pulse velocity and pulse period values used in Agrawal and He(2002) pulse model can be obtained through the Eq.(2.8) and Eq.(2.9). For generation of velocity pulse and acceleration pulse, value determination of maximum pulse velocity vp and pulse period tp is essential. Somerville (1998) proposed the relationship between these parameters. The simulation of the peak ground motion begins with moment magnitude Mw and r (km) the distance from the fault relationships given in Eq.(2.8) and the relationship of pulse period with moment magnitude is given in Eq.(2.9).

$$\ln(v_p) = -2.31 + 1.15M_w - 0.5\ln(r) \tag{2.8}$$

$$\log_{10}(T_p) = -2.5 + 0.425M_w \tag{2.9}$$

2.5 Rubber Base Isolation

In Section 2.1.1, the research study of Warn, Ryan(2012) is briefly explained. Bearings are of two types, elastomeric and sliding bearings given in Figure 2.7. Elastomeric bearings can form linear and as well as nonlinear isolation systems depending on their mechanical behavior. Low damping rubber bearing (LDRB) is the example of linear isolation system. Due its low damping ratio, it is used along with linear viscous dampers Constantinou et al(2007) and Alhan, Sürmeli (2011). Nonlinear isolation system consists of high damping rubber bearings (HDRBs) and lead rubber bearings (LRBs). Both systems demonstrate hysteretic energy dissipation. Figure 3.3 illustrates the sub type of two main bearings.

In this thesis, nonlinear rubber bearing isolation system is used as seismic isolation. Figure 2.8 is the hysteretic energy dissipation mechanism of the system. William Henry Robinson, is a New Zealand scientist and seismic engineer who invented the lead rubber bearing (LRB) seismic isolation device. Figure 2.9 is an example of elastomeric bearing i.e. lead rubber bearing. It is formed of two different functioning material. First, natural or synthetic rubber which contributes in lateral ductility and secondly, steel shims in between rubbers acts as reinforcing steel such that it helps in vertical load resistance of structure and also restrains from bulging reaction under compression force of structure. The rubber cover provides protection from environmental effects to steel layers (Buckle et al, 2006). Furthermore, in the same study material, design, and design related issues and analysis manual for elastomeric isolator and sliding isolator are given.

Bilinear isolator mechanical behavior shown in Figure 2.8 has F_Q as characteristic force, F_y as yield force, D_y as yield displacement, K_1 as pre-yield stiffness, K_2 as post-yield stiffness, α as post to pre yield stiffness ratio and effective Stiffness (ke) or in other words secant stiffness at any displacement. T_0 is the isolation period based on post yielding stiffness, K_2 of the seismic isolation building (Nagarajaiah et al. 1991; Matsagar and Jangid 2004; Öncü and Alhan 2012). In Eq. (2.11), W is the total weight of the building, g is the gravitational acceleration.

$$T_0 = 2\pi\sqrt{\frac{W}{(gK_2)}} \tag{2.11}$$

F_Q Characteristic force, D_y yield displacement, F_y yield force and α as post to pre yield stiffness of the system is calculated using following relationship

$$F_Q = \frac{F_y(K_1 - K_2)}{K_1} \tag{2.12}$$

$$D_y = \frac{F_y}{K_1} \tag{2.13}$$

$$F_y = \frac{F_Q\, K_1}{K_1 - K_2} \tag{2.14}$$

$$\alpha = \frac{K_2}{K_1} \tag{2.15}$$

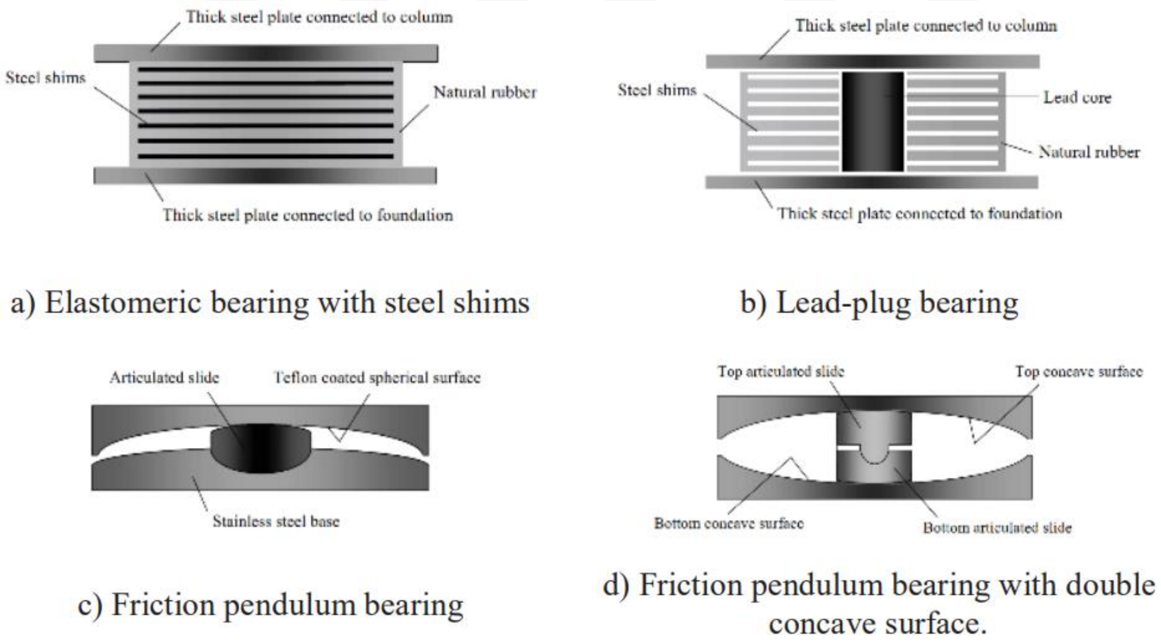

Figure 2.6: a) and b) are elastomeric, c) and d) are sliding bearings (M. Azimi, 2017)

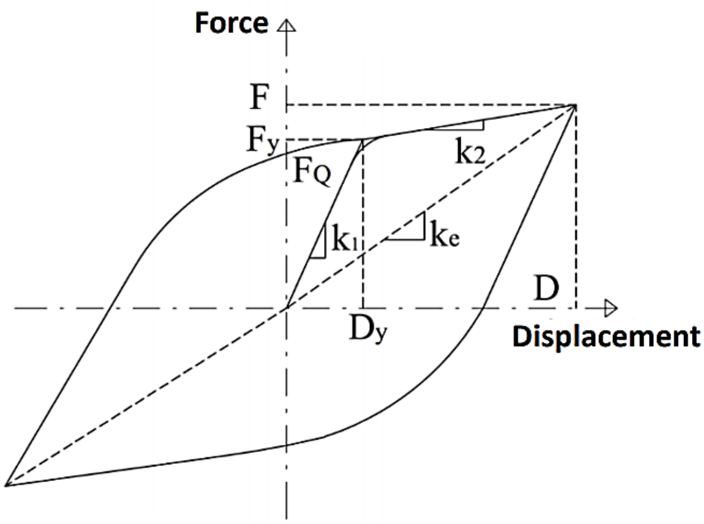

Figure 2.7: Non-linear rubber isolator Force-displacement Property

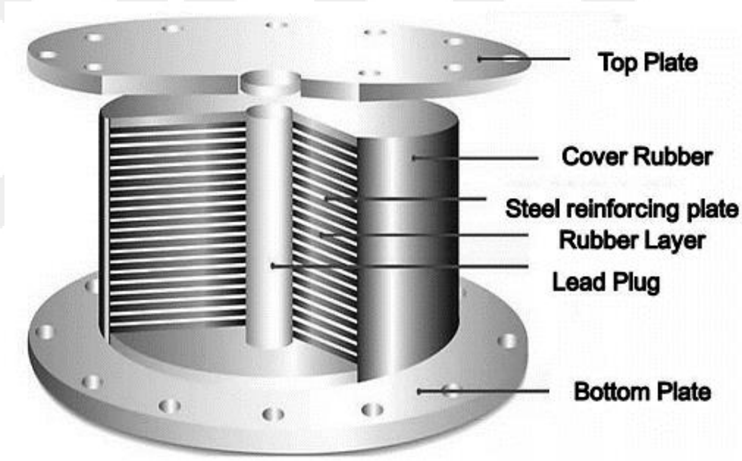

Figure 2.8: Lead rubber isolator (Z.Tafheem et al, 2015)

3 MATERIALS AND METHODS

3.1 Benchmark Base-isolated Building Model

In this thesis, investigation of the content behavior of the seismic isolated building is intended. To begin with, a building model and a rack model is assigned. The building model given by Alhan, Sürmeli (2011) is used in this study. In this subsection, the building model is presented. The building model is symmetrical in, in plan and regular vertically.

The model consists of base floor and five normal floors. Due to symmetrical plan, the mass is lumped at the center of gravity (G) which is the center of stiffness also. Figure 3.1 is the plan view of the building model, having 4 spans in x and as well as in y direction with 5 m distance. Seismic isolation system is situated under the base floor of the model.

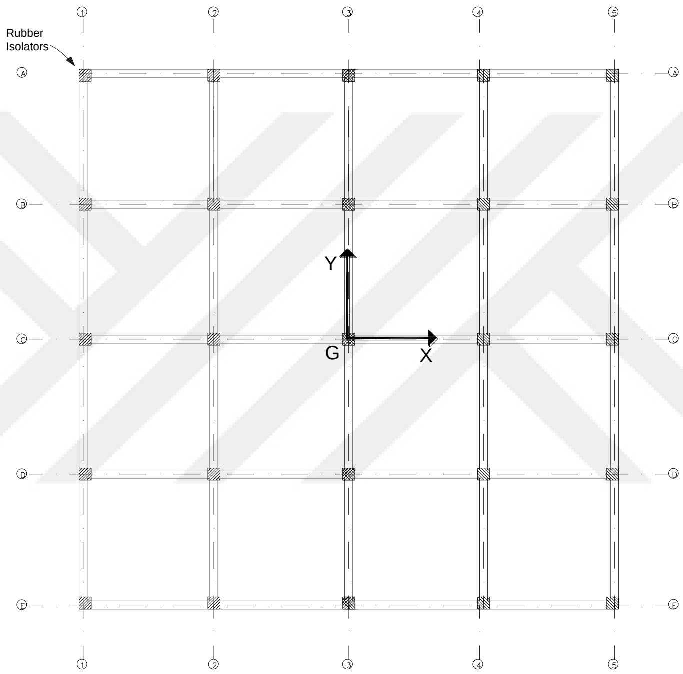

Figure 3.1: Plan view of the model

Plan of the base floor and normal floors are identical. Height of each floor is 3m. In Table 3.1 , the dimension of the structural elements are given. Diaphragms are constructed at floor levels in the structural model.

Table 3.1: Dimensions of the structural elements

Section Property	Dimension (m)	Cross-section Area(m)	Length (m)	Self-weight factor	Moment of Inertia y-axis (m^4)	Moment of Inertia z-axis (m^4)	Torsional Inertia (m^4)
Column	0.45×0.45	0.2025	3	1	0.00342	0.00342	0.005775
Beam	0.55×0.30	0.165	5	1	0.00124	0.00416	0.003262

Mass of normal floors and base isolation floor is 320 kNs^2/m respectively. In Table 3.2 the masses of different floors are given.

Table 3.2: Mass and weight of different floors

Floors	Mass (Ton)	Weight (kN)
Base isolation floor	320	3139.2
1st Floor	320	3139.2
2nd Floor	320	3139.2
3rd Floor	320	3139.2
4th Floor	320	3139.2
5th Floor	320	3139.2

Below the base floor (sub-structure), the seismic isolation is introduced as link elements. All the isolation members bear the same property with no variation. Figure 3.2 is the cross-sectional view of the benchmark building. The normal floors are named as super-structure and seismic isolation floor as sub-structure.

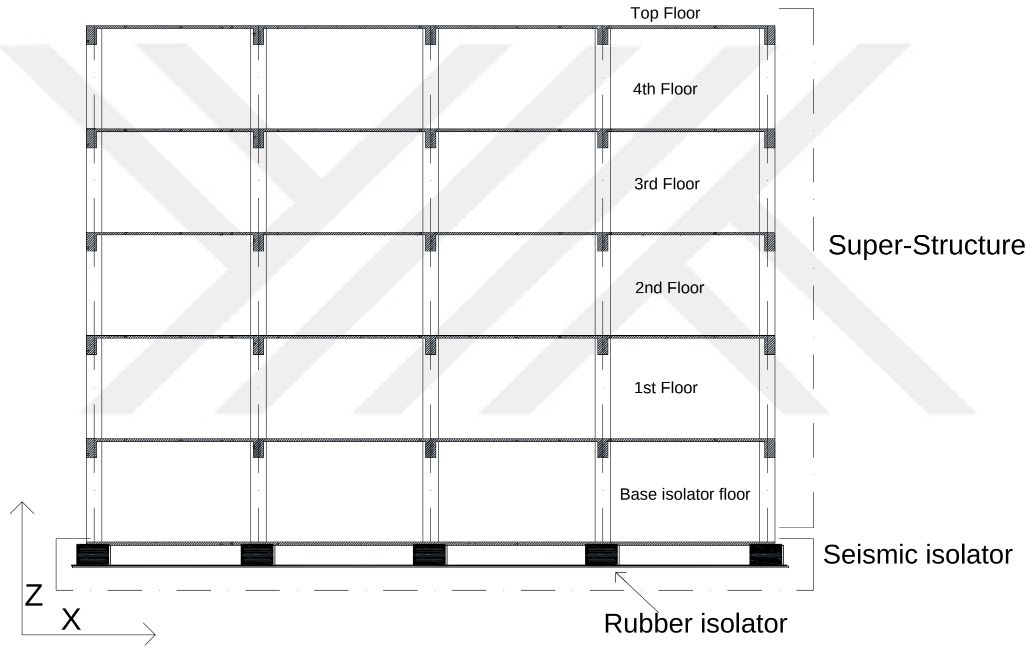

Figure 3.2: Cross-sectional view of the benchmark building

The model building characteristic is described in material section. In this section modeling detail and link element properties of the building using Sap2000 analysis program will be explained.

Computer and Structures incorporated (CSI) is a company that operates in the area of structural analysis and earthquake engineering and has produced Sap2000. Sap2000 is a structural analysis program widely used by engineers around the world. Dynamic or static, linear or non-linear analysis of structural systems can be performed by SAP2000 finite element program. Various codes like AISC building code, ACI and AASHTO standards can be used to meet the requirements of designing structures. It is easy to use with a graphical interface. So Initially, the building is modeled in Sap2000. First, the material property is introduced, which is composed of concrete compressive strength (σ_c) of 30Mpa as C30. The columns and beams are defined as frame elements. In Figure 3.3, 3d view of the subject building is shown and is modeled according to the plan. It includes sub-structure (base floor) and super-structure (Normal Floors).

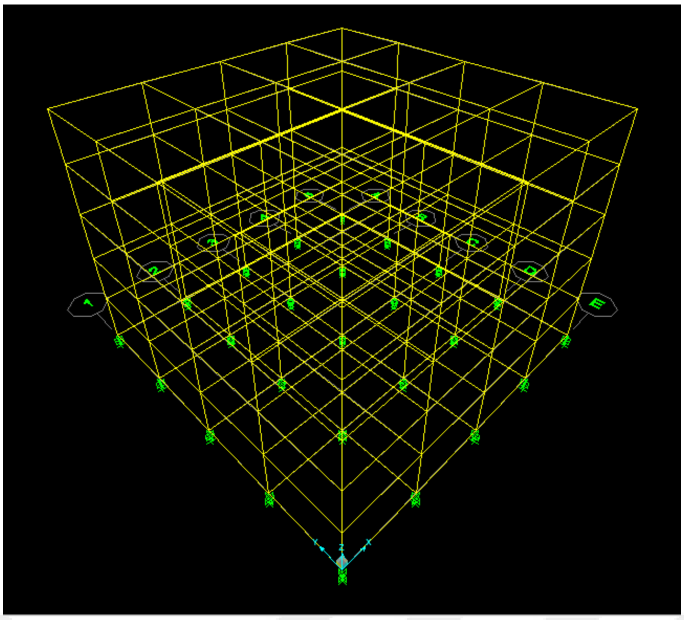

Figure 3.3: 3d view of the structural model

In this study, Non-linear rubber base isolator is used as seismic isolation elements. Elastomeric bearings are detailed in the study of Alhan, Sürmeli (2011) and Warn, Ryan(2012). In both studies, assumption, formulation and mechanical behavior of the elastomeric isolators are explained. Figure 3.4 is the cross-sectional view of the subject building and isolators are indicated by arrows. In analysis program, the seismic isolation system is introduced as link elements in the substructure. Figure 3.5 shows the option for defining section properties as link element.

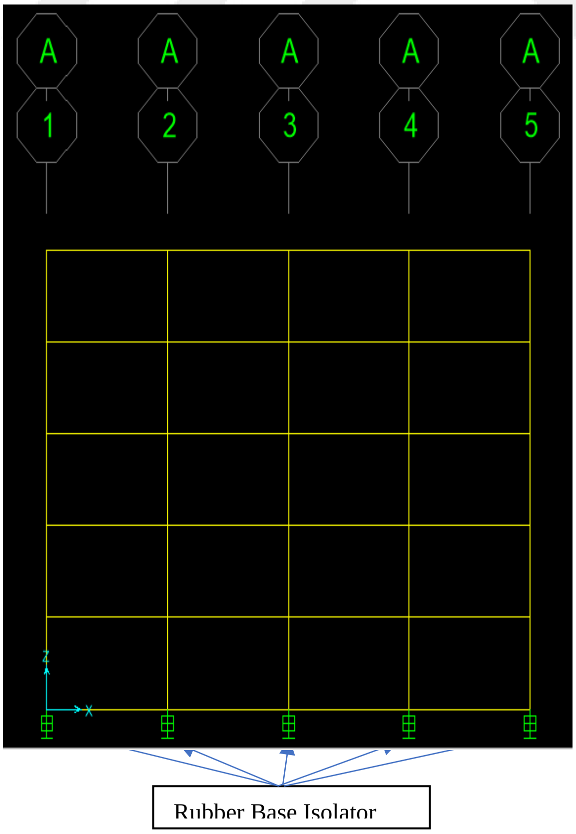

Figure 3.4: Cross-sectional view of the Benchmark building

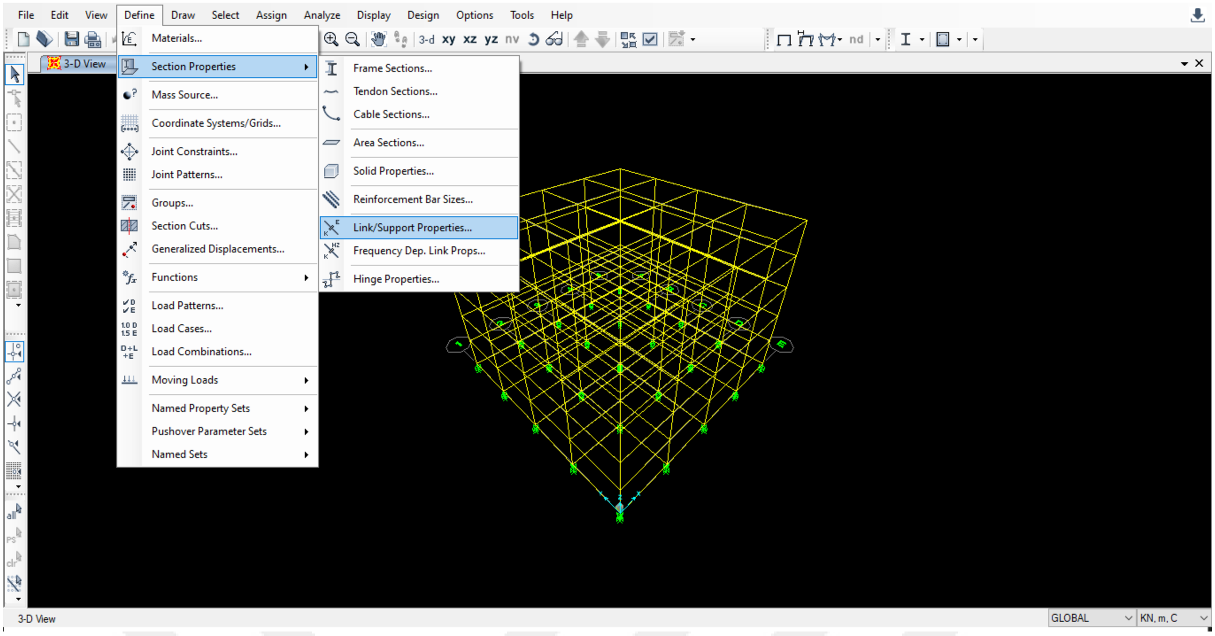

Figure 3.5: Seismic isolation option menu given in Sap2000 analysis program

Before introducing rubber base isolation into the building, mechanical properties of the seismic isolation system are defined by the parameters given in Figure 2.8 such as T_0, the isolation period based on K_{2sys} obtained using Eq. (2.11), Q/W is the nominal characteristic force ratio taken 10% to 20% in high seismicity regions, pre-yield stiffness as K_{1sys}, the post to pre yield stiffness ratio α given in Eq.(2.15). Target values are given in Table 3.3 and corresponding values are given in Table 3.4. The model has 6 floors including base floor. In plan n=25 rubber base isolators exist and stiffness values per isolator can be obtained by dividing to 25. Rubber isolator bears 20 mm of yield displacement (D_y). Weight of the building, W, is also given in Table 3.4. Additionally, the super-structure damping ratio is taken as 0.02.

Table 3.3: Initial target values for the isolation

T_0	Q/W	α
3.5 s	10 %	0.062

Table 3.4: Property of the non-isolation system

	Nonlinear isolation systems parameters							
Number of floors	n	$K_{1\ Sys}$ (kN/m)	$K_{2\ Sys}$ (kN/m)	D_y (mm)	$F_{y\ Sys}$ (kN)	$\alpha = K_2/K_1$	W=n*M*g, (kN)	$F_{y\ Sys}/W$ (%)
6	25	100363.75	6222.5	20	2007.25	0.062	18835.2	0.1066

Figure 3.6 shows how to assign the properties of link elements in link/support properties section. Each command boxes of data entry are labeled with red color as 1,2,3. in sequence. In the given box the link/support type is chosen as nonlinear rubber isolator. The introduced properties of elements from Table 3.4 is given in Figure 3.6.

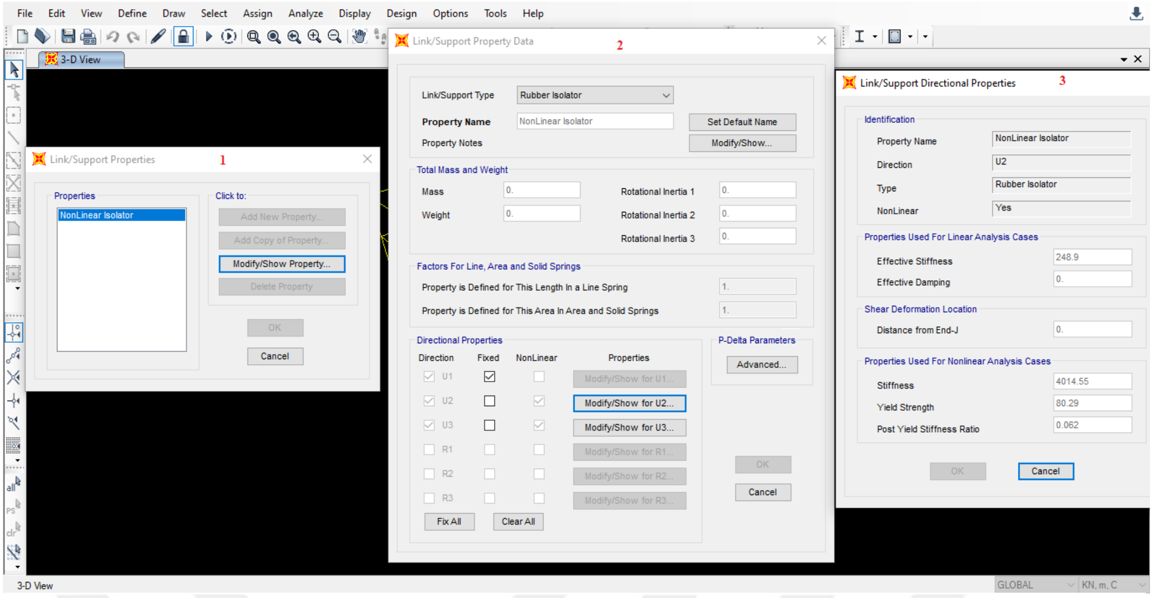

Figure 3.6: Link support properties

3.2 Rack Model

In this subsection, the rack model is presented. Rack is a useful tool to keep and organize small spaces that require a lot of technology packed into them. Most of the contents such as different hardware, goods, industrial machines and sensitive devices used in different fields are are kept in racks.

In order to investigate the acceleration levels sustained at the rack floors, benchmark rack given in Figure 3.7 is modeled. Protecting contents, particularly vibration sensitive contents, of the seismically isolated building, such as electronic devices, computers, testing machines etc are possible if the acceleration responses in different levels of rack are kept below the serviceable values.

The objective rack model is composed of 4 floors. Dimension of the model is 1m x 1 m. The height of each floor is 0.50 m. Properties of the rack model is given in Table 3.5.

Table 3.5: Benchmark rack properties

RACK MODEL PROPERTIES					
No. of Floors	Total Height	Floor Height	Length	Width	Weight of Rack
4	2 m	0.5 m	1 m	1 m	400kg/m^2

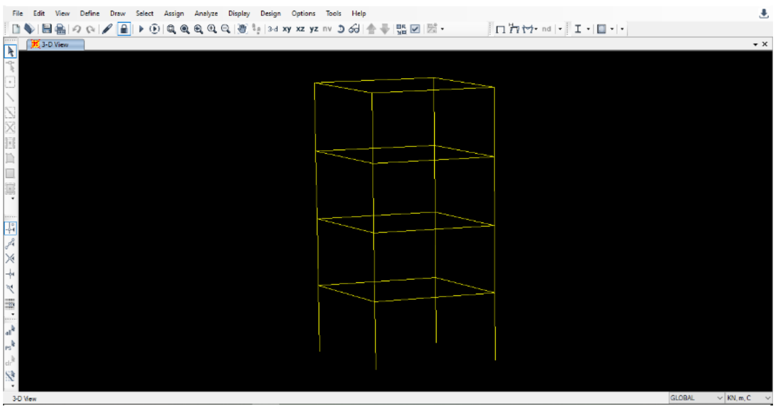

Figure 3.7: Perspective view of the rack model

The defined rack model is placed into the seismically isolated building model. To meet the requirements of the modeling, new sub-gridline is created. The sub-gridline represents the fictive secondary beams. The fictive secondary beams are hinged on the sides where it is connected to the main beams as shown in the plan veiw given in Figure 3.8. In Figure 3.8, orange arrows are pointing to main beams in plan, red color arrows are showing fictive beams named in Figure as secondary beams and blue arrows are indicating the introduced hinges. The benefit of appointing secondary beams hinged to main beam is that, secondary beams will only transfter the lateral loads to the rack. The secondary beam will not transfer any moment to the main beam. As a result, our objective of achieving the rack behaviour in analysis will be satisfied. But to confirm the approach and understanding, it is necessary to compare the rack model behaviour as dependent and independent. Thus, two types of rack model are created. Material and dimensional properties of both dependent and independent rack model are the same.

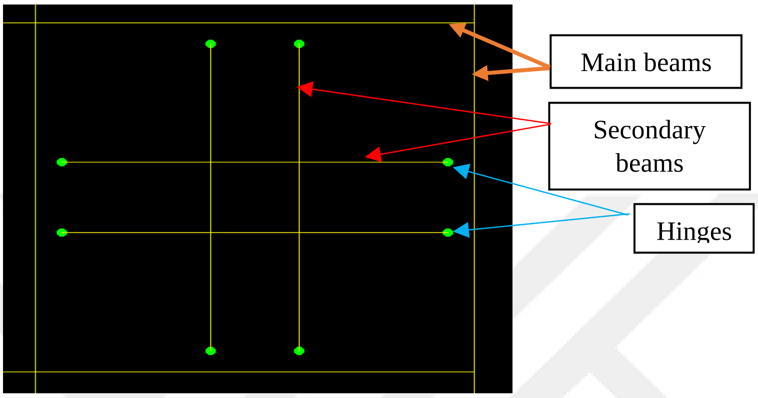

Figure 3.8: Allocated location for rack in plan view

3.2.1 Dependent Rack Model

Dependent rack model is the type of rack that is modeled together with the building. Dependent rack movement affects the building and vice versa, i.e. a coupled action is observed. For dependent rack model, the input is given as time history earthquake records to building through the ground, then the model is analyzed. In Figure 3.9 dependent rack model is shown, situated in allocated place of the floor over fictive secondary beams.

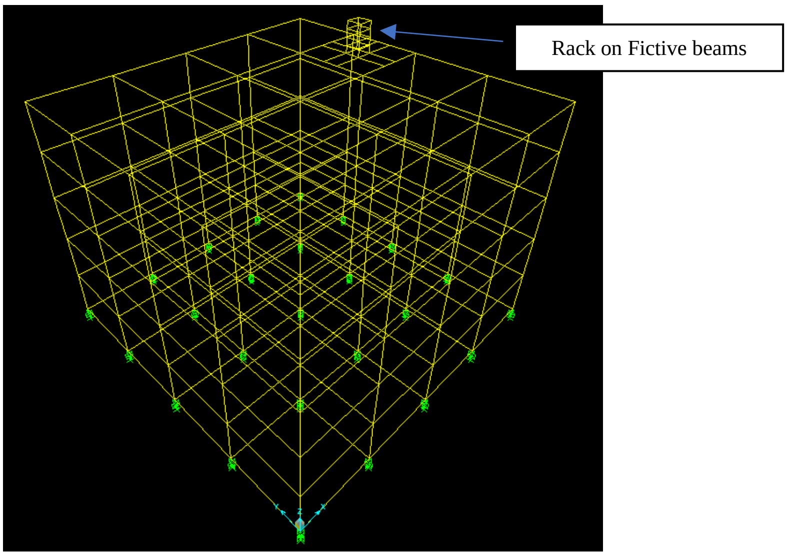

Figure 3.9: Perspective view of the building and benchmark rack

3.2.2 Independent Rack Model

Unlike the dependent rack model, which is placed on the floor of seismic isolated building, the independent rack model is the second type of rack, bearing the same property but is fixed to the ground shown in Figure 3.10. The building model without is given in Figure 3.9 and initially analyzed under time history earthquake record. The selected specific joint floor response of the building in the form of acceleration response recored is collected and saved into a txt file. Later on, the independent rack is subjected to the this building’s floor acceleration response history and examined.

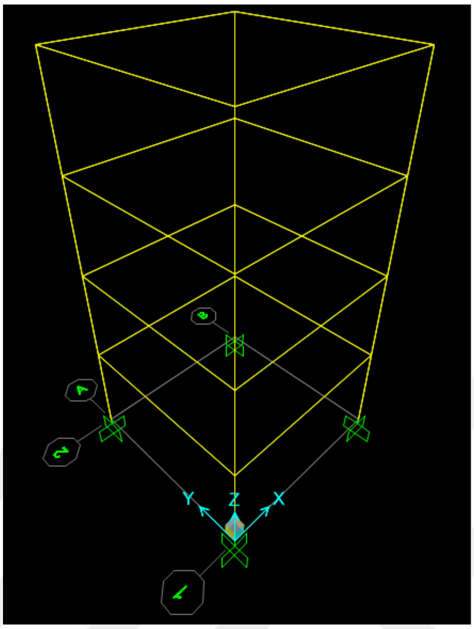

Figure 3.10: Perspective view of the Independent rack model

3.2.3 Rack Model Property

Before proceeding to the investigation of models. It is worth to mention how the rack model is selected. Selection of the rack model is based up on the fundamental mode period. Racks of natural periods with 0.2 s, 0.4 s, 0.6 s, and 0.8 s are obtained by playing with the stiffness of the structural members which were obtained by changing the modulus of elasticity as required. The advantage of keeping the natural period to a specific value is that it helps in practice and it provides easiness to systematically understand the behavioural variation of rack that is dependent upon the stiffness parameters.

3.2.4 Trial of Models

Before going onto investigation, analysis and collecting results, it is necessary to test the type of rack models. In other words to prove and compare the two dependent and independent rack model provide similar results. The building with rack (BWR) and building without rack (BWOR), rack dependent (R_d) and rack independent (R_I) model is set to trial under earthquake records. To fulfil the test, the near-fault 1994 Northridge Earthquake is selected from Table 3.8 (shown in bold character). In Figure 3.9 the subject building model and rack placed on top floor is shown.

The Earthquake record is uploaded to BWR and BWOR model through Functions as Time history given in Figure 3.11. After inputting the historical earthquake record to the models through function, the load case for models are setup as nonlinear analysis with direct-integration as solution type. In Figure 3.12 load case input values are shown.

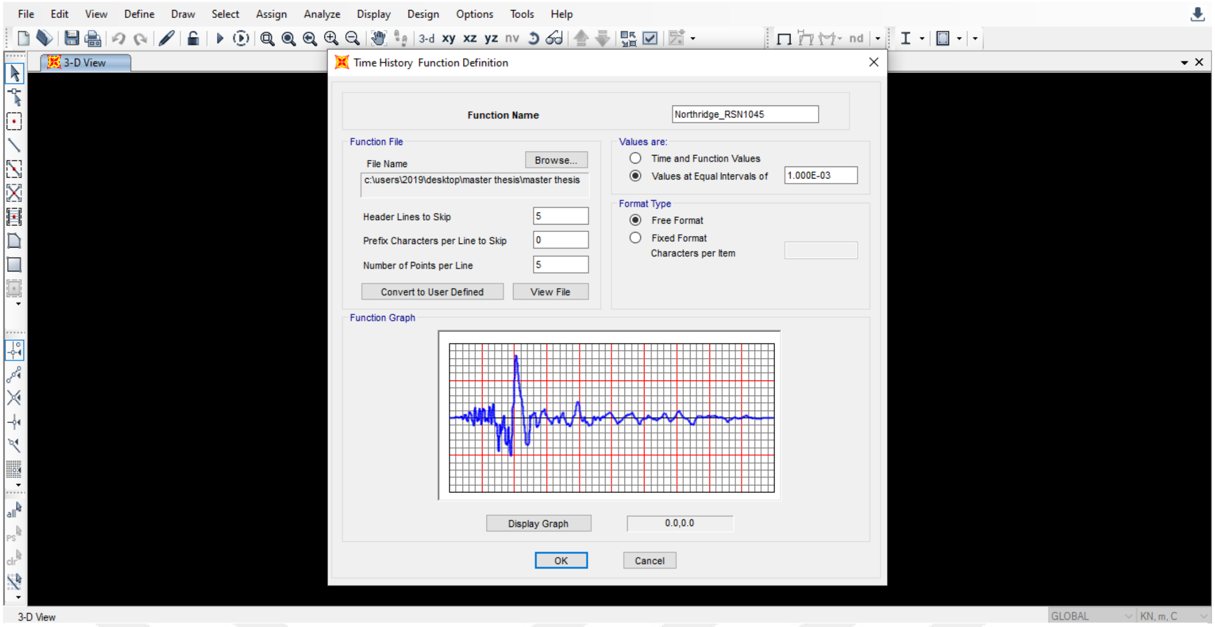

Figure 3.11: Time History Function properties

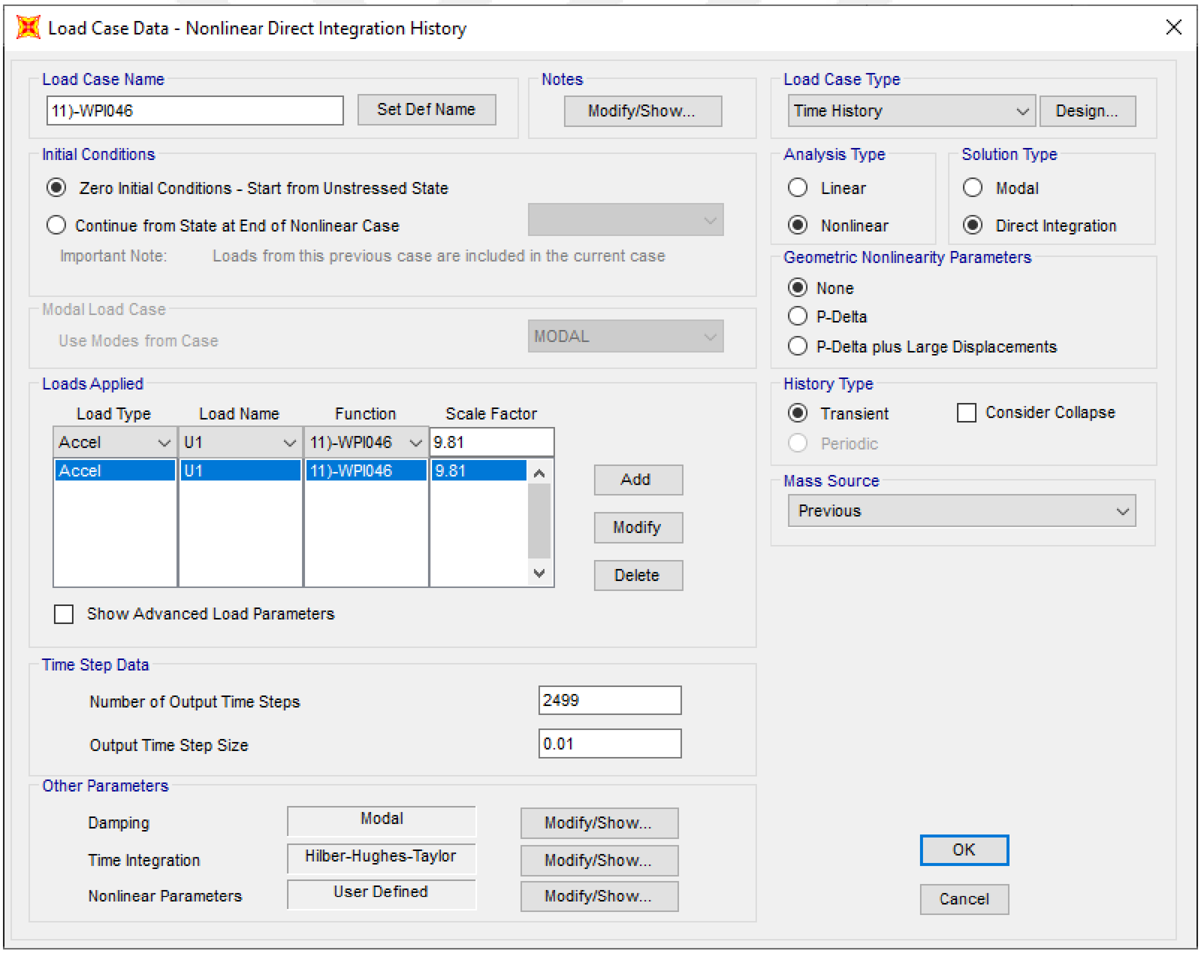

Figure 3.12: Load case data for BWR and BWOR

For the test, specific joints, for obtaining acceleration responses, are selected in the building and the rack. BWR and BWOR top floor accelertion of joint 161 given in Figure 3.13 is selected. As the building model is symmetrical, the result obtained from the specific joint is same as other joints of the floor. For rack dependent and rack independent cases, joint 18 shown in Figure 3.14 is seleceted and renamed shortly as J18.

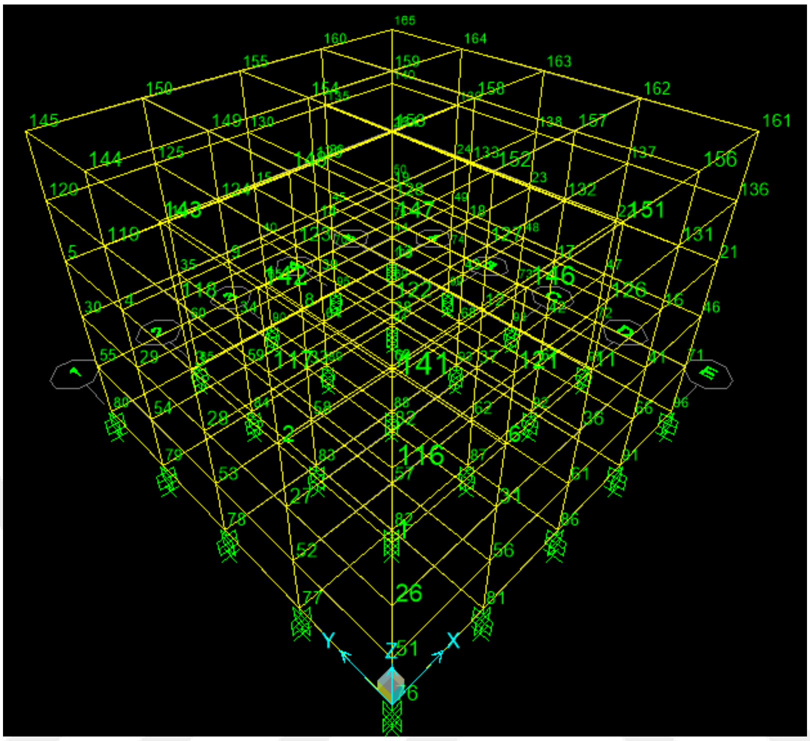

Figure 3.13: Benchmark building with joint labels

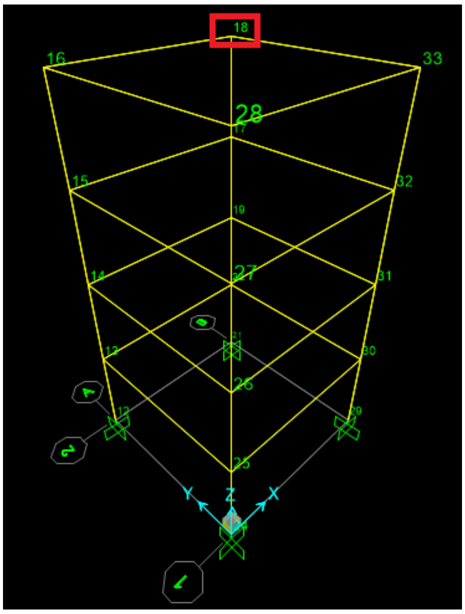

Figure 3.14: independent Rack Joint labels

First, the building with rack model (BWR) and building without rack (BWOR) is analyzed under the 1994 Northridge Earthquake record seperately and joint 161 acceleration responses for the dependent model building (BWR_TFA_J161) and the independent building model (BWOR_TFA_J161) are compared in Figure 3.15. As seen, the acceleration values match perfetctly, which shows that rack does not affect the response of the building significantly.

Secondly, joint 161 acceleration response of BWOR is collected into txt.file and used as ground motion for the independent rack analysis case. The independent rack model is subjected to this floor acceleration response and compared with dependent rack joint 18 acceleration response which is collected from the anlysis of BWR model. Joint 18 results are compared for the dependent case (R_D_TFA_J18) and independent case (R_I_TFA_J18). In Figure 3.16 shows that the results do not differ much. So, although the coupled and uncoupled analysis both give close results, it is concluded that using coupled model (dependent rack model) would be more realistic.

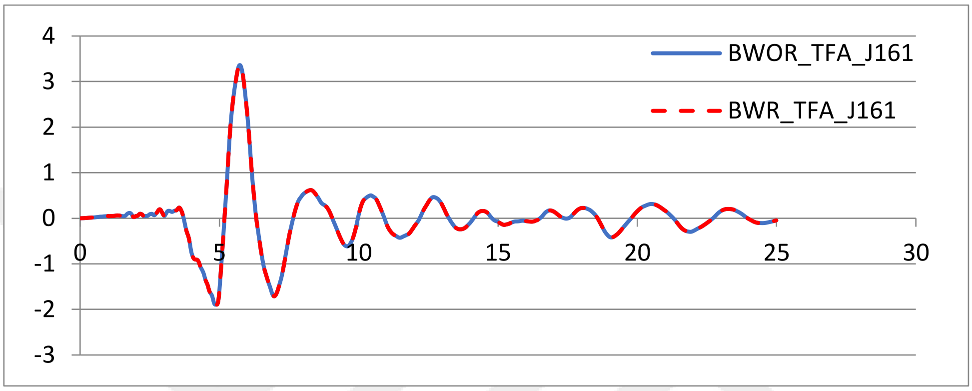

Figure 3.15: Top floor acceleration response of two Building models

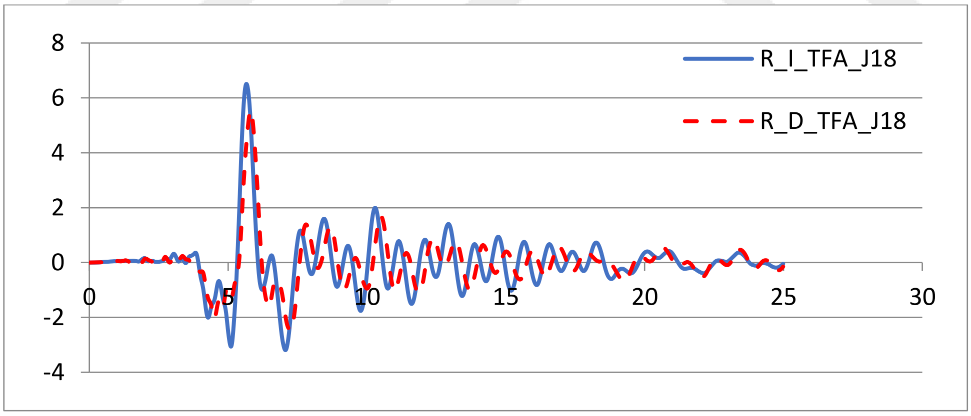

Figure 3.16: Top Floor Acceleration Response of rack types

3.3 Final Model

In Previous sections the building model and rack model protoype was intitally tested. In this section the thesis main objective will be attained using the benchmark building with racks. Previously, only one type of rack was used but now the final model building consists of four racks placed in three different floors (Figure 3.17) which will be futher explained in subsections.

In order to observe the behaviour of the building and racks under time history analysis, the building is loaded with historic and synthetic earthquakes loads presented in 3.4 section.

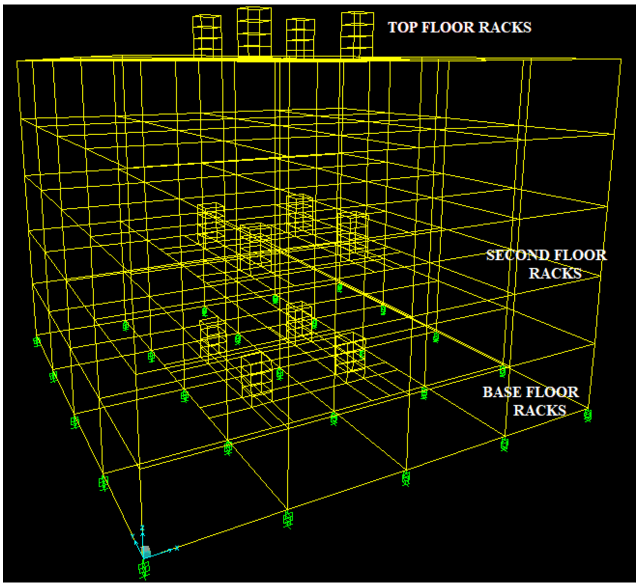

Figure 3.17: Subject Building with rack in different floors

3.3.1 Joint Selection of Building

In Figure 4.3, 3d view of the structure with different joint Ids is presented. From over all joints, the joint id given in Table 3.6 of specific floors are selected. Selection of different floors is based upon the structures different floor responses to the ground acceleration. In Table 3.6, base floor, 2nd floor and top floor of different joint id is described.

Table 3.6: Selected joints of different floors for accleration response result

Series no	Floor No	Joint ID	Renamed	Description
1	Base Floor	Joint 96	BWR_BFA_J96	Base floor Acceleration
2	2nd Floor	Joint 46	BWR_2FA_J46	2nd floor Acceleration
3	Top Floor	Joint 161	BWR_TFA_J161	Top floor Acceleration

The joint numbers given in Table 3.6 is labeled by default in Sap2000 program. The chosen Joints of different floor is framed with red lines shown In Figure 3.18.

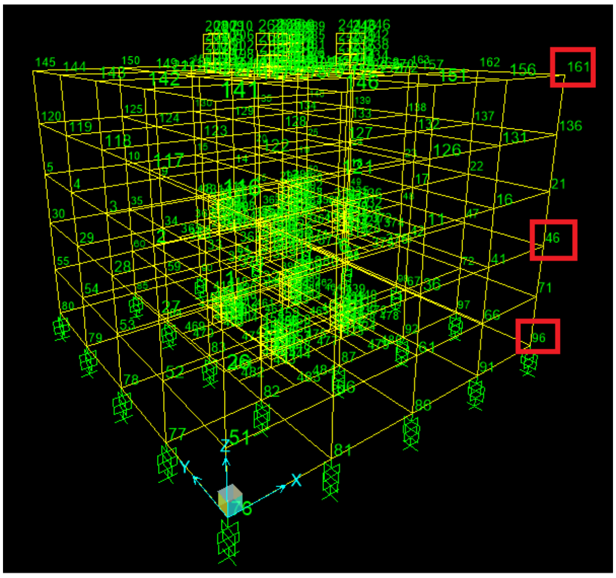

Figure 3.18: Base floor, 2nd floor and top floor Joints

3.3.2 Modeling Four Types Of Racks

For the analysis, four different racks are modeled. The differences of racks depend on their stiffness and fundamental period (0.2 s, 0.4 s, 0.6 s, 0.8 s) parameters. The modeling concept is defined in Section 3.1. The new gridline plan view, overall plan view and modeled structure preview is given in Figures 3.19, Figure 3.20 and Figure 3.17. In Figure 3.17, the 3d veiw of structure modeled along racks is shown. The 6th floor is named as top floor, the 2nd floor is named as second floor and base floor respectively.

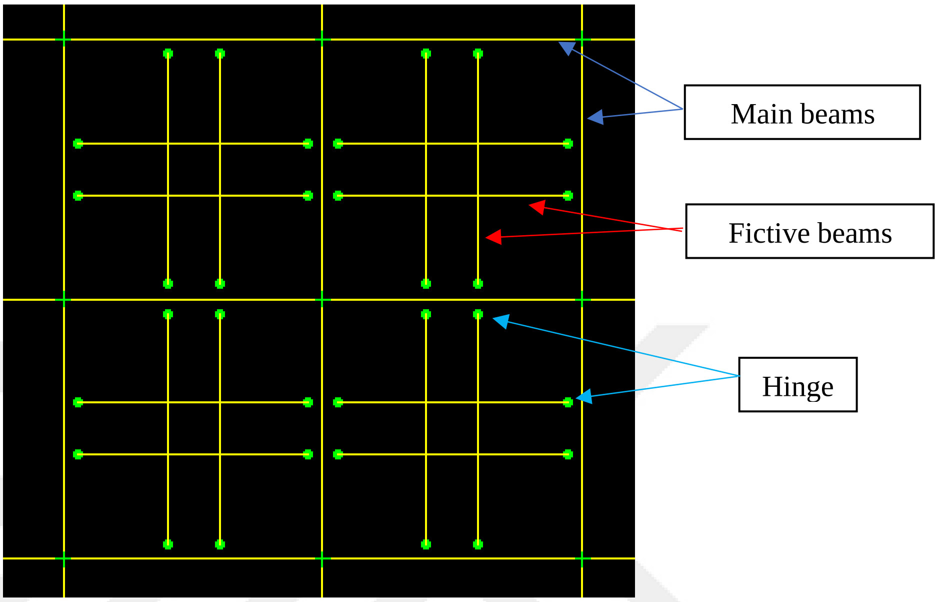

Figure 3.19: Gridline introduced for Allocation of Racks

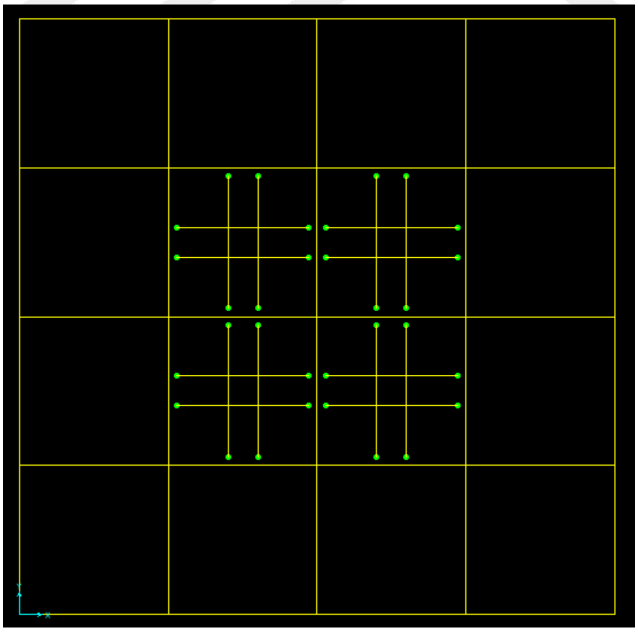

Figure 3.20: Overall plan view of the subject building

3.3.3 Joint Selection For Racks

The building with rack joints are labeled in Sap2000 by default. Building with four different rack types in different floor is previewed in Figure 3.18. In Figure 3.21, four different racks having time period of

T= 0.2 s, T= 0.4 s, T= 0.6 s and T= 0.8 s situated on Base floor with their joint label is shown. The chosen joints for acceleration response of each rack floor is highlighted in red color.

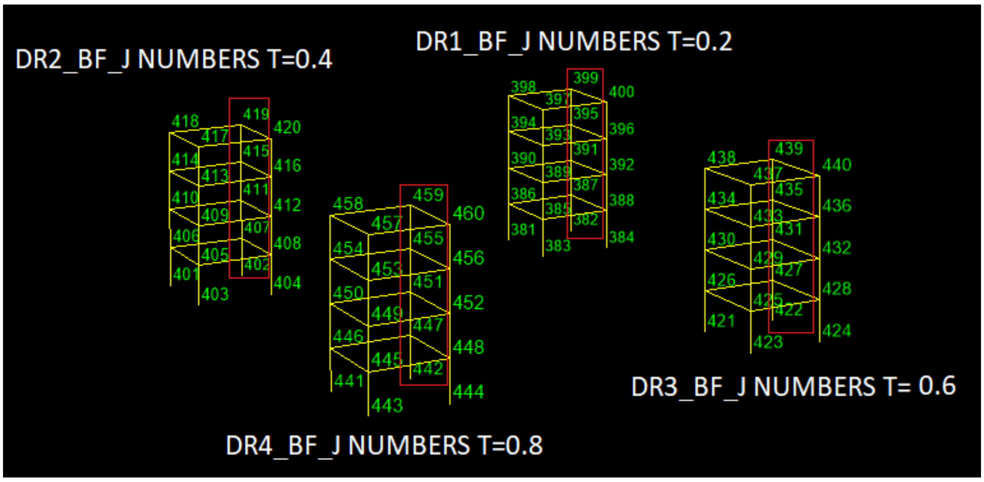

Figure 3.21: Base Floor Joint Labels

In Figure 3.22 and Figure 3.23, four different racks having time period of T= 0.2 s, T= 0.4 s, T= 0.6 s and T= 0.8 s situated on 2nd floor and top floor with their joint label are shown, respectivley. The chosen joints for acceleration response of each rack floor is highlighted in red color.

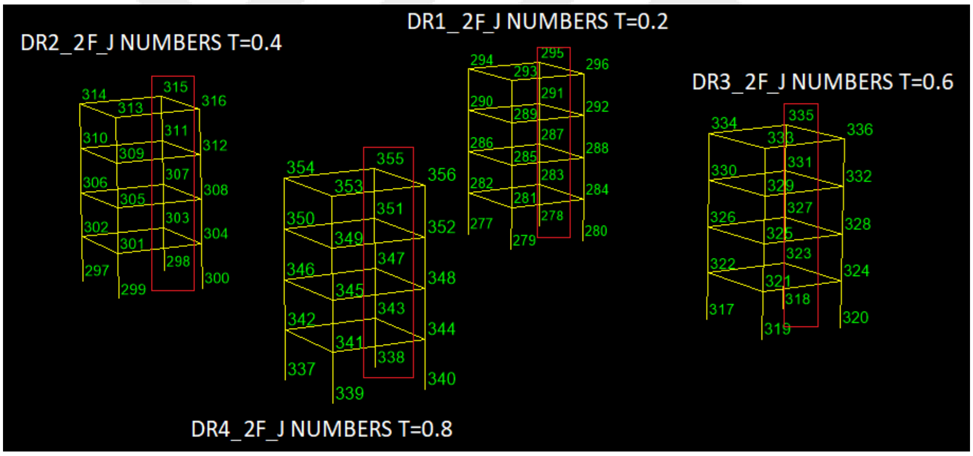

Figure 3.22: Second Floor Joint Labels

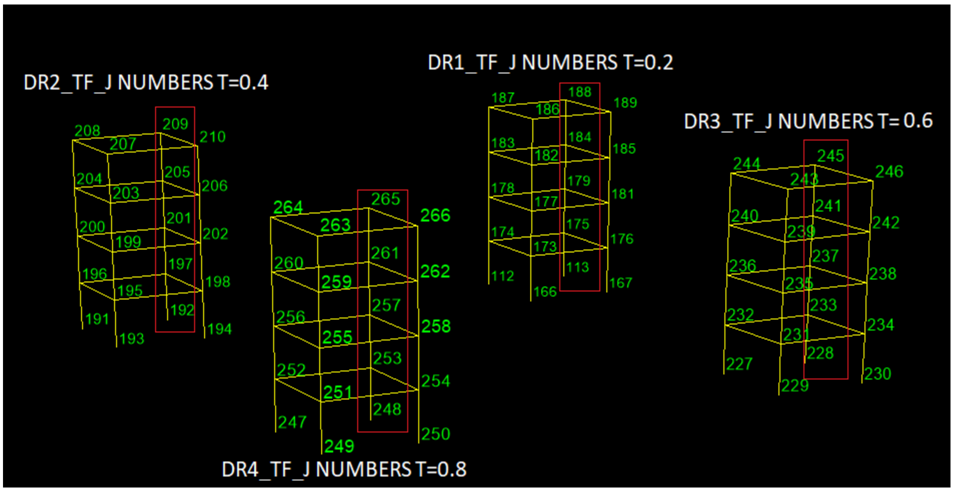

Figure 3.23: Top Floor Joint Labels

In Table 3.7, the chosen specific joint IDs of 4 different racks are listed. Highlighted joint id's are renamed with abbreviations. The abbreviations are briefly described in description column.

Table 3.7: Rack Joint Id and description

S. No	Joint ID	Renamed	Description	S. No	Joint ID	Renamed	Description
1	387	R151 Acc	Rack 1 top floor 1st floor	25	427	R351 Acc	Rack 3 top floor 1st floor
2	391	R152 Acc	Rack 1 top floor 2nd floor	26	431	R352 Acc	Rack 3 top floor 2nd floor
3	395	R153 Acc	Rack 1 top floor 3rd floor	27	435	R353 Acc	Rack 3 top floor 3rd floor
4	399	R154 Acc	Rack 1 top floor 4th floor	28	439	R354 Acc	Rack 3 top floor 4th floor
5	283	R121 Acc	Rack 1 2nd floor 1st floor	29	323	R321 Acc	Rack 3 2nd floor 1st floor
6	287	R122 Acc	Rack 1 2nd floor 2nd floor	30	327	R322 Acc	Rack 3 2nd floor 2nd floor
7	291	R123 Acc	Rack 1 2nd floor 3rd floor	31	331	R323 Acc	Rack 3 2nd floor 3rd floor
8	295	R124 Acc	Rack 1 2nd floor 4th floor	32	335	R324 Acc	Rack 3 2nd floor 4th floor
9	175	R1B1 Acc	Rack 1 base floor 1st floor	33	233	R3B1 Acc	Rack 3 base floor 1st floor
10	179	R1B2 Acc	Rack 1 base floor 2nd floor	34	237	R3B2 Acc	Rack 3 base floor 2nd floor
11	184	R1B3 Acc	Rack 1 base floor 3rd floor	35	241	R3B3 Acc	Rack 3 base floor 3rd floor
12	188	R1B4 Acc	Rack 1 base floor 4th floor	36	245	R3B4 Acc	Rack 3 base floor 4th floor
13	407	R251 Acc	Rack 2 top floor 1st floor	37	447	R451 Acc	Rack 4 top floor 1st floor
14	411	R252 Acc	Rack 2 top floor 2nd floor	38	451	R452 Acc	Rack 4 top floor 2nd floor
15	415	R253 Acc	Rack 2 top floor 3rd floor	39	455	R453 Acc	Rack 4 top floor 3rd floor
16	419	R254 Acc	Rack 2 top floor 4th floor	40	459	R454 Acc	Rack 4 top floor 4th floor
17	303	R221 Acc	Rack 2 2nd floor 1st floor	41	343	R421 Acc	Rack 4 2nd floor 1st floor
18	307	R222 Acc	Rack 2 2nd floor 2nd floor	42	347	R422 Acc	Rack 4 2nd floor 2nd floor
19	311	R223 Acc	Rack 2 2nd floor 3rd floor	43	351	R423 Acc	Rack 4 2nd floor 3rd floor
20	315	R224 Acc	Rack 2 2nd floor 4th floor	44	355	R424 Acc	Rack 4 2nd floor 4th floor
21	197	R2B1 Acc	Rack 2 base floor 1st floor	45	253	R4B1 Acc	Rack 4 base floor 1st floor
22	201	R2B2 Acc	Rack 2 base floor 2nd floor	46	257	R4B2 Acc	Rack 4 base floor 2nd floor
23	205	R2B3 Acc	Rack 2 base floor 3rd floor	47	261	R4B3 Acc	Rack 4 base floor 3rd floor
24	209	R2B4 Acc	Rack 2 base floor 4th floor	48	265	R4B4 Acc	Rack 4 base floor 4th floor

3.4 Historic Earthquake Records

In this study, the historic earthquake records used for time history analysis of the model is obtained from Öncü-Davas (2018). In Table 3.8 the earthquake record list is given.

Historic Earthquake records listed in the Table 3.8 have the distance ranging from 0km – 6km and 6km – 10km, both near-fault historical earthquake records but first is much closer than the second set. The details of the earthquake records are given in Table 3.9 and Table 3.10, for 0km – 6km and 6km – 10km, respectively.

In Figure 3.24, several joint acceleration response of the building model and rack model under a historic (Chi-Chi Taiwan) earthquake is given.

Table 3.8: Near-fault historic earthquake records

Abbreviaton	Earthquake	Date	Mw	r (km)	Tp (s)	Abbreviaton	Earthquake	Date	Mw	r (km)	Tp (s)
TCU065	Chi-Chi Taiwan	1999	7.6	0.6	5.7	CHY024	Chi-Chi Taiwan	1999	7.6	9.6	6.7
TCU068	Chi-Chi Taiwan	1999	7.6	0.3	12.3	SPV	Northridge	1994	6.7	8.4	0.9
YPT	Kocaeli	1999	7.5	4.8	4.9	NWH	Northridge	1994	6.7	5.9	1.4
BPTS	Superstition Hills-02	1987	6.5	1.0	2.4	LDM	Northridge	1994	6.7	5.9	1.6
HE05	Imperial Valley	1979	6.5	4.0	4.1	HECC	Imperial Valley	1979	6.5	7.3	4.4
TAZ	Kobe	1995	6.9	0.3	1.8	HE04	Imperial Valley	1979	6.5	7.1	4.8
HE06	Imperial Valley	1979	6.5	1.4	3.7	HE10	Imperial Valley	1979	6.5	8.6	4.5
HE07	Imperial Valley	1979	6.5	0.6	4.4	PUL	Northridge	1994	6.7	7.0	0.8
LCN	Landers	1992	7.3	2.2	5.1	WVC	Loma Prieta	1989	6.9	9.3	5.6
TAB	Tabas	1978	7.4	2.1	6.2	HHVP	Imperial Valley	1979	6.5	7.5	4.8
WPI	**Northridge**	**1994**	**6.7**	**5.5**	**3**	PET	Cape Mendocino	1992	7.0	8.2	3
JEN	Northridge	1994	6.7	5.4	3.2	LINC	Darfield	2010	7.0	7.1	7.4
SCE	Northridge	1994	6.7	5.2	3.5	HORC	Darfield	2010	7.0	7.3	9.9
SYL	Northridge	1994	6.7	5.3	2.4	GRO	Montenegro	1979	7.1	7.0	1.4
SFERN	San Fernando	1971	6.6	1.8	1.6	TCU063	Chi-Chi Taiwan	1999	7.6	9.8	6.6

Table 3.9: Historic earthquake record and details (0-6 km)

Earthquakes	Station	Acronym	EQ Components	PGD (cm)	PGV (cm/s)	PGA (g)
Chi-Chi Taiwan	TCU065	TCU065	TCU065-E	108.7	92.1	0.8
			TCU065-N	50.2	125.3	0.6
Chi-Chi Taiwan	TCU068	TCU068	TCU068-E	297	249.5	0.5
			TCU068-N	421.5	264	0.4
Kocaeli	Yarımca	YPT	YPT150	47.3	71.9	0.3
			YPT060	62.3	69.7	0.2
Superstition Hills-02	Parachute Test Site	BPTS	B-PTS225	46.1	134.2	0.4
			B-PTS315	17.8	53	0.4
Imperial Valley	El Centro Array #05	HE05	H-E05230	75.2	96.9	0.4
			H-E05140	48.9	48.9	0.5
Kobe	Takarazuka	TAZ	TAZ000	26.7	68.4	0.7
			TAZ090	20.8	86.2	0.6
Imperial Valley	El Centro Array #06	HE06	H-E06230	72.9	113.5	0.4
			H-E06140	27.9	67	0.4
Imperial Valley	El Centro Array #07	HE07	H-E07230	46.9	113.1	0.5
			H-E07140	28	51.7	0.3
Landers	Lucerne	LCN	LCN260	113.9	133.3	0.7
			LCN345	25.5	28.1	0.8
Tabas	Tabas	TAB	TAB-T1	93.6	123.3	0.9
			TAB-L1	37.5	98.8	0.9
Northridge	Newhall - W. Pico Canyon Rd.	WPI	WPI046	42.5	118.1	0.4
			WPI316	16	59.2	0.4
Northridge	Jensen Filter Plant	JEN	JEN022	44.6	111.4	0.4
			JEN292	23.4	97.3	0.6
Northridge	Sylmar - Converter Sta East	SCE	SCE011	34	120.9	0.9
			SCE281	18.8	60.4	0.4
Northridge	Sylmar - Olive View Med FF	SYL	SYL360	32.1	129.3	0.8
			SYL090	16	77.5	0.6
San Fernando	Pacoima Dam (upper left abut)	SFERN	PUL194	39	114.4	1.2
			PUL254	12.8	57.2	1.2

Table 3.10: Historic earthquake record and details (6-10 km)

Earthquakes	Station	Acronym	EQ Components	PGD (cm)	PGV (cm/s)	PGA (g)
Chi-Chi Taiwan	CHY024	CHY024	CHY024-E	53.73	51.11	0.28
			CHY024-N	29.81	43.5	0.17
Northridge	LA-Sepulveda VA Hospital	SPV	SPV270	11.84	77.63	0.75
			SPV360	17.66	76.23	0.93
Northridge	Newhall - Fire Sta	NWH	NWH360	34.32	96.54	0.59
			NWH090	17.54	74.86	0.58
Northridge	LA Dam	LDM	LDM064	19.05	74.8	0.43
			LDM334	24.56	47.35	0.32
Imperial Valley	EC County Center FF	HECC	H-ECC092	47.98	73.35	0.24
			H-ECC002	16.98	38.42	0.21
Imperial Valley	El Centro Array #4	HE04	H-E04230	74.23	80.37	0.37
			H-E04140	25.12	39.62	0.48
Imperial Valley	El Centro Array #10	HE10	H-E10320	35.38	50.66	0.17
			H-E10050	28.77	46.35	0.23
Northridge	Pacoima Dam (upper left)	PUL	PUL194	22.17	103.33	1.29
			PUL104	5.51	54.85	1.58
Loma Prieta	Saratoga - W Valley Coll.	WVC	WVC270	24.26	42.04	0.26
			WVC000	37.83	64.88	0.33
Imperial Valley	Holtville Post Office	HHVP	H-HVP315	35.81	51.43	0.22
			H-HVP225	39.13	53.11	0.26
Cape Mendocino	Petrolia	PET	PET090	33.2	88.47	0.66
			PET000	16.59	49.3	0.59
Darfield, New Zeland	LINC	LINC	LINCN23E	66.65	108.69	0.46
			LINCN67E	33.81	56.88	0.39
Darfield, New Zeland	HORC	HORC	HORCN18E	52.93	105.87	0.45
			HORCN72E	29.67	69.82	0.48
Montenegro, Yugoslavia	GRO	GRO	BSO090	15.97	52.79	0.37
			BSO000	10.4	41.22	0.37
Chi-Chi Taiwan	TCU063	TCU063	TCU063-N	52.66	82.79	0.13
			TCU063-E	43.66	43.96	0.18

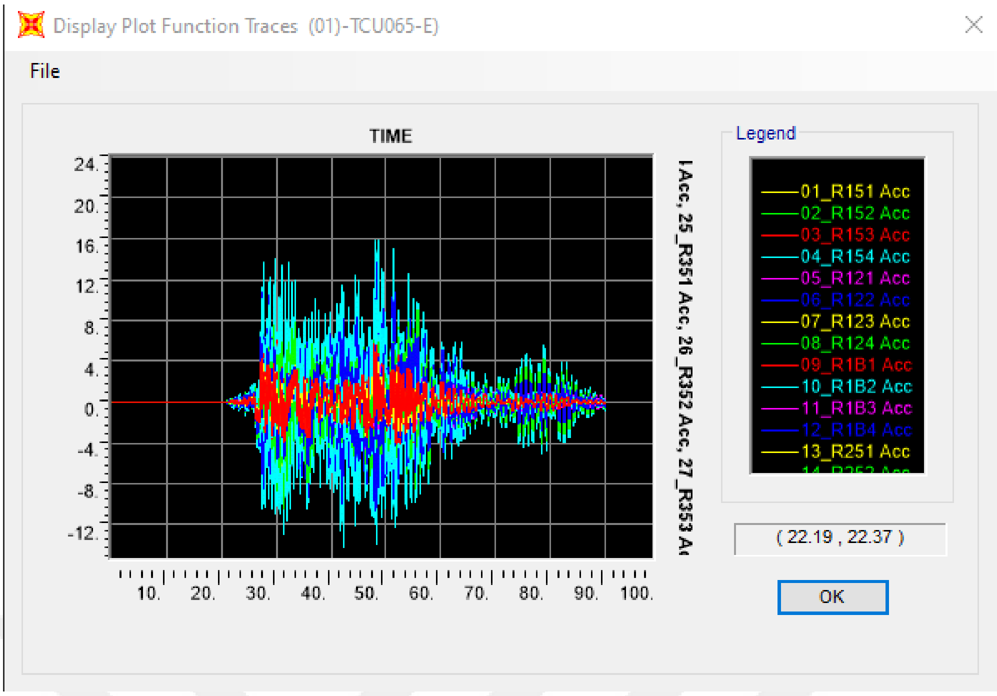

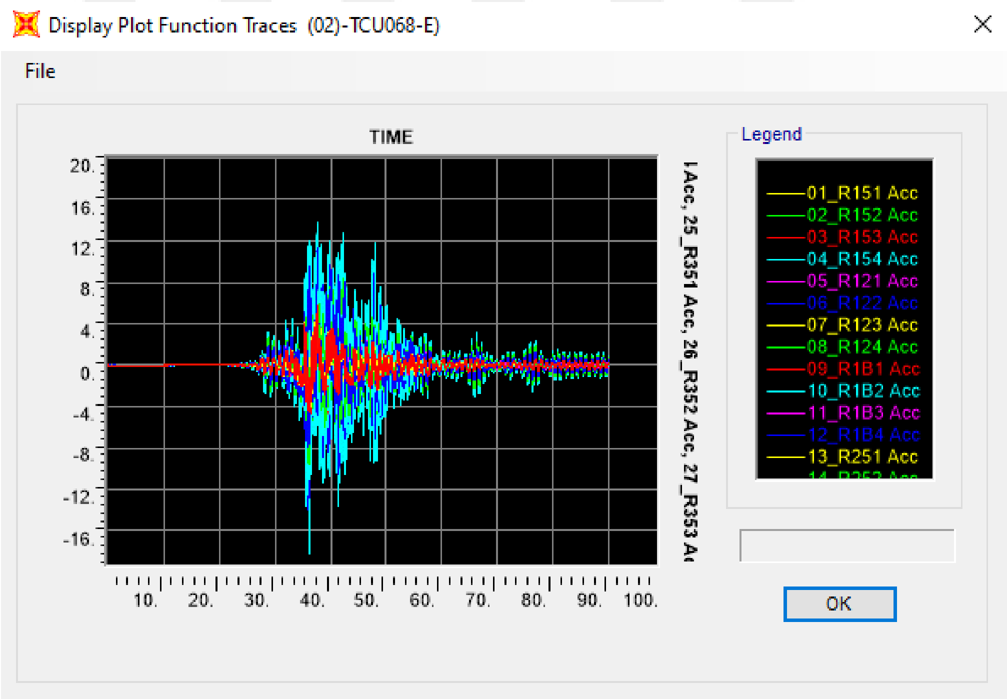

Figure 3.24: Joint Acceleration Response of the model under Chi-Chi Taiwan Historic Earthquake

3.5 Synthetic Earthquake Records

The recorded historical near-fault earthquake ground motions are characterized by different parameters such as the magnitude of the earthquake, the closest distance of the region to the fault and the existence of pulses. The parameters in question do not change systematically in the available historic near-fault earthquake records. Historic earthquakes records for near-fault specially near 10 km is rare. Thus, synthetic records are needed. For years several researches has been done in this field by different researchers to generate controlled, systematic and precise distant earthquakes in the form of a pulse which resembles the historic near-fault earthquakes. Synthetic earthquake model to be used in this study is presented by Agrawal and He (2002). Details of this model are given in Section 2.4.3.

In this study, for synthetic earthquake record generation parameters defined given in Table 3.12 are considered. Magnitude (Mw) of the earthquake are 6.0, 6.5, and 7.0 with the fault distance as r 3, 6, 9, 12 km. The synthetic earthquake velocity and acceleration is genereated by using pulse model equations Eq.(2.3) and Eq.(2.4). Prerequisite to velocity and acceleration generation, parameters such as wp sinusoid frequency given in Eq.(2.5), Tp pulse period given in Eq.(2.6), Vp max pulse velocity given in Eq.(2.8) must be calculated. Figure 3.25 illustrate's the parameter evaluation using Excel Spreadsheet. Synthetic earthquake record (both acceleration and velocity record) is produced in the Excel program. In Figure 3.28, examples of pulse model acceleration responses under Mw = 6.0 with r = 3, 6, 9, 12 km are given.

Table 3.11: Magnitude and Fault distance of the Synthetic Earthquakes

Mw	r (km)	M_w	r (km)	M_w	r (km)
	3		3		3
	6		6		6
6.0	9	6.5	9	7.0	9
	12		12		12
	15		15		15

Mw	r	Vp	Tp	wp	zetap	sqrt(1-zetap^2)	tp	s	zetap*wp
	3	57.74	1.122	5.72	0.2	0.98	0.245	77.93	1.14
	6	40.82	1.122	5.72	0.2	0.98	0.245	55.10	1.14
6	9	33.33	1.122	5.72	0.2	0.98	0.245	44.99	1.14
	12	28.87	1.122	5.72	0.2	0.98	0.245	38.96	1.14
	15	25.82	1.122	5.72	0.2	0.98	0.245	34.85	1.14
	3	102.67	1.830	3.50	0.2	0.98	0.399	138.58	0.70
	6	72.60	1.830	3.50	0.2	0.98	0.399	97.99	0.70
6.5	9	59.28	1.830	3.50	0.2	0.98	0.399	80.01	0.70
	12	51.33	1.830	3.50	0.2	0.98	0.399	69.29	0.70
	15	45.91	1.830	3.50	0.2	0.98	0.399	61.98	0.70
	3	182.57	2.985	2.15	0.2	0.98	0.651	246.44	0.43
	6	129.10	2.985	2.15	0.2	0.98	0.651	174.26	0.43
7	9	105.41	2.985	2.15	0.2	0.98	0.651	142.28	0.43
	12	91.29	2.985	2.15	0.2	0.98	0.651	123.22	0.43
	15	81.65	2.985	2.15	0.2	0.98	0.651	110.21	0.43

Figure 3.25: Synthetic Earthquake Parameters

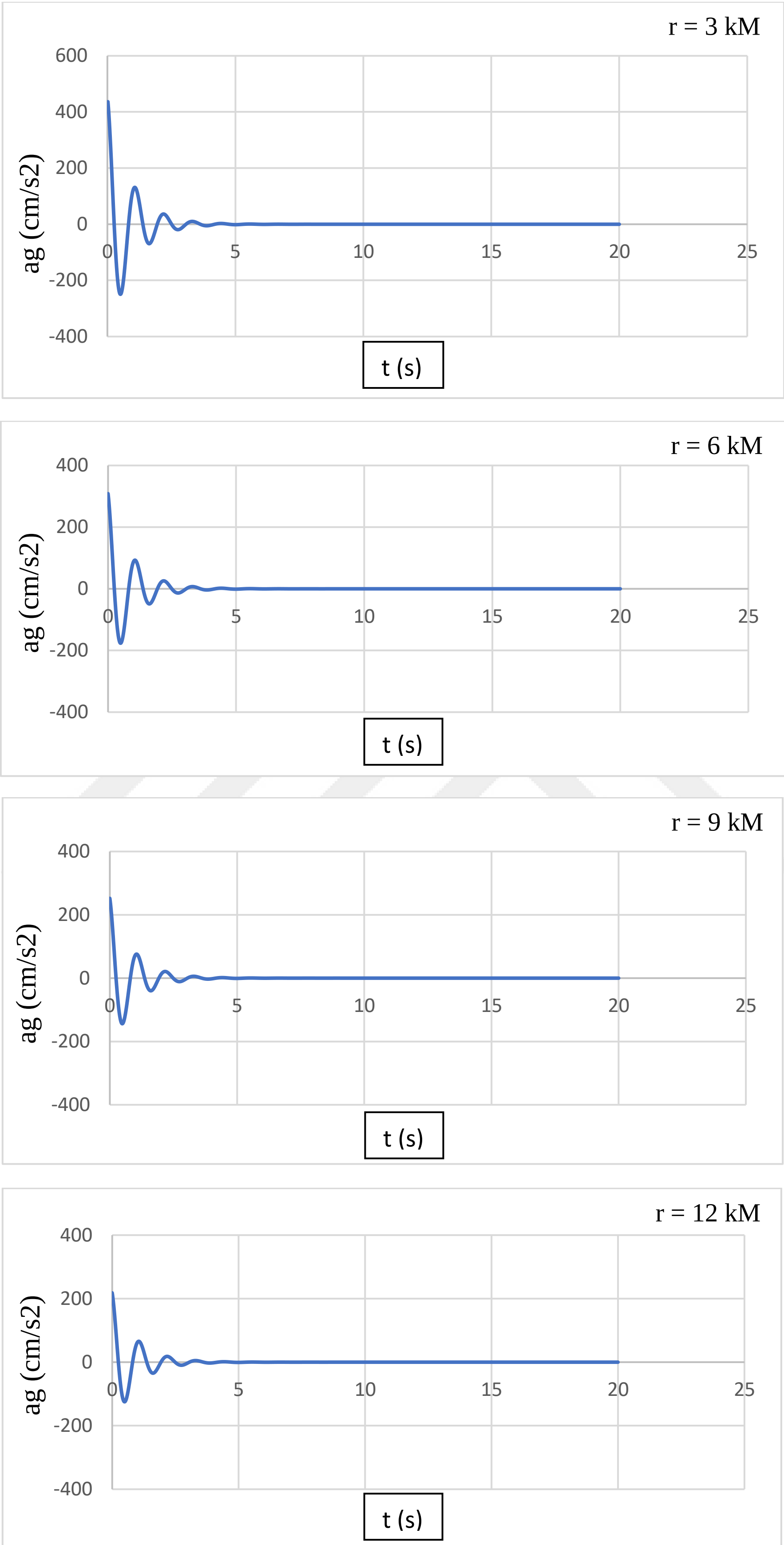

Figure 3.26: Synthetic Earthquake pulse model, Acceleration response under M_w = 6.0

4 DISCUSSION OF RESULTS

4.1 Response Under Historical Earthquakes

The building model with rack is analyzed underr real historic earthquakes. The time history record of near-fault earthquakes ranging from 0 km to 6 km and 6 km to 10 km are examined. The earthqauke records used for the model is given in Table 3.8 and are detailed in Table 3.9 and 3.10, respectively. In this section, responses of the model under historic earthquake is explained. The responses are collected from the specific joints mentioned in Sections 3.3.1 and 3.3.3 of the building and rack models, respectively. Collected responses of historic earthquake is presented in four different sets of graphs. The first set of graph, starts from Figure 4.1 and ends with Figure 4.3. The second set of graph starts from Figure 4.4 to Figure 4.6. Third set of graph starts from Figure 4.7 and ends with Figure 4.9.

In first set of graphs, x-axis represents peak acceleration values and on y-axis rack floor level, where rack base floor is labeled as 0, is given. Acceleration limits are drawn perpendicular to x-axis with black colored lines at 3.5, 5.0, 6.5 and 8.0 m/s^2. Blue color and red color graph represents immediate vicinity (0-6 km) and close to (6-10 km) near-fault results, each with 15 different earthquake responses (a total of 30). Each figure (Figs 4.1-4.3) contains four different graphs for racks, representing different racks of natural period with Tr=0.2s ,0.4s, 0.6s, 0.8s.

For instance, in Figure 4.1, the graph representing rack with period of Tr =0.2s can be summarized as follows. Under 0-6 km near-fault earthquakes, rack base floor and as well as different rack floor levels are seen to pass the 3.5 m/s^2 peak acceleration limits for almost all the earthquakes. And certain earthquake responses of rack can be seen starting over 5.0 m/s^2 at rack base floor while crossing all the peak acceleration limits and ending at the rack top floor with nearly 15 m/s^2. In contrast to 0-6 km earthquakes, under certain 6-10 km earthquakes, rack base floor is seen to be within 3.0 m/s^2 limit. However, some earthquake responses are over 3.0 m/s^2 and are within 5.0 m/s^2 and 8.0 m/s^2 limits at first two rack floors. Rack's third and fourth floor is noticed to drastically cross all the limits and reach to peak acceleration of 12.0 m/s^2.

When Figure 4.1 to Figure 4.3 are examined. It is seen that regardless of the rack period and rack building floor number, all near-fault 0-6 km responses tend to give higher values compared to all 6-10 km responses. From Figure 4.1 we can see that the racks with period Tr = 0.6s generally gives low responses however when we look at Figure 4.2, rack placed at 2nd floor with Tr =0.4s gives the lowest values. Therefore, it is important that what kind of rack period you have and which floor you place it.

Finally, when Figure 4.3 is checked, this time the largest responses are obtained by Tr = 0.4s racks. As seen in Figure 4.1, rack with period of Tr = 0.4s exceed 7.5 m/s^2 limit. However, when we go to Figure 4.2, the responses with these rack periods are smaller and the responses with other rack periods are higher. When you go to Figure 4.3, we see that regardless of the rack period, all of them give very high responses. Moreover, when we compare Figures 4.1, 4.2 and Figure 4.3, we see that largest responses for all rack periods tend to be observed at the top floor. In a nutshell, it is essential to consider rack base and rack's different floor and specifically at different building floor. Moreover, natural period of racks are also important.

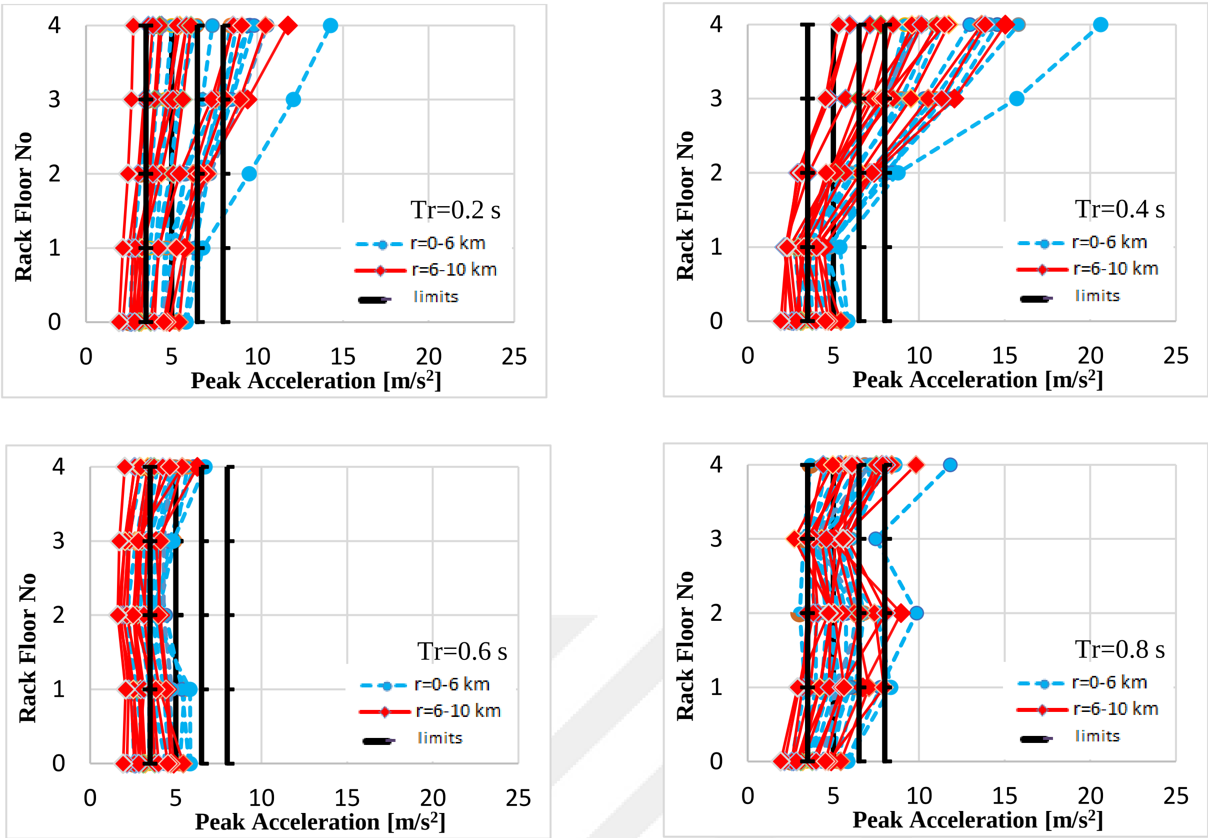

Figure 4.1: Peak acceleration profile of racks at base floor. Limits are drawn at 3.5, 5.0, 6.5, 8.0 m/s^2

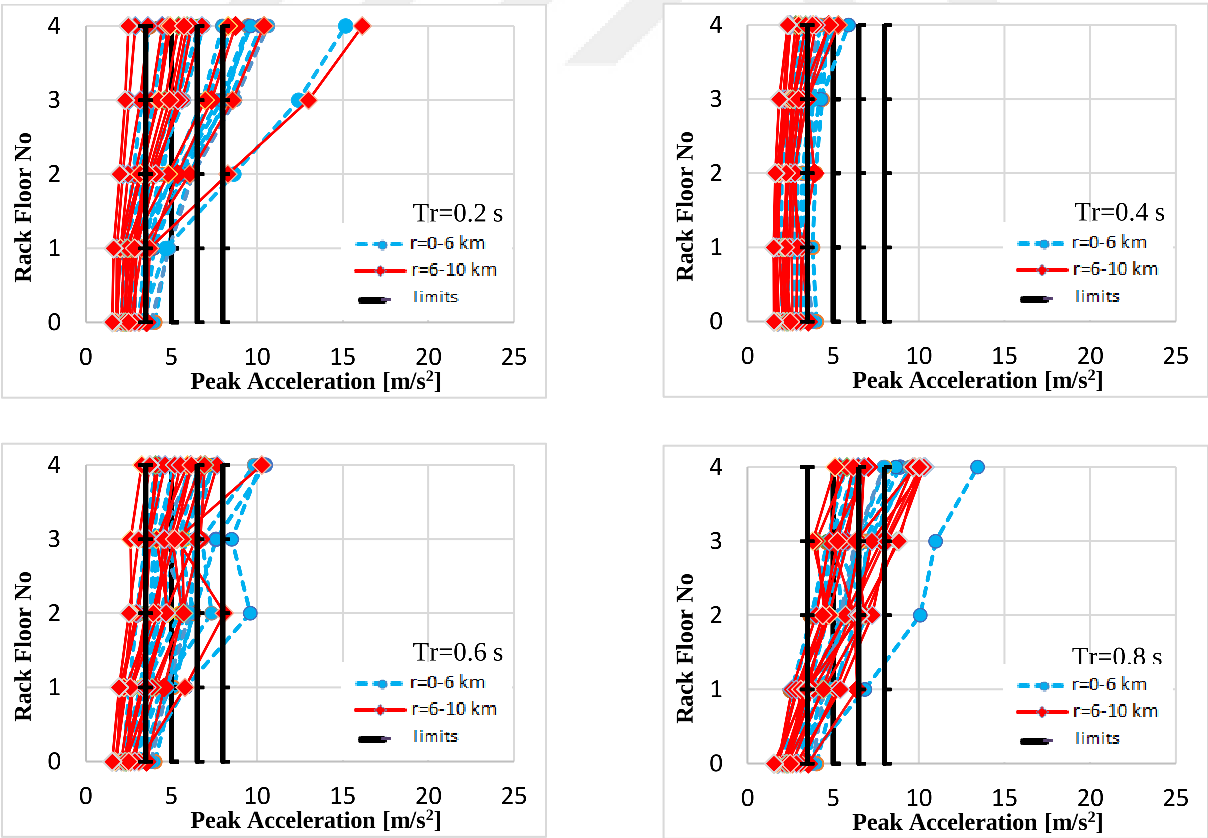

Figure 4.2: Peak acceleration profile of racks at 2nd floor. Limits are drawn at 3.5, 5.0, 6.5, 8.0 m/s^2

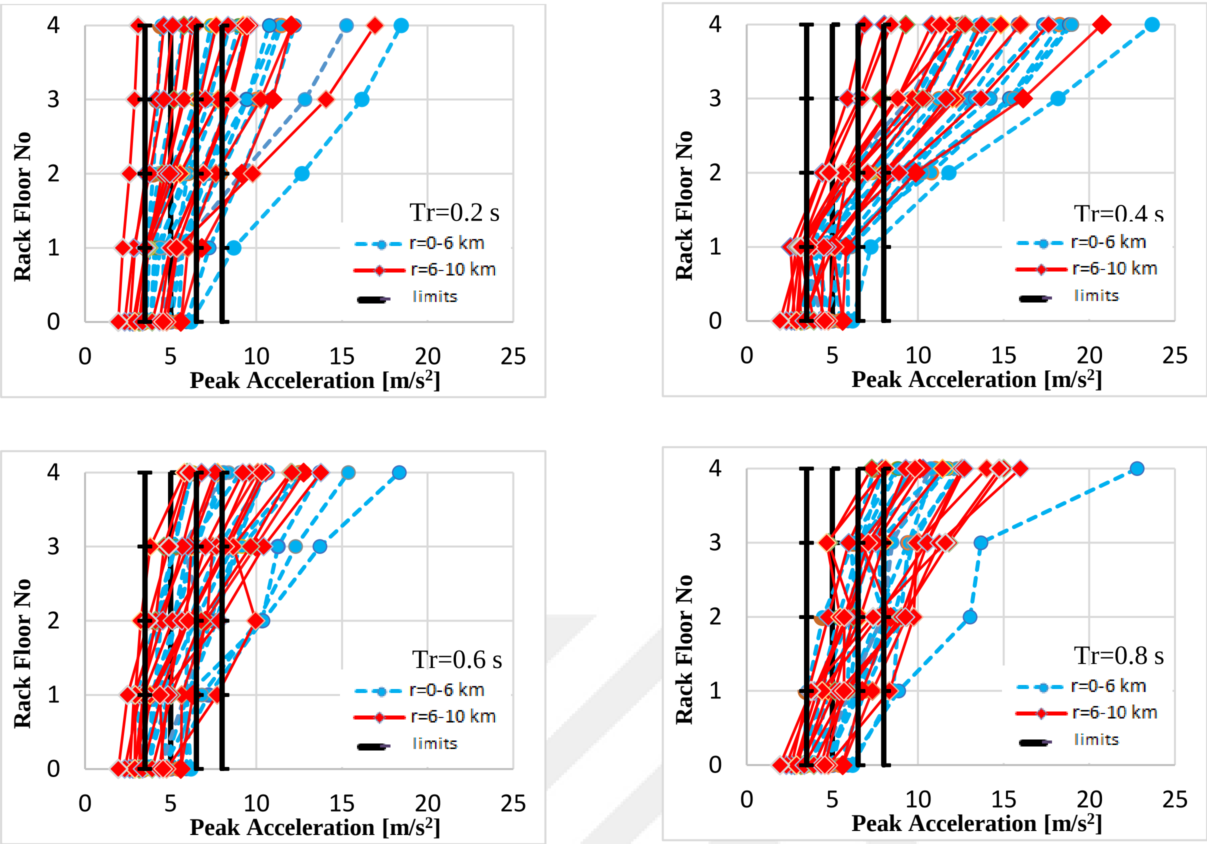

Figure 4.3**:** Peak acceleration profile of racks at top floor. Limits are drawn at 3.5, 5.0, 6.5, 8.0 m/s^2

The second set of graph explains acceleration amplification ratio of all earthquakes as an average between rack base and rack floors regardless of 0-6 km and 6-10 km earthquakes. Ratios for rack models located at different building floors are given in Figures 4.4 to 4.6. The earthquake responses as a ratio of rack model (Tr=0.4s) at base floor to building base floor, clearly tells us that under historic earthquake it can monotonically increase at different rack levels and can be multiple of rack base floor. When Figures 4.4 to 4.6 are compared, it is seen that acceleration amplification ratios are different for racks located at different floors. A combination of the rack period and rack floor location results in different amplifications.

Figure 4.4, it is seen that the rack with period of Tr=0.2 s has increased nearly 250% compared to its base and for rack with Tr = 0.4 s, the amplification ratio can be seen to reach almost 400%. On the other hand, rack with Tr = 0.6s and rack with Tr = 0.8s are showing 20% reduction in responses but Tr = 0.8s in rack top floor again increases 3 times with respect to its base, i.e. building floor.

In Figure 4.5, rack with Tr = 0.2s, Tr = 0.6s and Tr = 0.8s increased 350% to 500% compared to its base but rack with Tr = 0.4s has hardly increased by 150%. Rack with Tr = 0.8 s contains unique earthquake response. When investigated, the Earthquake is found to be CHICHI_TCU063-N with Mw=7.6 at r =9.8km distance from fault having Tp= 6.6s, when compared to other earthquakes, drastically increases 6.5 times at rack top floor with respect to its base floor.

In Figure 4.6, racks with Tr = 0.2 s, Tr = 0.4 s and Tr = 0.6 s has monotonically increased 4 times compared to its base but with few in rack with Tr = 0.6s, showing 40% reduction. Lastly, rack with Tr = 0.8 s has a blazing earthquake response with an increase of nearly 8 times its base floor. Hence base and top floor rack models with its base when compared to 2nd floor is proved to be not a good option for sensitive equipment placements.

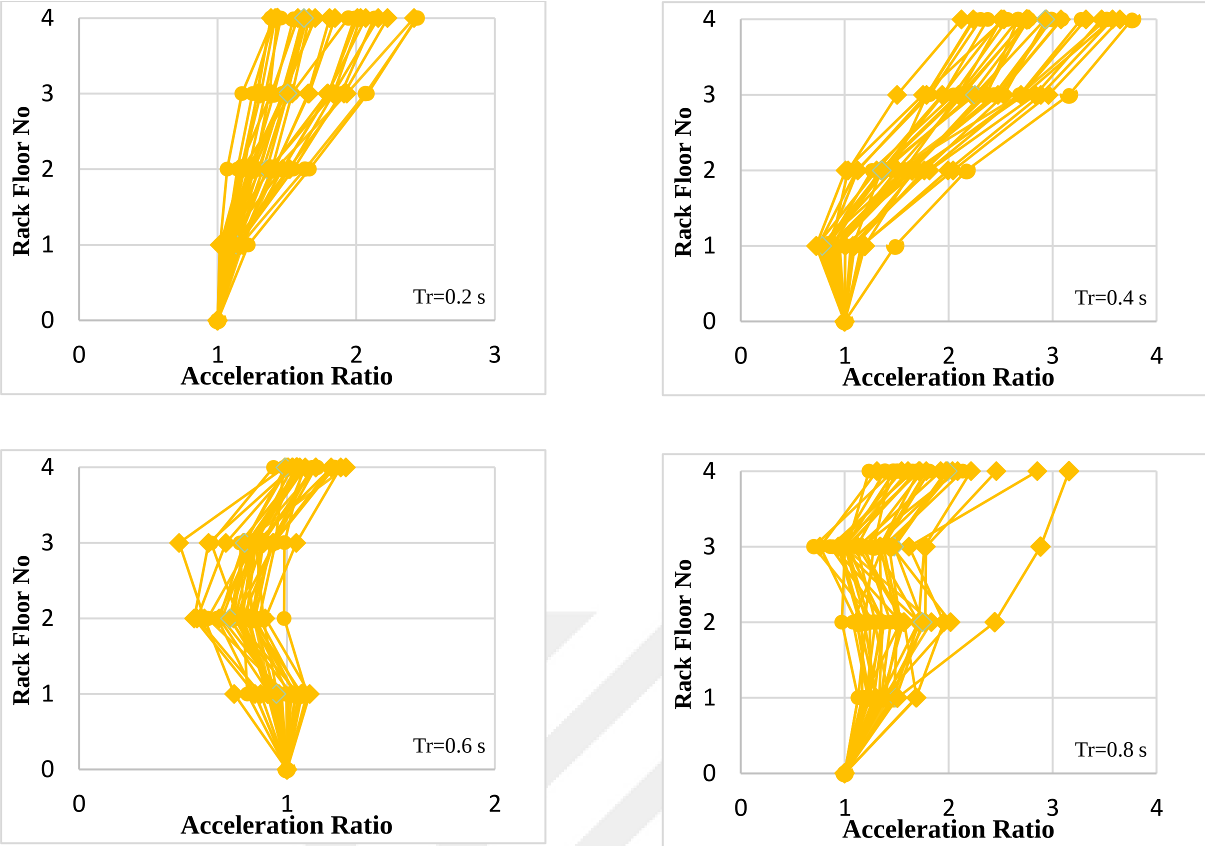

Figure 4.4: Ratio of peak rack floor accelerations at base floor to peak building base floor acceleration

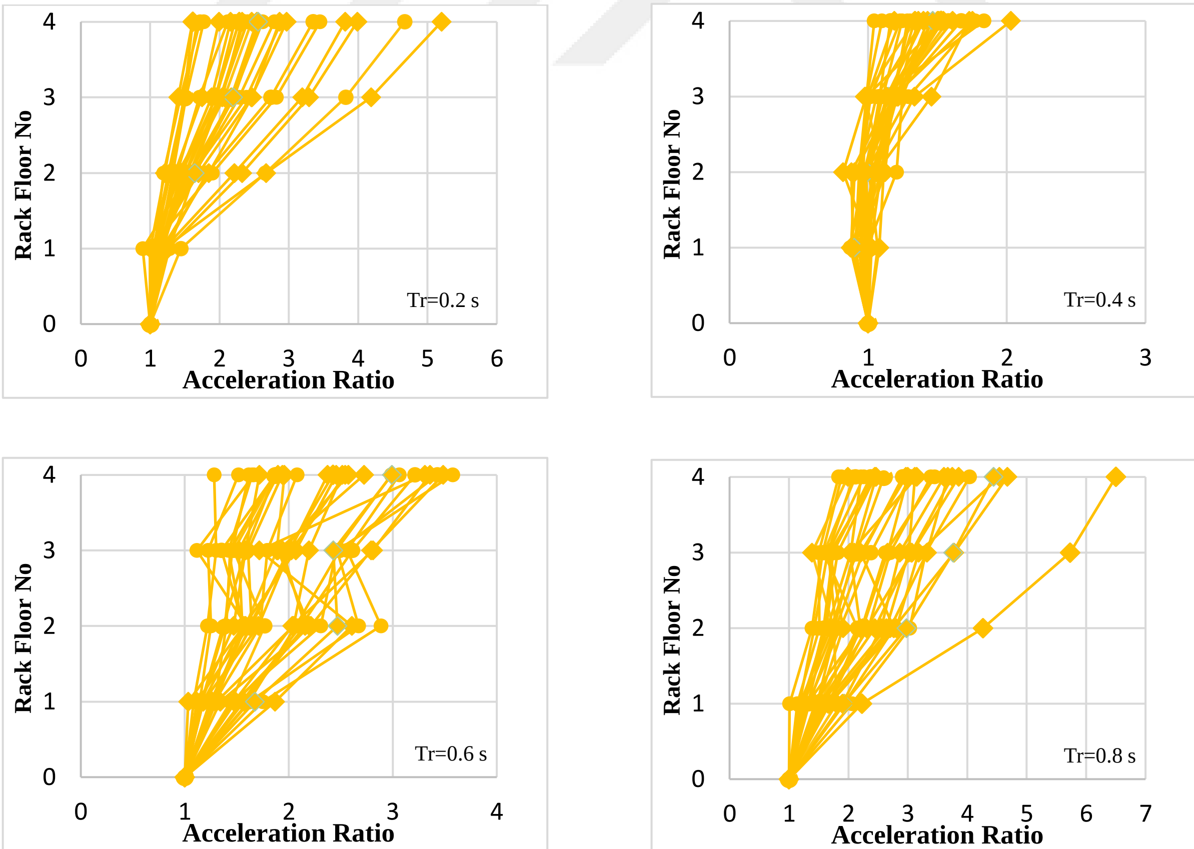

Figure 4.5: Ratio of peak rack floor accelerations at 2nd floor to peak building 2nd floor acceleration

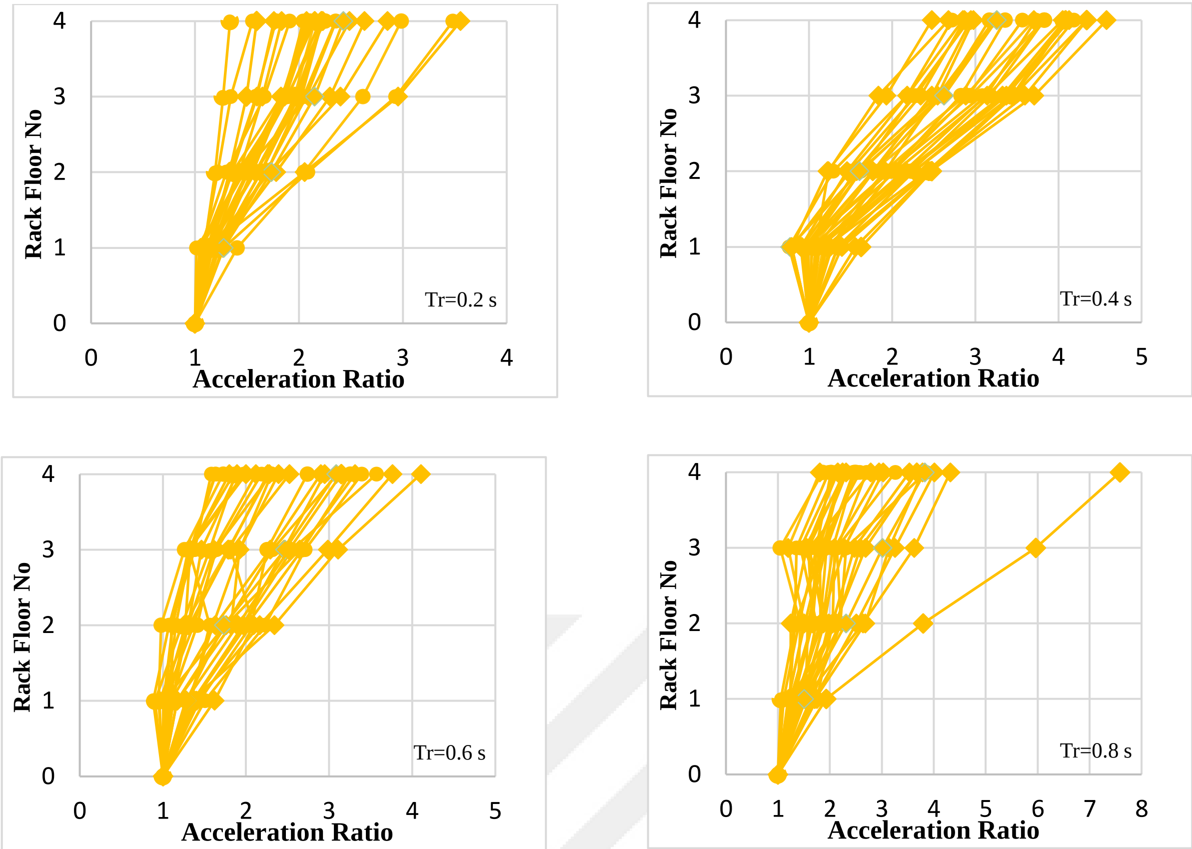

Figure 4.6**:** Ratio of peak rack floor accelerations at top floor to building top peak floor acceleration

The third set of graphs are the summary of results in the form of probability of exceeding specified limits under historic earthquake response at rack base and different rack floors. Purple color represents those cases exceeding the most stringent limit of 3.5 m/s^2, light green 5.0 m/s^2, dark red 6.5 m/s^2, and blue 8.0 m/s^2.

Generally, in Figure 4.7, for all racks and rack floors, 3.5 m/s^2 acceleration limit is seen passed at serious rate. The same is applicable to building top floor given in Figure 4.9 but in Figure 4.8, building 2nd floor is the exception at rack base and rack initial floors for 3.5 m/s^2 acceleration limit. It's worth to mention that very close and thorough examination of every floor in rack and rack base is important. For example, in building base floor rack with Tr = 0.4 s for limit 5.0 m/s^2 at rack base, is seen 20% exceeding probability but in rack 1st floor it decreases to 5% and then monotonically increases again till rack top floor. Likewise, rack with Tr=0.6s at rack base and rack 1st floor and 4th floor passes 5.0 m/s^2 exceedance probability limit but rack 2nd and 3rd floor is exception. Rack with Tr= 0.8 s is a good example for variable changes regarding floor levels. At rack base 20% acceleration exceedance probability, 15% for rack 1st floor, 60% for rack 2nd floor, 20% for rack 3rd floor and 80% for rack 4th floor for limit 5.0 m/s^2 is found. So, it can be said, that rack base and rack 1st floor interaction can be different for acceleration responses and in between rack floors sudden decrease from 60% to 20% is also possible moreover from decreased point it can drastically increase from 20% to 80%. In Figure 4.7, rack with Tr = 0.6s and Tr = 0.8s when compared to other racks are found better in least acceleration possession. For instance, in building base floor, rack with Tr = 0.6s and in 2nd floor given in Figure 4.8, rack with Tr = 0.4s are the best option with an alternative of placing sensitive equipment. And for this model, it is important to consider building top floor to be the worst scenario for sensitive equipment. But still in top floor, rack base and rack initial floor limit 4 can be achieved.

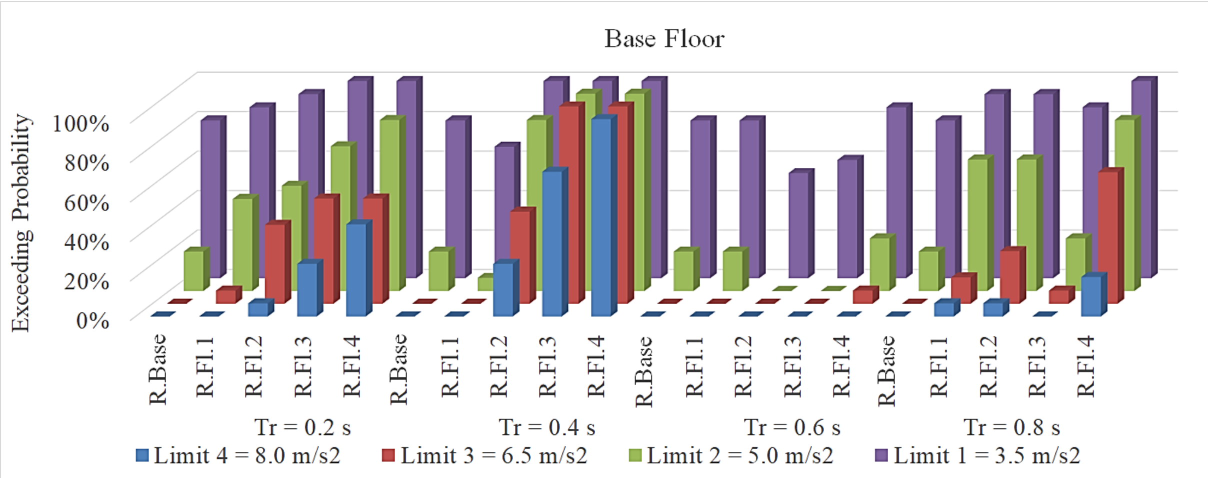

Figure 4.7: Base Floor Acceleration Exceedance Probability under Limit 3.5, 5.0, 6.5 and 8.0 m/s^2

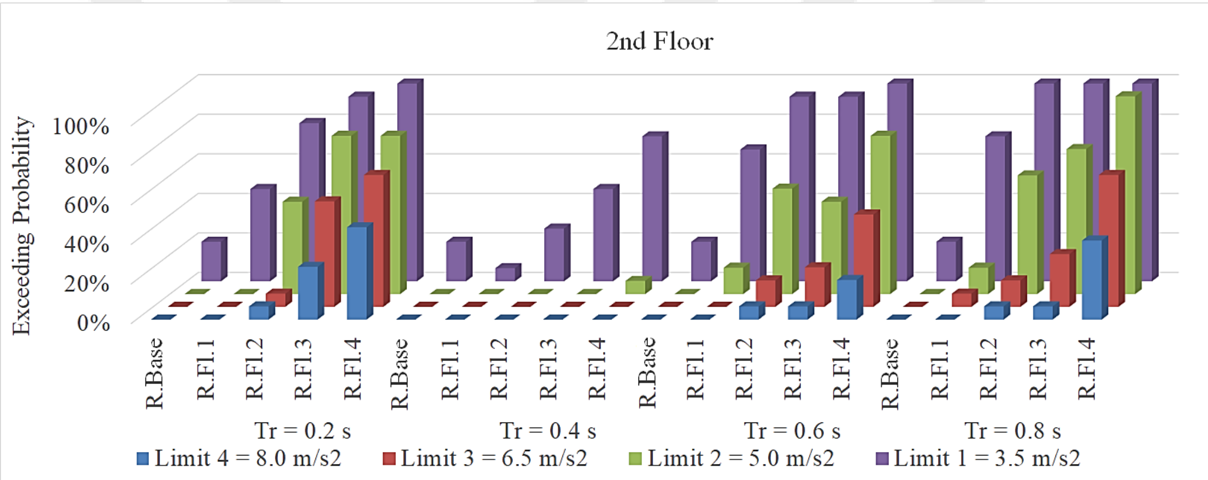

Figure 4.8: 2nd Floor Acceleration Exceedance Probability under Limit 3.5, 5.0, 6.5 and 8.0 m/s^2

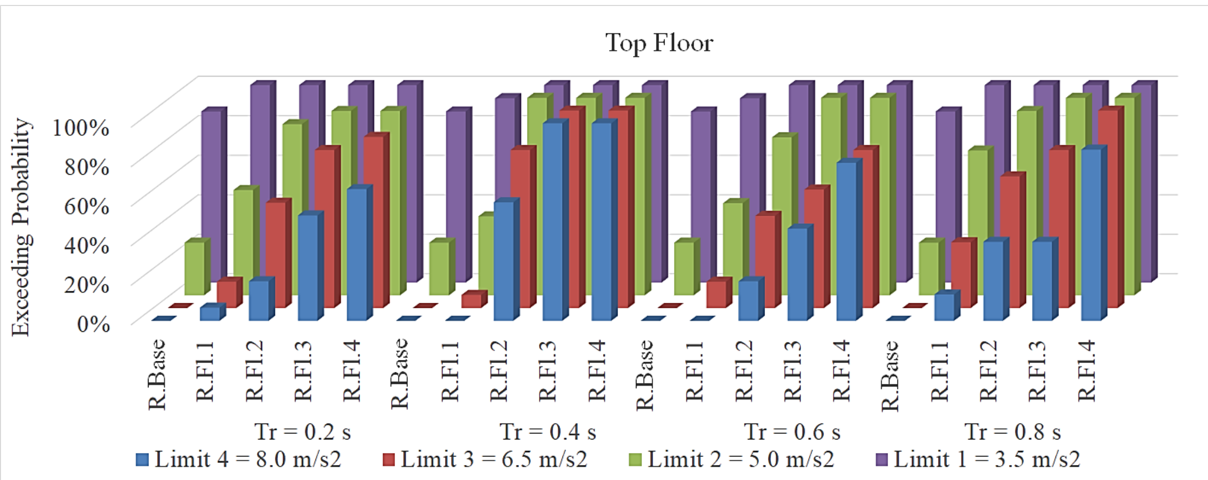

Figure 4.9: Top Floor Acceleration Exceedance Probability under Limit 3.5, 5.0, 6.5 and 8.0 m/s^2

4.2 Response Under Synthetic Earthquakes

The selected historic earthquakes within 10km range from fault, between 0km - 6km and 6km - 10km behaved differently. That is to say, there is a change depending on r (fault distance), but exactly how it changes depending on r and with the different earthquake magnitudes? in order to understand and observe systematically, synthetic earthquakes are generated depending on the fault distance (r) and the moment magnitude (Mw). Thus, it created a chance to compare them based on fault distances, different earthquake magnitudes, different pulse periods and on a rack type basis. The synthetic earthquake in the form of pulses are generated using parametric equations and are detailed in Sections 2.4.3 and 3.5.

In this section, synthetic earthqauke responses achieved systematically are presented in two sets of graphs and are briefly expalined in the passage. The first set of graph covers Figure 4.10, Figure 4.11 and Figure 4.12. Second set of graphs starts at Figure 4.13 and ends at Figure 4.24. Each set of graph is explained below.

The first set of graphs are the peak acceleration profile of racks under Mw = 6.0, 6.5 and 7.0 respectively. As an example, rack responses located at base floor response graph given in Figure 4.10 can be summarized as follows. X-axis represents the fault distance with 3 km increments, starting from fault distance of 3 km and ending at 15 km. Y-axis represents peak acceleration values of relative subject model base and floors in m/s^2. Acceleration limits are drawn horizontally with dashed lines at 3.5, 5.0, 6.5 and 8.0 m/s^2. Rack location as a title is given on the right corner and suitable place of different graphs. In the mentioned floor graph, dark green color as R.base represents rack base (which is also the base floor), blue color as R1B4 Acc represents the **R**ack **1** (with Tr=0.2 s) located at **B**ase floor, **4**th rack floor acceleration, Red color as R2B4 Acc represents **R**ack **2** (with Tr=0.4 s) located at **B**ase floor, **4**th rack floor acceleration. In these graphs rack top floor (4th floor) accelerations located at base, 2nd and top floor of the building are compared. There exist five different colored lines for 4 different racks and also the floor itself. Brown colored line is building floor acceleration response and different rack types color designation is briefly explained in Table 4.1.

Table 4.1: Rack types and their designation on graphs

Rack Type	Colour designation	Time period
Rack 1	Blue colour	T = 0.2s
Rack 2	Red colour	T = 0.4s
Rack 3	Green colour	T = 0.6s
Rack 4	Yellow colour	T = 0.8s

Summary of data used to construct Figures 4.10, 4.11, and 4.12 are given in Table 4.2. In the table, building top floor and base floor accelerations are seen to be close to each other but rack floor accelerations present in both floors show variation. 2nd floor when compared with both floors, show minimum acceleration in building floor as well as in different rack floors. For example in near-fault distance of r = 3km and under Mw=6.0, 2nd floor response acceleration is 2.39 m/s^2 and top and base floor are 3.74 m/s^2. With same fault distance under Mw=6.5 and Mw=7.0, all floors show higher response acceleration compared to earthquake magnitude of Mw=6.0. In the same way rack types also show variant values. For instance, rack one top floor in building base floor, 2nd floor and top floor at 3 km distance from fault under Mw=6.0 values are 6.33 m/s^2, 6.02 m/s^2 and 7.68 m/s^2 respectively. In 2nd floor of the building model, different rack and building floor acceleration is minimal compared to building base and top floor. On the other hand, since different rack models have different properties, the acceleration responses of the rack floors vary. Rack 3 in building base floor, Rack 2 in building 2nd floor and Rack 1 in building top floor show minimum acceleration value.

It is also seen that by setting the building period and rack period correctly it can target a realistic value without exceeding 5.0 m/s^2 limit. But it is difficult to achieve 3.5 m/s^2 limit and fortunately 6.5 m/s^2 and

8.0 m/s^2 limits can be achieved if equipment is not installed at rack top floors. Moreover, by including fault distance and earthquake magnitude, 3.5 m/s^2 is not a limit that can be easily achieved. But what is noticed is that 3.5 m/s^2 limit can be provided on 2nd floor only for certain cases.

Table 4.2: Building Floors and rack's top floor response acceleration under Mw = 6.0, 6.5, 7.0.

	Mw=6.0					Mw=6.5					Mw=7.0				
r (kM)	**3**	**6**	**9**	**12**	**15**	**3**	**6**	**9**	**12**	**15**	**3**	**6**	**9**	**12**	**15**
Top Floor	3.74	3.18	2.84	2.60	2.41	3.96	3.12	2.75	2.55	2.42	7.24	5.10	4.21	3.63	3.19
R154 Acc	7.68	6.04	5.06	4.37	3.85	7.38	5.02	4.29	3.94	3.80	11.98	8.44	6.21	5.24	5.01
R254 Acc	10.73	9.67	8.97	8.70	8.32	17.49	14.91	11.64	10.26	9.21	19.06	14.94	12.90	11.34	9.38
R354 Acc	8.83	7.87	7.29	6.83	6.45	7.99	6.94	6.17	6.72	6.66	11.28	9.02	7.47	6.63	5.96
R454 Acc	9.14	8.27	7.63	7.12	6.68	7.81	6.73	5.96	5.58	5.41	9.94	7.45	6.98	6.43	5.78
2nd Floor	2.39	2.05	1.85	1.71	1.62	2.78	2.21	2.07	1.93	1.82	5.80	3.75	3.00	2.50	2.23
R124 Acc	6.02	4.47	3.80	3.25	2.96	5.77	4.13	3.17	2.79	2.51	9.21	6.78	4.30	3.22	3.01
R224 Acc	3.43	2.98	2.72	2.52	2.37	3.01	2.90	2.21	2.03	1.94	7.20	4.70	3.74	3.13	2.69
R324 Acc	5.22	4.39	3.90	3.67	3.54	5.44	4.35	4.42	4.36	4.29	8.74	5.20	4.09	3.58	3.24
R424 Acc	5.94	5.59	5.30	5.04	4.81	5.97	4.44	4.23	3.77	3.69	8.77	6.71	5.56	4.77	4.14
Base Floor	3.74	3.16	2.82	2.57	2.39	3.71	2.97	2.64	2.48	2.38	6.89	4.94	4.01	3.51	3.13
R1B4 Acc	6.33	4.95	4.28	3.83	3.49	5.80	4.06	3.99	3.79	3.58	11.66	7.62	5.27	4.74	4.37
R2B4 Acc	8.01	6.76	6.43	6.09	5.75	13.47	10.88	9.17	8.27	7.55	16.06	12.58	10.52	8.89	7.23
R3B4 Acc	3.65	3.09	2.74	2.50	2.33	4.26	3.25	2.72	2.49	2.45	7.38	5.04	4.14	3.56	3.20
R4B4 Acc	6.69	5.85	5.29	4.87	4.52	5.90	4.74	3.98	3.53	3.34	8.96	6.81	5.45	4.43	3.87

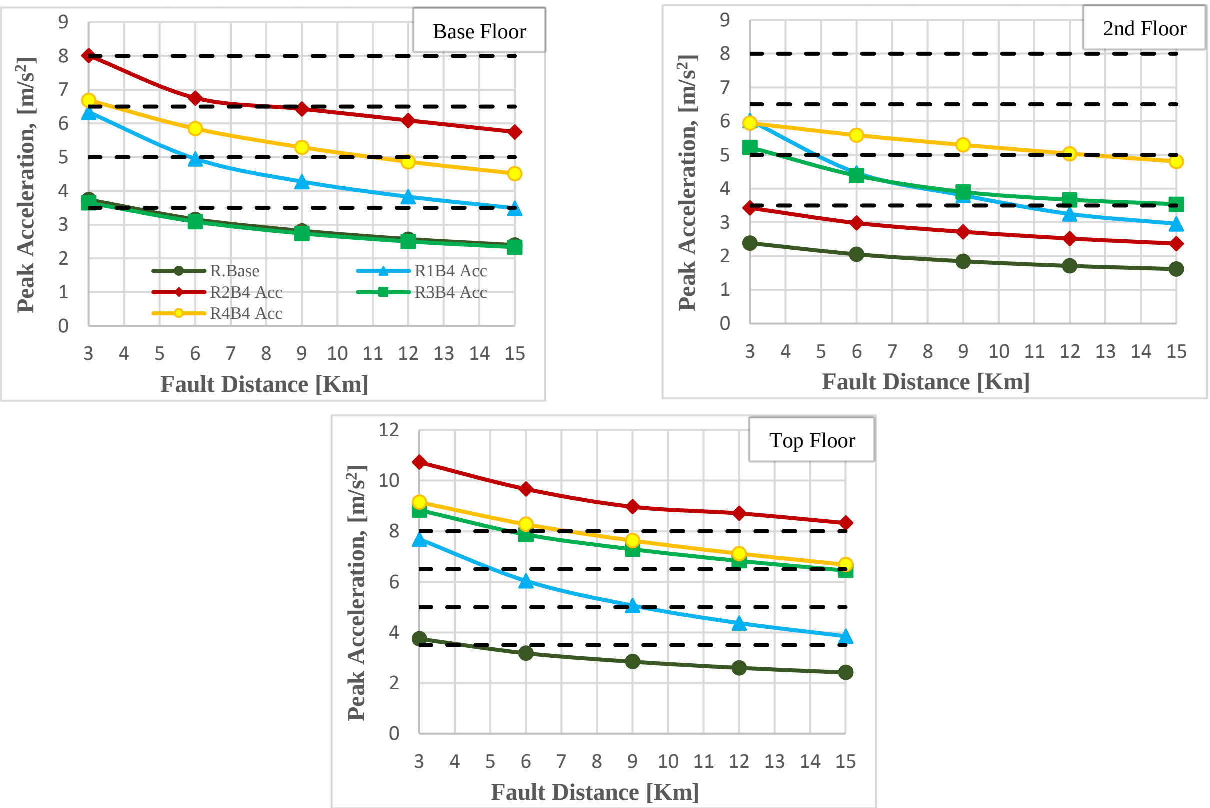

Figure 4.10**:** Peak acceleration profile of racks for Mw=6.0. Limits are drawn at 3.5, 5.0,6.5, 8.0 m/s^2

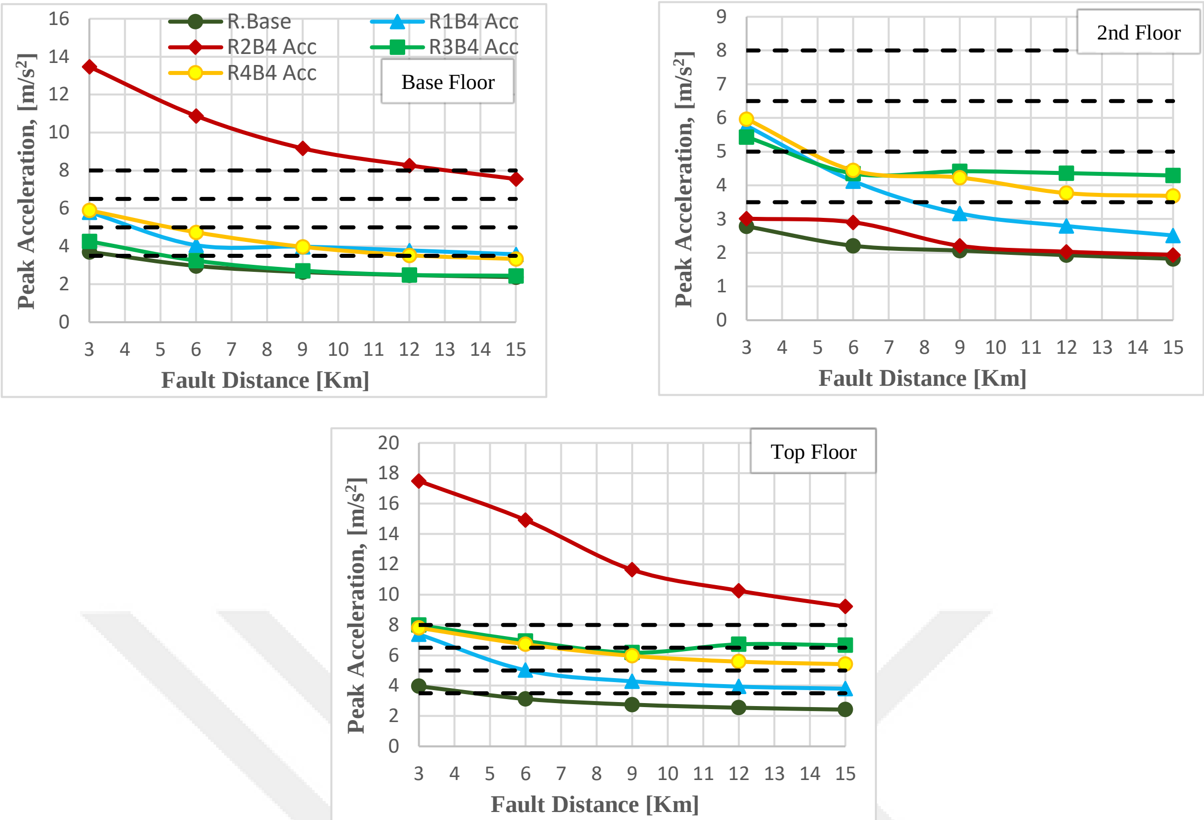

Figure 4.11: Peak acceleration profile of racks for Mw=6.5. Limits are drawn at 3.5, 5.0,6.5, 8.0 m/s²

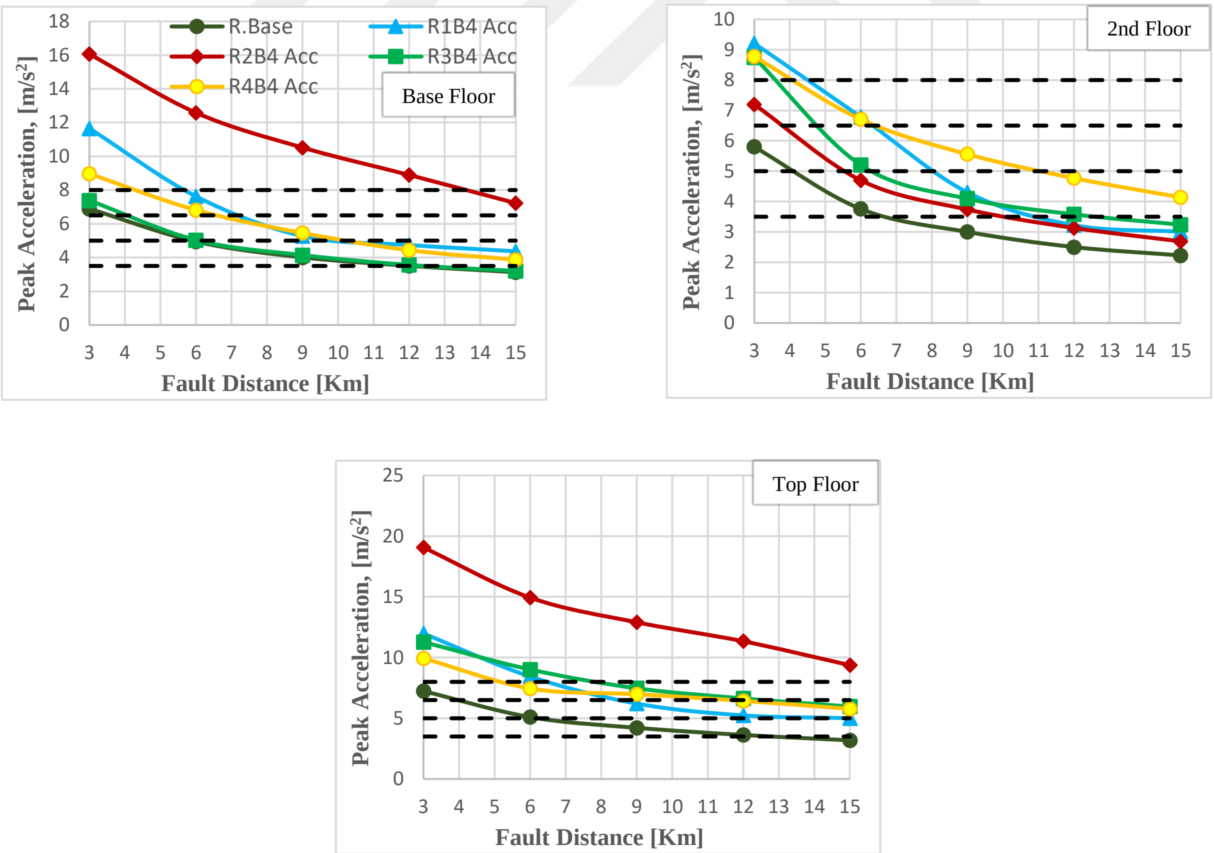

Figure 4.12: Peak acceleration profile of racks for Mw=7.0. Limits are drawn at 3.5, 5.0,6.5, 8.0 m/s²

In the second set of graphs, each set represents separate rack types. Rack one (R1) graphs cover Figures 4.13, 4.14 and Figure 4.15. Rack two (R2) graphs cover Figures 4.16, 4.17 and Figure 4.18. Rack three (R3) graphs cover Figures 4.19, 4.20 and Figure 4.21. Rack four (R4) graphs cover Figures 4.22, 4.23 and Figure 4.24. Each case is exposed to earthquakes with three different magnitudes at fault distances of 3, 6, 9, and 12 km. For example Rack one's four different floor responses under Mw=6.0 m/s^2, 6.5 m/s^2 and 7.0 m/s^2 are given for cases where it is located in building base floor, 2nd floor and top floor.

In Figure 4.13 graph, all the model racks in near-fault distance starts with higher acceleration response but as soon as the distance from fault increases the acceleration response values accordingly decreases. Moreover, rack responses are different in different building floors. As an example, blue color representing Rack one in base and top floor at distance of r =3km is 4.17 m/s^2 crossing the limit of 3.5 m/s^2 but in 2nd floor the response is half of both floors. Under earthquake magnitudes of 6.5 and 7.0, the same rack is seen to proportionally increase in all floors. When rack one is compared to rack two under earthquake magnitudes and different floors of the building model, Rack two bearing different property is seen to have 2.58 m/s^2 and 3.68 m/s^2 acceleration response in base floor and top floor, respectively. In comparison to rack one, rack two is found out to have lower acceleration response. Same way, under different magnitudes, rack two can behave better than rack one. The plots give a complete picture for all racks. Under Mw=6.0 and 6.5, Rack 3 at building base floor at r=3km distance, performed better and 3.5 m/s^2 limit is secured in rack base and intial floors and as a result it can be said that is may be a good option for vibration sensitive equipement ranging within and above 3.5 m/s^2 limit.

Additionally in building 2nd floor and top floor rack base and rack first floor hardly crosses 3.5 m/s^2 limit but in other rack floors 3.5 m/s^2 limit and 5.0 m/s^2 limit is seen crossing at r=3km. It is important to mention that rack top floor at specially r=3km crosses all the given limits. Rack 3 when examined under Mw=7.0 is seen to be crossing all the limits at r=3km and decreasing gradually as distance from fault increases. Specifically at r=3km in building base floor only 8.0m/s^2 limit could be secured, when compared to other limits and other building floors, however in 2nd floor and top floor it seems impossible

Rack 4 response is quite different than Rack 3. Under Mw=6.0, in building base floor in near-fault r=3km maximum acceleration response is noticed in rack top floor as 6.5 m/s^2 and it proportionally decreases at r=15km to 5 m/s^2. The minimum acceleration value is seen in rack base and rack first floor at r=3km to be 3.5 m/s^2, which likewise decreases to 2.71 m/s^2 in 15km distance from fault. In comparison to building base floor, building 2nd floor shows close values in rack top floor like 5.94 m/s^2 in r=3km and in r=15km declines to 5 m/s^2. Rack base demonstrates least acceleration response and proves to be a good place to consider for important equipment placement. Rack base acceleration value in r=3km is 2.39 m/s^2 but rack first floor is 3.5 m/s^2. Carelessly if a machine with 3.5 m/s^2 limit is placed in rack first floor, it can consequently leave it useless by damaging the machine. Here, rack base also is a good option in far-fault earthquake. For instance, in r=15km rack base maximum lateral acceleration is 1.62 m/s^2 and rack first floor is 2.62 m/s^2 in r=15km. now it is important to discuss building top floor, which is totally different and high when compared to building base and 2nd floor. Rack top floor is almost a disaster in near-fault earthquakes due to the fact that it crosses all the given limits. Rack third floor in comparison to rack second and first floor tends to be less affected. Numerically, rack second and first floor shows 6.5 m/s^2 and 5.58 m/s^2 respectively, where Rack third floor responds with 5.5 m/s^2 acceleration limit. To sum up, under Mw=6.0, building second floor and exactly rack base and rack first floor is suggestable for sensitive equipment placements due to lower and satisfactory acceleration values.

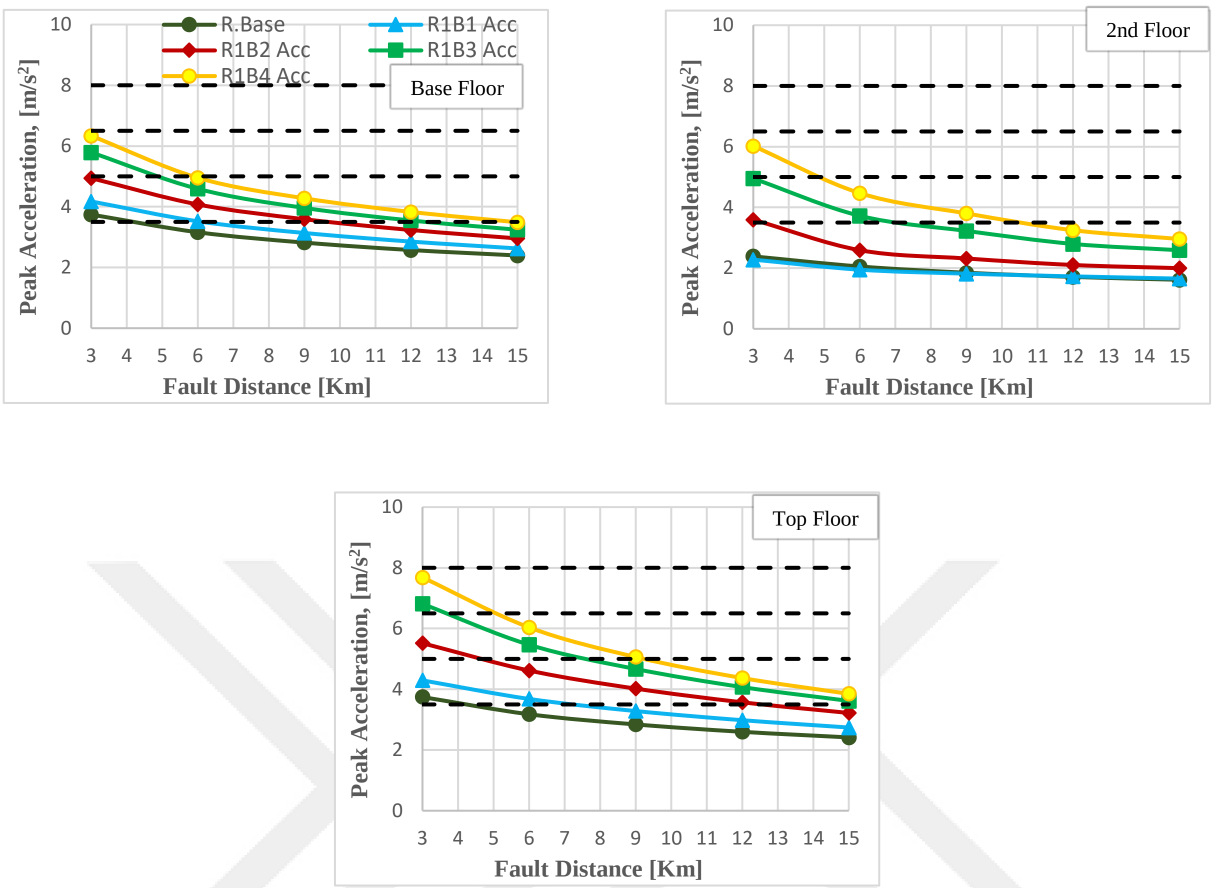

Figure 4.13: Peak acceleration of Rack-1 floor for Mw=6.0. Limits are drawn at 3.5, 5.0,6.5, 8.0 m/s^2

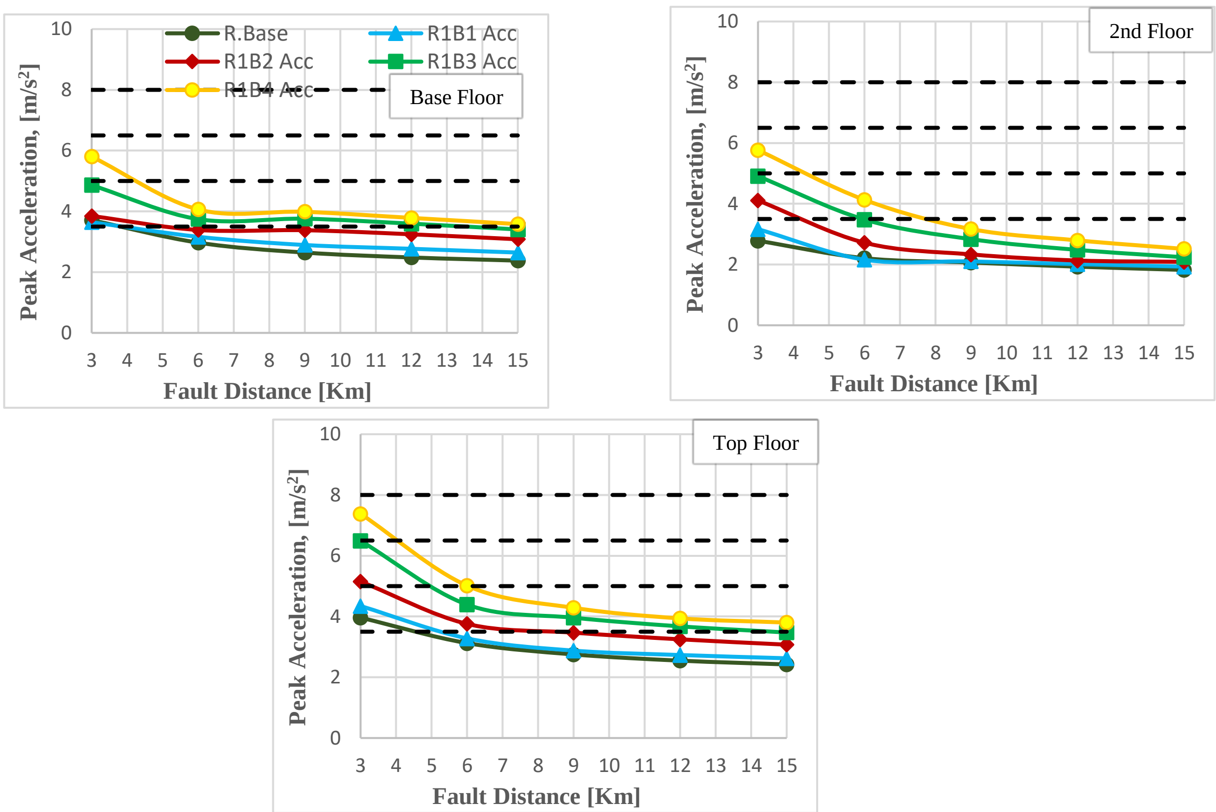

Figure 4.14: Peak acceleration of Rack-1 floor for Mw=6.5. Limits are drawn at 3.5, 5.0,6.5, 8.0 m/s^2

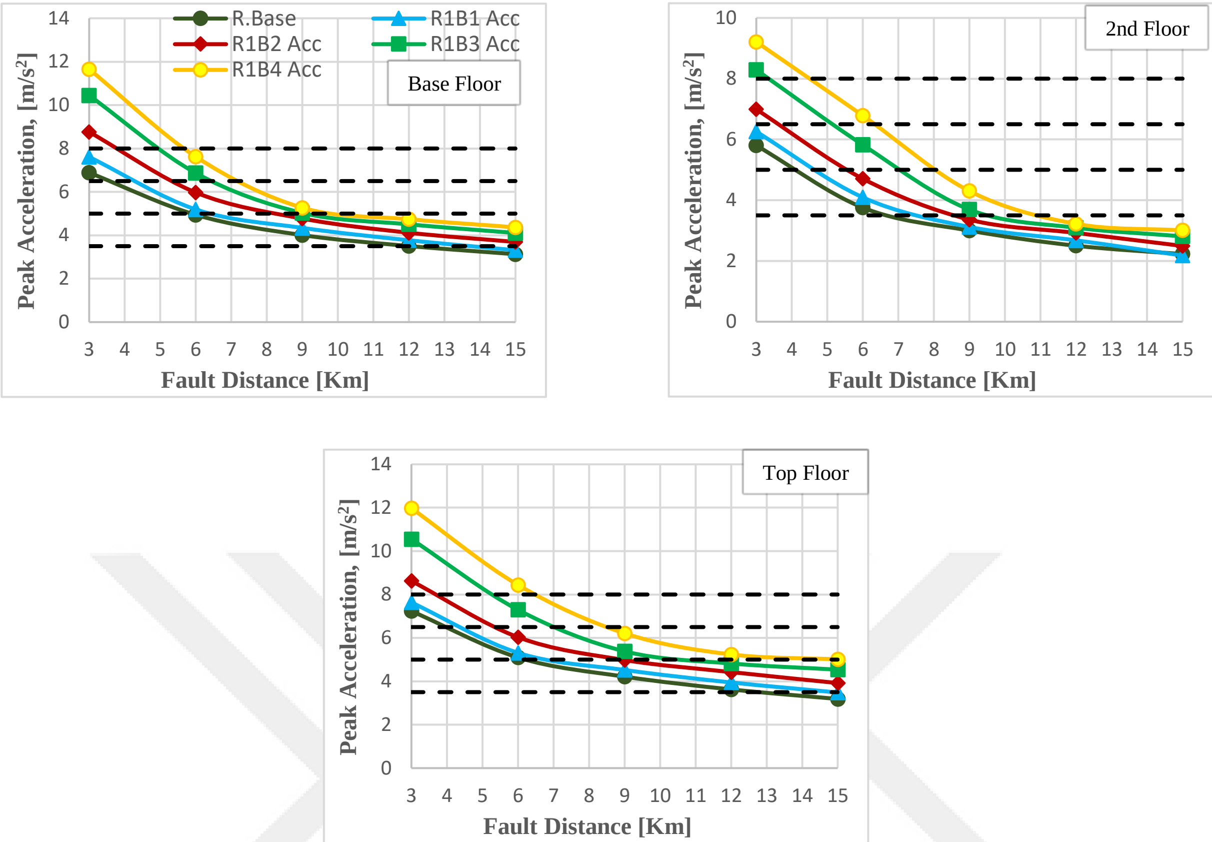

Figure 4.15: Peak acceleration of Rack-1 floor for Mw=7.0. Limits are drawn at 3.5, 5.0,6.5, 8.0 m/s^2

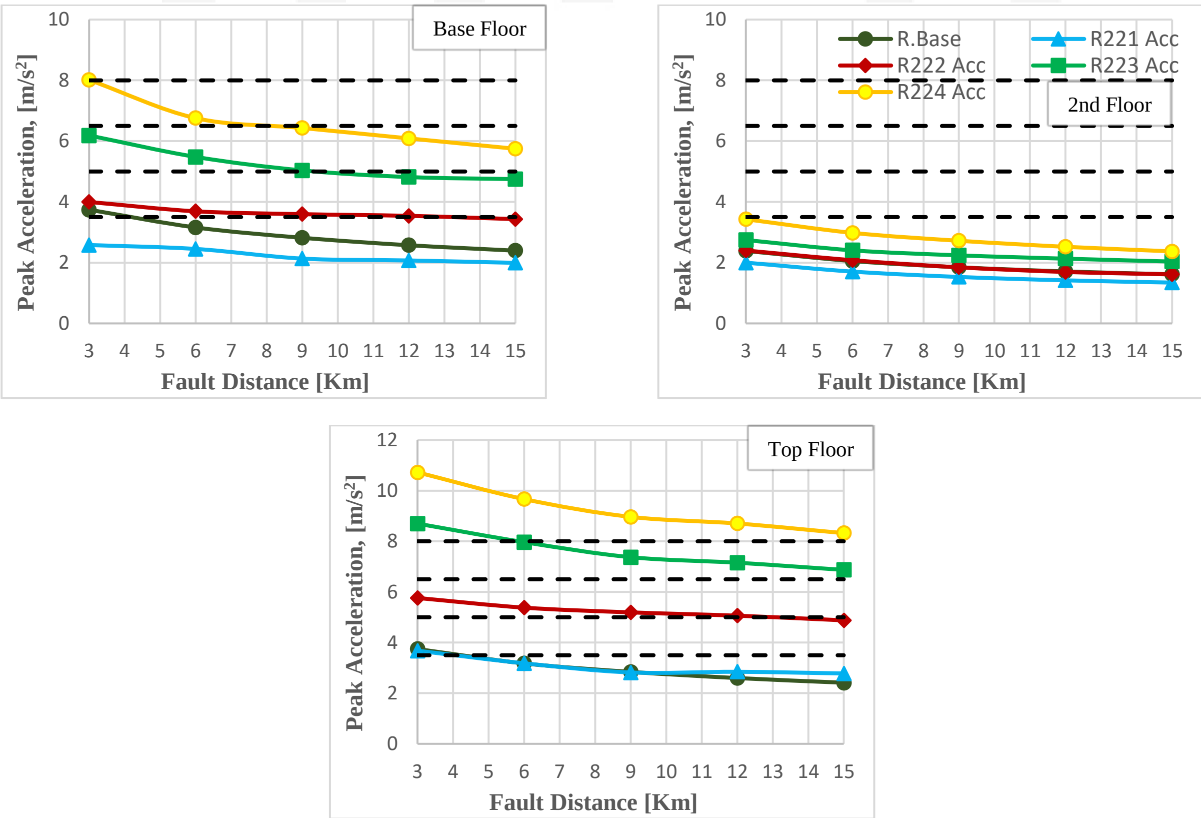

Figure 4.16: Peak acceleration of Rack-2 floor for Mw=6.0. Limits are drawn at 3.5, 5.0,6.5, 8.0 m/s^2

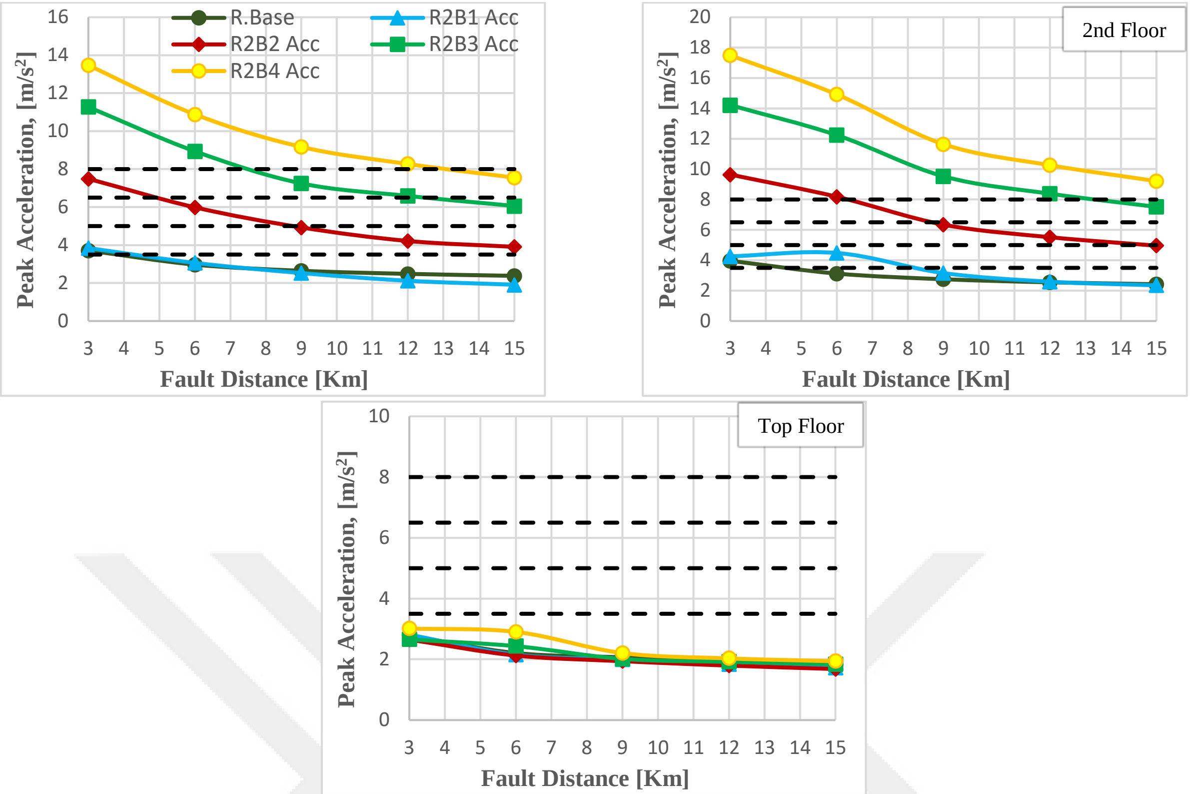

Figure 4.17**:** Peak acceleration of Rack-2 floor for Mw=6.5. Limits are drawn at 3.5, 5.0,6.5, 8.0 m/s^2

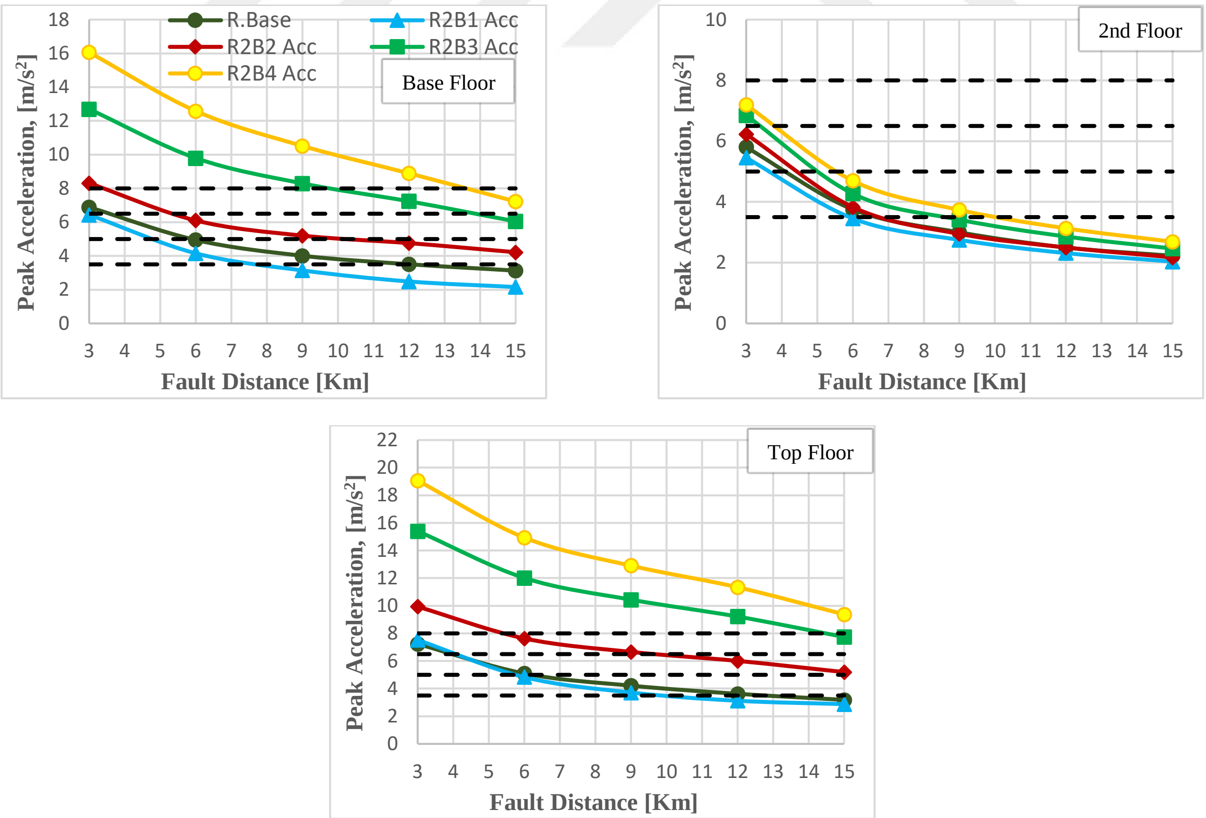

Figure 4.18**:** Peak acceleration of Rack-2 floor for Mw=7.0. Limits are drawn at 3.5, 5.0,6.5, 8.0 m/s^2

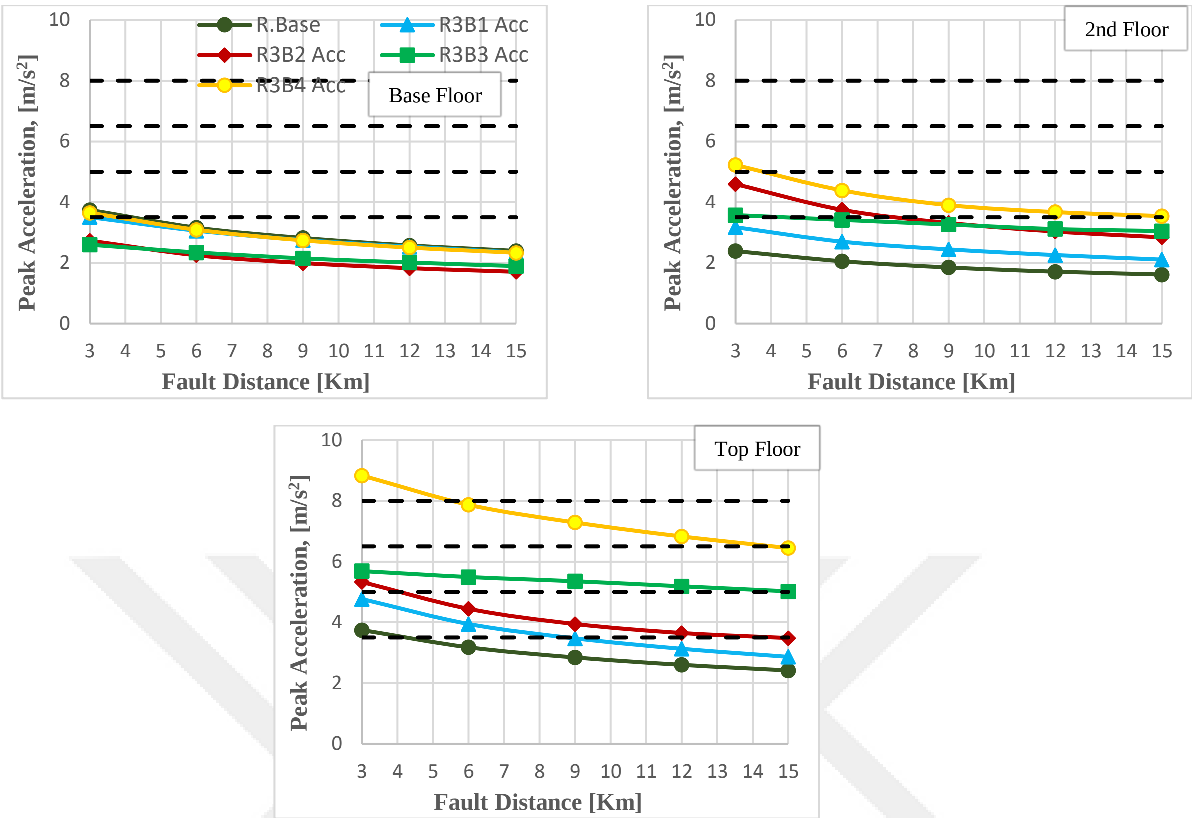

Figure 4.19: Peak acceleration of Rack-3 floor for Mw=6.0. Limits are drawn at 3.5, 5.0,6.5, 8.0 m/s^2

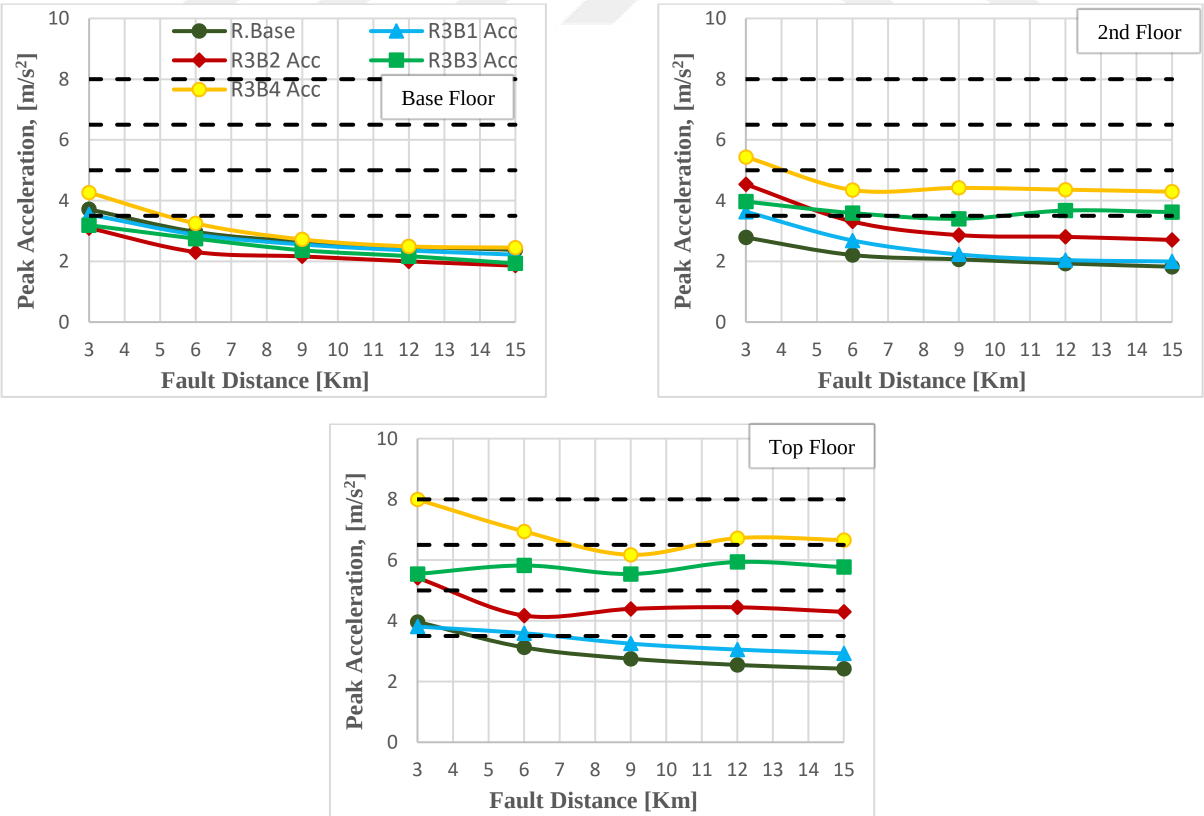

Figure 4.20: Peak acceleration of Rack-3 floor for Mw=6.5. Limits are drawn at 3.5, 5.0,6.5, 8.0 m/s^2

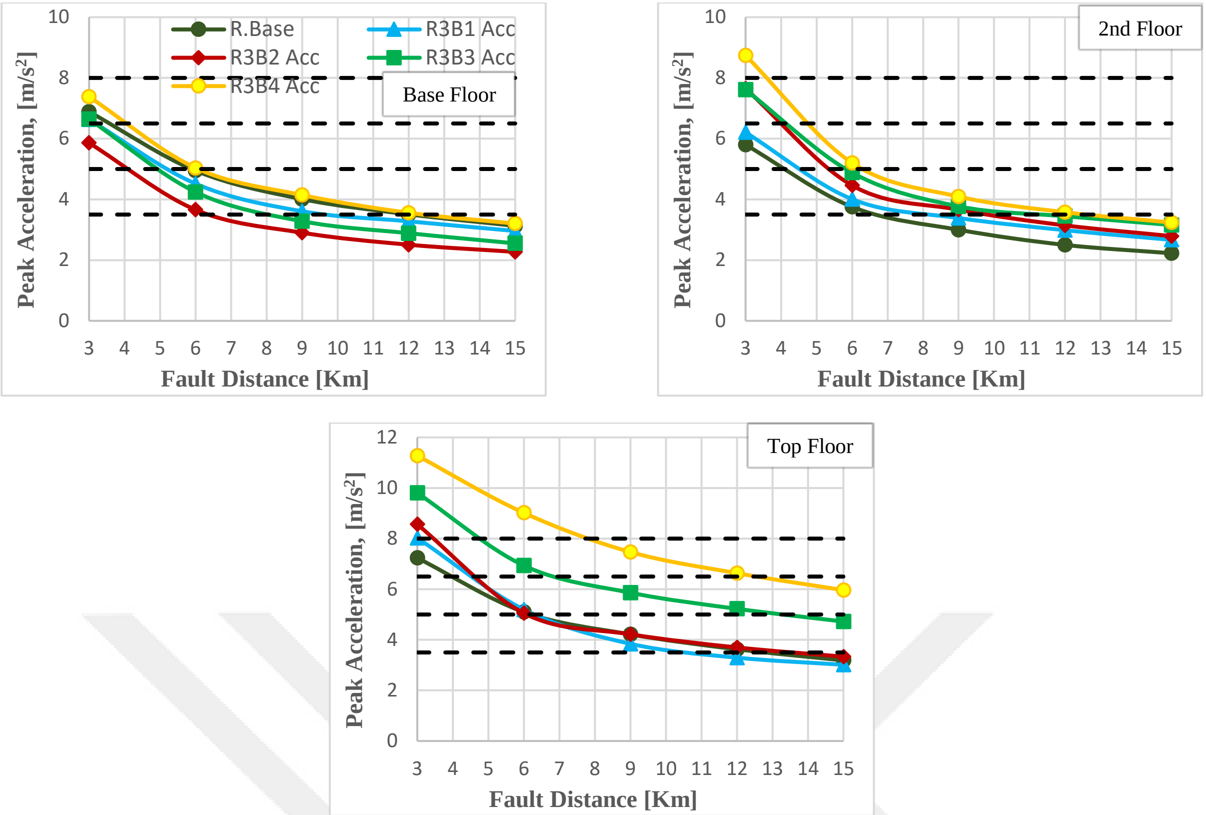

Figure 4.21: Peak acceleration of Rack-3 floor for Mw=7.0. Limits are drawn at 3.5, 5.0,6.5, 8.0 m/s²

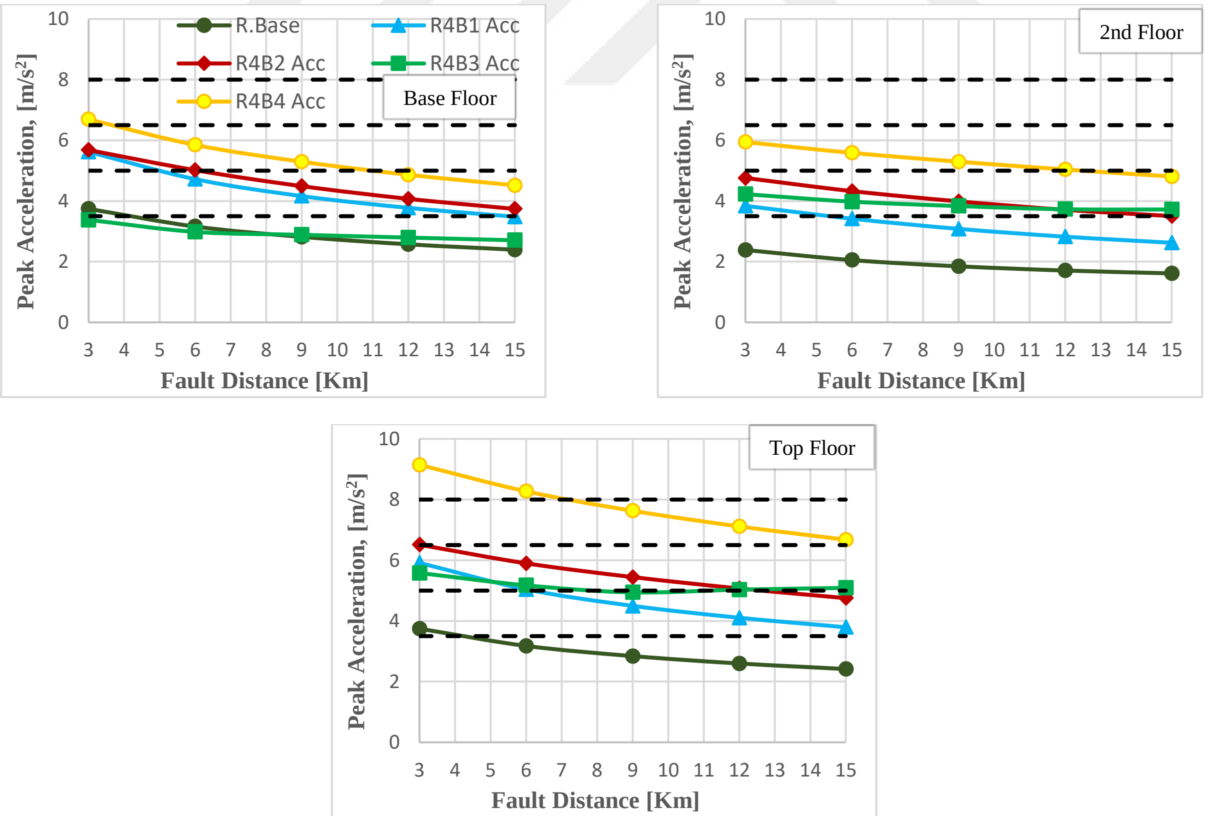

Figure 4.22: Peak acceleration of Rack-4 floor for Mw=6.0. Limits are drawn at 3.5, 5.0,6.5, 8.0 m/s²

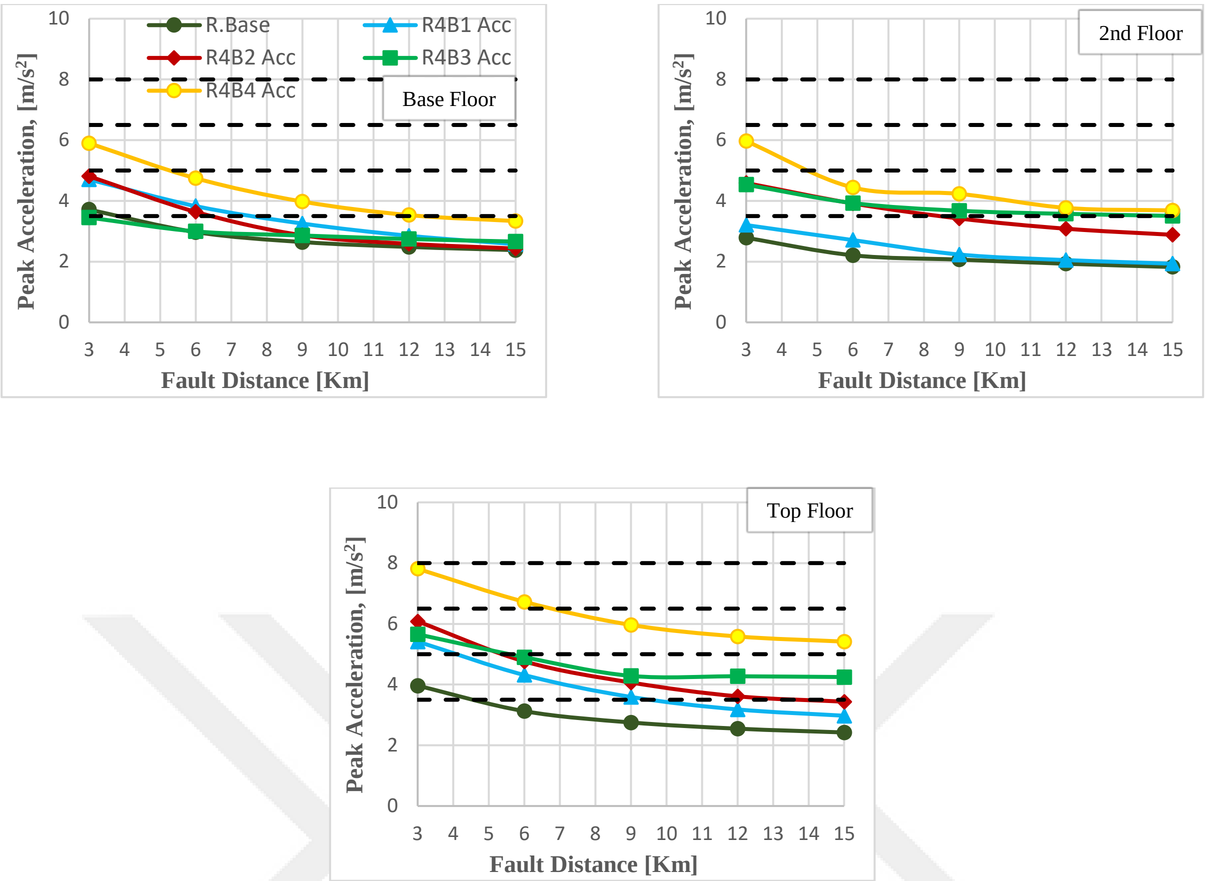

Figure 4.23: Peak acceleration of Rack-4 floor for Mw=6.5. Limits are drawn at 3.5, 5.0,6.5, 8.0 m/s^2

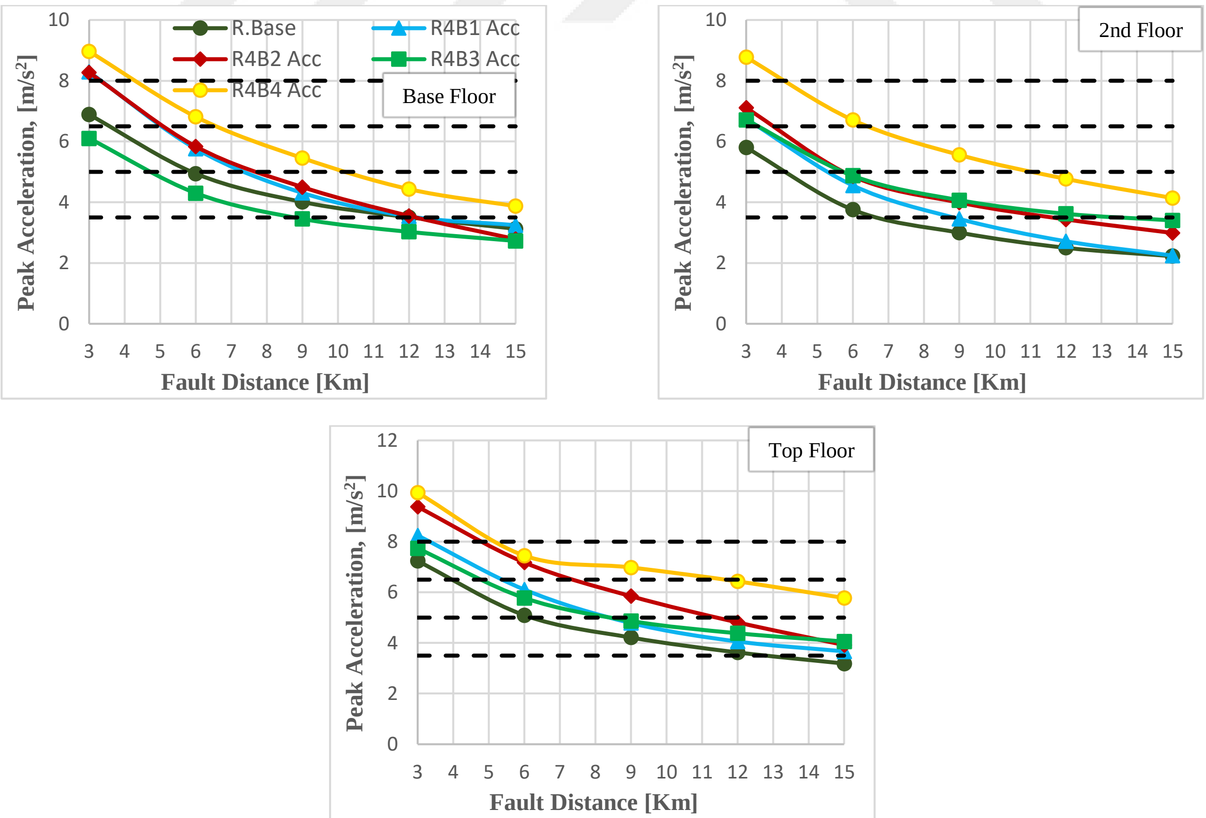

Figure 4.24: Peak acceleration of Rack-4 floor for Mw=7.0. Limits are drawn at 3.5, 5.0,6.5, 8.0 m/s^2

5 CONCLUSIONS

Seismic isolation technology has proved to be quite successful in reducing lateral equivalent earthquke forces. Moreover, it helps content protection of the seismic isolated building in typical far-fault earthquakes. But in near-fault earthquakes, the functionability of such systems is challenged. In order to find out the extent of this challenge and the potential success of seismic isolation, it is important to assess a subject model response under different near-fault earthquakes. Generally earthquake records can be divided into two types: natural historic and synthetic earthquake records. Natural historic earthquake records are actual records of real earthquake events. In this study, 15 historic records with 0-6 km fault distance and 15 historic records with 6-10 km fault distance are used. Alternatively, synthetic earthquakes are also generated. In this study, Agrawal and He(2002) pulse model is employed to systematically generate earthquake records of different magnitudes (Mw=6.0, 6.5, 7.0) and fault-distances (r=3, 6, 9, 12 km). It is intended in this thesis to find the response outcomes of a subject model and its contents placed on racks under historic and synthetic earthquakes. A building model comprised of six stories and housing four different type of racks with fundamental periods of 0.2 s, 0.4 s, 0.6 s, 0. 8 s are modeled using Sap2000 computer program. Racks are used for keeping vibration sensitive equipment. Most of the previous research studies mainly focused on floor accelertions but the assessment of the influence of rack behaviour is equally important. In this study, the racks are placed on subject building's different floors. Peak rack floor accelerations are obtained at different fault distances and for different earthquake magnitudes and compared to set acceleration limits that may damage vibration sensitive equipment. The outcomes of model presented are summarized in two different categories:

(A) In the first category, under historic earthquake what outcomes of building and rack model is achieved is explained. And for the easy comprehension, each building floor and relative rack behaviour is elaborated. Under historic earthquake, when racks are examined, it is seen that regardless of the rack period and rack building floor number, all 0-6 km near-fault responses tend to give higher values compared to all 6-10 km responses. In base floor, racks with period Tr = 0.6s generally give low responses however when the same rack in 2nd floor is compared, the rack with Tr =0.4s is found out to give the lowest values. Finally, when top floor is checked, this time the largest responses are obtained by Tr = 0.4s racks. Largest responses for all rack periods tend to be observed at the top floor. In a nutshell, it is essential to consider rack base and different floors of rack and different floors of the building where the racks are located. Moreover, natural period of racks and isolation period of the buildings are also important.

Table 5.1: Racks responses with their relative locations

Building floor	Lowest Acceleration values	Highest Acceleration values
Base Floor	Tr = 0.6s	Tr=0.4s
2nd Floor	Tr=0.4s	Other racks are higher, mostly crosses all benchmark limits
Top Floor	All rack responses are higher in the top floor	

Acceleration amplification ratios defined as between rack base and rack floors are assessed for all near-fault earthquakes. It is seen that these ratios increase towards the upper floors of racks and can be multiple of the floor at which rack is supported. In addition, it is observed that a combination of the rack period and rack floor location results in different amplifications.

Finally, the results are also evaluated in the form of probability of exceeding specified limits at rack base and different rack floors Limits of 3.5 m/s^2, 5.0 m/s^2, 6.5 m/s^2, and 8.0 m/s^2 are checked.

For all racks and rack floors, 3.5 m/s^2 acceleration limit is passed significantly. 8.0 m/s^2 can conveniently be met particularly at lower floors of the building and the lower levels of the rack. It is determined that building top floor and rack top floor are the worst-case scenarios for sensitive equipment.

(B) In the second category, peak acceleration response profiles of racks under synthetic earthquakes of Mw=6.0, 6.5 and 7.0 are presented, which give a complete picture. Synthetic earthquake results are found to comply with the results of the historical earthquakes. Building top floor and base floor acceleration is seen to be nearly the same but accelerations of racks present in these floors show variation. 2nd floor when compared with both floors, show minimum acceleration in building floor as well as in different rack floors.

It is observed that increasing magnitude and decreasing fault distance result in higher accelerations. It is seen that by setting the building period and rack period correctly, one can target a realistic value without exceeding 5.0 m/s^2 limit. But it is difficult to achieve 3.5 m/s^2 limit and fortunately 6.5 m/s^2 and 8.0 m/s^2 limits can be achieved as long as the equipment is not installed at rack top floors.

In summary, it is shown in this thesis that racks located in seismically isolated buildings containing vibration sensitive equipment need to be closely examined in order to provide adequate safety for the equipment. The accelerations in rack floors can be significantly higher than that of building floor where it is located. Therefore, seismic isolation may fail short in protecting vibration sensitive equipment if they are placed on racks and the building is located in a near-fault region that is closer than 6 km. It is shown that the risk of exceeding a specified acceleration limit is a function of earthquake magnitude, fault distance, isolation period of the building, period of the rack, and building floor and rack floor where the equipment is located.

REFERENCES

A. Barka, H. S. Akyüz et al, "The Surface Rupture and Slip Distribution of the 17 August 1999 Izmit Earthquake (M 7.4), North Anatolian Fault", *Bulletin of the Seismological Society of America, 92, 1, pp. 43–60, February* 2002.

A. Bayraktar, H. Keypour, A. Naderzadeh, "Application of Ancient Earthquake Resistant Method in Modern Construction Technology.", in *15th World Conference on Earthquake Engineering,* (2012).

A. Daei, M. Poursha, "A Comprehensive Review on the Characteristics of Near-Fault Earthquakes" (2016).

A. Mohammadia, G. Nouri, "Investigation on the Effect of Near-Fault Earthquake on Double Concave Friction Pendulum (DCFP) Base Isolated Buildings", *Procedia Engineering 199 (2017) 1731–1736*

Afet ve Acil Durum Yönetim Başkanlığı. (2014). Müdahale, İyileştirme ve Sosyoekonomik Açıdan Van Depremi 2011. AFAD Yayınları, Ankara.

B. Atmaca , M. Ergun, Ş. Ateş, "The Most Appropriate Earthquake Record Groups For Dynamic Analysis Of A Building", *Sigma journal of engineering and natural sciences , (2018) 1047-1079*

B. Carpani, "Base Isolation From A Historical Perspective", in *16th World Conference on Earthquake, 16WCEE,* (2017).

B. Mohraz, "Recent studies of earthquake ground motion and amplification", *Earthquake engineering, Tenth World Conference 1994 Balkerna, Rotterdam (wcee), article 10_vol11_6695* (1994).

C. Alhan, F. Sahin, "Protecting vibration-sensitive contents: an investigation of floor accelerations in seismically isolated buildings*.", Bulletin of Earthquake Engineering, 9, 1203-1226,* (2011).

C. Alhan, M. Sürmeli, **"**Shear building representations of seismically isolated buildings", *Bulletin Of Earthquake Engineering, 9(5), 1643-1671,* (2011).

C. Alhan, M. Sürmeli, "Necessity and adequacy of near-source factors for not-so-tall fixed-base buildings", *Earthq Eng And Eng Vib (2015), 14: 13-26*

C. Lu, "Research on Near-fault Problems in Earthquake Engineering", *Telkomnika, Vol.10, No.5, pp. 1033-1039* (2012).

C. G. Gordon, "Generic Vibration Criteria for Vibration-Sensitive Equipment", *Proc. SPIE 3786, Optomechanical Engineering and Vibration Control,* (28 September 1999)

C. Scawthorn, G. S. Johnson, "Preliminary report: Kocaeli (izmit) earthquake of 17 August 1999", *Engineering Structures,* Volume 22, Issue 7, July 2000, Pages 727-745 (2000).

D. B. Montessus. "The Seismological Work of John Milne", *Bulletin of the Seismological Society of America. 4 (1), 1-24* (1914).

D. Stevenson (1868), “Notice of Aseismatic Arrangements, adapted to Structures in Countries subject to Earthquake Shocks”, *Transaction of the Royal Scottish Society of Arts. 7, 557-566.*

D. Konstantinidis, F. Nikfar, “Seismic response of sliding equipment and contents in base-isolated buildings subjected to broadband ground motions”, *Earthquake Engng Struct. Dyn. 2015; 44:865–887* (2014).

Earthquake in Turkey Article, Tectonics Information, Earthquake Facts -- National Geographic.” [Online]. Available: https://www.nationalgeographic.com/science/earth/the-dynamic-earth/anatolian-fault/.

G. P. Warn, K. L. Ryan," A Review of Seismic Isolation for Buildings: Historical Development and Research Needs", *Buildings 2012, 2, 300-325* (2012).

H. Karayiğit, Ö. Özkul, “First Application of Base Isolation in an Existing Residential Building in Istanbul”, in *fifth conference on smart monitoring, Assessment and Rehabilitation of Civil Structures SMAR* (2019).

Bringing to life the largest base-isolated building in the world.” [Online]. Available: https://www.arup.com/projects/basaksehir-city-hospital

Event Report, kocaeli Turkey Earthquake [Online]. Available: https://www.preventionweb.net/files/2667_TurkeyEvent.pdf and [Online]. Available: https://www.rms.com/about

KOBİ'lerde Dayanıklılık: Yeni Riskler, Yeni Öncelikler, [Online]. Available:https://www.tr.undp.org/content/turkey/tr/home/library/poverty/cbi-report.html

Deadliest earthquakes of the past decade [Online] Available: https://www.usatoday.com/story/news/world/2017/09/20/deadliest-earthquakes-past-decade/684109001/

Seismicity Study in Turkey, [Online] Available: https://www.usgs.gov/about/organization/science-support/international-programs/seismicity-study-turkey

The Science of Earthquakes, Lisa Wald (U.S. Geological Survey) for “The Green Frog News”, [Online] Available: https://www.usgs.gov/natural-hazards/earthquake-hazards/science/science-earthquakes?qt-science_center_objects=0#qt-science_center_objects

İ. Şahin, T. Kılınç, “Türkiye’de 1980-2014 Yılları Arasında Görülen Depremlerin Ekonomik Etkileri”, *Siirt Üniversitesi İktisadi ve İdari Bilimler Fakültesi İktisadi Yenilik Dergisi,* Cilt: 4, Sayı: 1, Temmuz 2016

I. G. Buckle, “Passive Control Of Structures For Seismic Loads”, *Bulletin of the New Zealand Society for Earthquake Engineering* 33(3), (2000).

J. V. Amiri, M.R. Davoodi, A.Sahafi, "Simulation of Near-Fault Ground Motions With Equivalent Pulses & Compare Their Effects on MRF Structures", *in The 14th World Conference on Earthquake Engineering, (2008) 12-17*

J.F. Hall and K.L. Ryan, “Isolated Buildings and the 1997 UBC Near-Source Factors,” *Earthquake Spectra, (2000) 16, 393–411*.

Türkiye'de Doğal Afetler Konulu Ülke Strateji Raporu, *Japonya Uluslararası İşbirliği Ajansı (JICA) Yayınları, Türkiye Ofisi,* Ankara, İçişleri Bakanlığı. (2004).

K.Yamanturk, C.Dogruoz "Application of Seismic Isolators in Kutahya City Hospital Project Utilizing Double Friction Pendulum Type Devices", *World Academy of Science, Engineering and Technology International Journal of Civil and Environmental Engineering* Vol:13, No:8, (2019).

L. Haj Najafi, M. Tehranizadeh, "Evaluation Of Seismic Behavior For Moment Frames And Eccentrically Braced Frames Due To Near-Field Ground Motions", *Asian Journal Of Civil Engineering (Bhrc)* Vol. 14, No. 3 (2013).

Matsagar VA, Jangid RS, "Influence of isolator characteristics on the response of base-isolated structures". *Eng Struct (2004) 26:1735–1749*

M. Azimi, "Design Of Structural Vibration Control Using Smart Materials And Devices For Earthquake-Resistant And Resilient Buildings", *Civil & Environmental,* Engineering Masters Theses (2017).

M. Diclelia, S. Buddaram, "Equivalent Linear Analysis Of Seismic-Isolated Bridges Subjected To Near-Fault Ground Motions With Forward Rupture Directivity Effect", *Engineering structures 29, (2007) 21-32*

M. Erdik , Ö. Ulker , B. Şadan and C. Tüzün, "Seismic isolation code developments and significant applications in Turkey", *M. Erdik et al. Soil Dynamics and Earthquake Engineering 115 (2018) 413–437* (2018).

M.C. Constantinou, A.S. Whittaker and E. Velivasakis. "Seismic Evaluation and Retrofit of the Ataturk International Airport Terminal Building", *MCEER Bulletin: Research Accomplishments, 2000-2001Chapter: 15Publisher: University at Buffalo* (1999).

M.C. Constantinou, A.S. Whittaker, Y. Kalpakidis, D.M. Fenz, and G.P. Warn, "Performance of Seismic Isolation Hardware under Service and Seismic Loading", *Technical Report, Report number: MCEER-07-0012 Affiliation: Multidisciplinary Center for Earthquake Engineering Research,* State University of New York, Buffalo, New York (2007).

M.Erdik, Y.Alpay Biro, T.Onur, K.Sesetyan and G.Birgoren, "Assessment Of Earthquake Hazard In Turkey And Neighboring Regions", *INGV, Istituto Nazionale di Geofisica e Vulcanologia, Vol 42, No 6* (1999).

M.Lashgari, "Comparative Study Of Base-Isolated And Fixed-Base Buildings Using A Damage/Cost Approach". *Construction Systems* -- Dissertations & Theses. 16. (2014).

M.V.Kishor, " Comparison Of Experimental Seismic Response Of Conventional And Base Isolated Buildings With Analysis". *Thesis for: Masters of Technology* (2010).

Makris N. and Chang S… "Effect of viscous, Viscoplastic and Friction Damping on the Response of seismic Isolated Structures", *Earthquake Engng Struct. Dyn. 2015;* 44:865–887 (2000).

Nagarajaiah S, Reinhorn AM, Constantinou MC, "Nonlinear dynamic analysis of 3-D base-isolated structures", *J Struct Eng (1991) 117:2035–2054*

N. Makris, “Seismic isolation: Early history.”, *Earthquake Engng Struct Dyn.* 2018;1–15 (2018).

N. N. Ambraseys, J. A. Jackson, “Seismicity of the Sea of Marmara (Turkey) since 1500”, *Geophys. J. Int. 141, F1-F6* (2000).

O. Tan, M. C. Tapirdamaz, A. Yörük, “The Earthquake Catalogues for Turkey”, *Turkish Journal of Earth Sciences,* Vol. 17, pp. 405–418 (2008).

P. G. Somerville, "Development of an improved representation of near fault ground motions", *In SMIP98 Seminar on Utilization of Strong-Motion Data (1998) Vol. 15.*

S. Grimaz, P. maliSan,"Near field domain effects and their consideration in the international and Italian seismic codes", *Bollettino di Geofisica Teorica ed Applicata 55(4):717-738* (2014).

S.A. Kabeer, S.kumar, "Comparison of Two Similar Buildings with and without Base Isolation", *Kabeer et al., International Journal of Advance research , Ideas and Innovations in technology. (Volume 1, Issue 1; Oct,2014).*

S.N. Fathima, “Base isolation of structures”. [Online]. Available: https://www.slideshare.net/khushinusrath/base-isolation-of-structures (2016)

S.Ö. Davas, “Puls periyotlarının sismik izolasyonlu binaların performansına etkisi*”, İnşaat Mühendisliği Anabilim Dalı, yüksek lisans tezi* (2011).

S. Öncü, C. Alhan, "Effectiveness of Seismic Isolation in Protecting Sensitive Contents against Near-Fault Earthquakes of Various Magnitudes", in 10th International Congress on Advances in Civil Engineering, *(2012) 17-19*

S. Öncü Davas, “Yari-Aktif Sismik İzolasyon Sistemlerine Sahip Binalarin Deprem Yükleri Altindaki Olasiliksal Davranişi”, *İnşaat Mühendisliği Anabilim Dalı, Doktora Tezi* (2018)

V. K. Mahadik, D. K. Paul, G. R. Reddy, P. N. Dubey, S. K. Deb, "Comparison Of Recorded Response Of Conventional And Base Isolated Buildings With Analysis", *Conference: Structural Mechanics in Reactor Technology (SMiRT 21)At:* New Delhi, IndiaVolume: Div-V (2011)

W.Lu Shun, Z. Fu Lin, “Vibration And Seismic Isolation Design For Builidings On Subway Platform”, *The 14th World Conference on Earthquake Engineering, Beijing China* (2008).

Z. Tafheem, T.A. Arafat, A. Chowdhury and A. Iqbal, “Seismic Isolation Systems in Structures-the State of Art Review”, *Proceedings of 11th Global Engineering, Science and Technology Conference* 18 - 19, BIAM Foundation, Dhaka, Bangladesh (2015).